Radiation Response of Head and Neck Squamous Cell Carcinoma Using Early Markers of Apoptosis and Proliferation, Utilising a Microfluidic Approach

Rishi Srivastava

MD MRCS DOHNS

MD by Thesis

The University of Hull and the University of York

Hull York Medical School

August 2016

Abstract

Introduction

The purpose of this study was to assess the response to irradiation of HNSCC tissue samples maintained in a microfluidic device, utilising early markers of apoptosis and proliferation.

Materials and Methods

Rat liver had initially been used to optimise the conditions so HNSCC tissue biopsies could be maintained in a pseudo *in vivo* environment. Parameters assessed were different flow rates, oxygenated media and concentrations of sera in the medium, buffer components and infusion times with bromodeoxyuridine. HNSCC tissue samples from the oral cavity, oropharynx, larynx, metastatic lymph node and maxillary sinus were obtained. Tissue from each subsite was irradiated with doses of 5Gy, 10Gy, 15Gy and 20Gy. Cell death was measured using LDH and the morphology of the tissue was assessed using H&E staining. Apoptosis was calculated using immunohistochemical techniques to detect cytokeratin and the M30 antibody; and proliferation was assessed using the bromodeoxyuridine assay.

Results

HNSCC tissue samples could be maintained in the microfluidic device after an initial rise in LDH levels and assessment of the tissue architecture using H&E staining. Statistically, there was no significant difference observed in LDH post irradiation. Apoptotic indices calculated for all subsites revealed variation within the same tissue with the same dose, statistically no significant difference between irradiation with different doses of the head and neck subsites. Proliferation was noted with the bromodeoxyuridine assay in three out of the five subsites but no significant pattern was observed.

Conclusion

The microfluidic device is capable of maintaining HNSCC tissue in a viable state and is able to withstand rigorous testing. This study did not demonstrate a dose dependent relationship and suggests HNSCC intratumour heterogeneity would

account for the variation in responses with irradiation. The microfluidic technique is a very useful method in assessing a patient's response to radiotherapy and allows a personalised treatment approach for the future.

Contents

Chapter 1 - Introduction

Chapter 2 – Materials and Methods

Chapter 3 - The optimisation of the microfluidic device

Tables

Figures

Acknowledgements

The author would like to express his deepest gratitude to Prof. J. Greenman, Dr V. Green and Prof. N. Stafford for their expertise, insight and unwavering support throughout this study. Mr J. Jose Consultant Head and Neck surgeon and Mr. S. Crank Consultant Maxillofacial surgeon are based at Hull and East Yorkshire hospitals and assisted with the provision of the HNSCC tissue biopsies for this study. Prof. A. Beavis, Consultant Medical Physicist and his team at the radiotherapy suite supported this study by staying well beyond their working hours and aided with the irradiation of the tissue specimens. I would like to thank Ms Elaine Brookes, Dr. Roger Sturmey and Dr. Tom McCreedy without whom this would not have been possible. My extended gratitude goes to Ramsah Cheah who I collaborated with for part of this research. Finally, I would like to thank my wife and parents for their never-ending support, specifically to shine the light when all that remained was darkness.

Thesis associated abstract publications and presentations

1. Cheah R., **Srivastava R**., Stafford N., Green V., and Greenman J. 2015. Exploiting microfluidic culture to determine the radio-sensitivity of head and neck squamous cell carcinoma tissue. *Hull York Medical School (HYMS).* (Poster) 2015 HYMS Postgraduate Research Conference (June 2015, Hull).

2. Cheah R., **Srivastava R**., Stafford N., Green V., and Greenman J. 2015. Can microfluidic culture be used to determine the response of head and neck squamous cell carcinoma tissue to irradiation using different markers of cell death? *European Association for Cancer Research (EACR)*. (Poster) EACR Conference Series 2015. (February 2015, Essen)

3. Cheah R., **Srivastava R**., Stafford N., Green V., and Greenman J. 2014. Analysis of cell death in head and neck squamous cell carcinoma (HNSCC) tissue in response to irradiation during microfluidic culture. *The National Cancer Research Institute.* (Poster) 2014 NCRI Cancer Conference (November 2014, Liverpool).

4. Cheah R., **Srivastava R**., Stafford N., Green V., and Greenman J. 2014. Investigation of the response of head and neck squamous cell carcinoma (HNSCC) to irradiation using a microfluidic device. *Hull York Medical School (HYMS).* (Poster) 2014 HYMS Postgraduate Research Conference (June 2014, York).

5. **Srivastava R**., Cheah R., Green V., Stafford N. and Greenman J. 2013. Monitoring Response To Irradiation In Head And Neck Squamous Cell Carcinoma Biopsies Using A Microfluidic-based Approach. The 6th European Congress on Head and Neck Oncology. (Poster) (April 2014, Liverpool)

6. Cheah R., **Srivastava R**., Kazmierow H., Patel R., Stafford N., Green V., and Greenman J. 2013. Optimisation of culture conditions for the maintenance of viable tissue samples in a microfluidic device and the study of tissue response to irradiation. *The National Cancer Research Institute.* (Poster) 2013 NCRI Cancer Conference (November 2013, Liverpool).

7. Patel R., Green V., **Srivastava R**., Cheah R., Hunter, I. A., and Greenman J. 2013. The use of apoptotic markers to predict rectal cancer response to neo-adjuvant therapy. *The National Cancer Research Institute.* (Poster) 2013 NCRI Cancer Conference (November 2013, Liverpool).

8. Cheah R., **Srivastava R**., Kazmierow H., Patel R., Stafford N., Green V., and Greenman J. 2013. Optimisation of culture conditions for the maintenance of viable tissue samples in a microfluidic device. *Hull York Medical School*. (Poster) 2013 HYMS Postgraduate Research Conference (June 2013, Hull).

Author's declaration

'I confirm that this work is original and that if any passage(s) or diagram(s) have been copied from academic papers, books, the internet or any other sources these are clearly identified by the use of quotation marks and the reference(s) is fully cited. I certify that, other than where indicated, this is my own work and does not breach the regulations of HYMS, the University of Hull or the University of York regarding plagiarism or academic conduct in examinations. I have read the HYMS Code of Practice on Academic Misconduct, and state that this piece of work is my own and does not contain any unacknowledged work from any other sources'. If applicable, the declaration should also include; 'I confirm that any patient information obtained to produce this piece of work has been appropriately anonymised'.

Chapter 1

Introduction

1.1 Background

The initial section consists of the background to head and neck cancer, why it is important and sets the goals of this research.

Cancer can be defined as a malignant neoplasm characterised by an abnormal growth of anaplastic cells, which can invade local structures and potentially metastasize to distant body sites. Head and neck squamous cell carcinomas (HNSCC) comprise a heterogeneous group of tumours that are located in the lip, oral cavity, nasal cavity, paranasal sinuses, pharynx and larynx.

Patients with head and neck and cancer can present with a variety of symptoms, depending on the function of the site where the cancer originates. Some examples include hoarseness, dysphagia, unilateral otalgia, cranial nerve palsy, an enlarging neck lump, a sore throat and stridor. Signs of cancer on examination include, but are not limited to, an abnormal looking ulcerative mass in any of the head and neck sites, leukoplakia or erythroplakia in the mouth, cranial nerve palsy, an orbital mass and unilateral ear effusion *(Mehanna et al., 2010)*. Diagnosis and staging consists of the following: examination by a specialist clinician, fibre optic endoscopy, fine needle aspiration (for cytology) or core biopsy of any neck masses, with subsequent examination under an anaesthetic with biopsies of the primary site if required. Once a malignancy is confirmed, the extent of the primary tumour and regional lymph node metastasis (if any) needs to be assessed. Radiological staging (using computerized tomography (CT) or magnetic resonance imaging (MRI)) will achieve this; not only to confirm the anatomical extent of the disease and metastasis, but also to locate any synchronous malignancies *(Paleri and Roland (ed), 2016)*. Tumours are staged according to the TNM classification system; and once the findings have been

discussed at a multi-disciplinary head and neck meeting, a decision is made regarding the appropriate treatment (which can be surgical, non-surgical or a combination of both). Each of these will be discussed in turn with a particular focus on radiotherapy. Depending on the staging, treatment can be with curative or palliative intent *(Scottish Intercollegiate Guidelines Network, 2006)*.

The clinical course of head and neck squamous cell carcinomas is highly variable as is their response to treatment. Survival data analysed by the Oxford Cancer Intelligence Unit *(Oxford Cancer Intelligence Unit, 2010)* stated there had been significant improvement in the 1-year and 5-year relative survival rates for oral, oropharyngeal, nasopharyngeal and hypopharyngeal cancers. However, even though the 1-year relative survival rate for laryngeal cancer has shown a small but significant increase (82.75% to 85.33%), the 5-year relative survival rate has remained unchanged (65%) over the study period (1990 – 2006). This is thought to mirror the lack of major new treatments throughout this study period *(Oxford Cancer Intelligence Unit, 2010)*. Therefore, a better understanding of individual malignancies is required to allow the most appropriate treatment for patients. More recently, a subgroup of patients with HNSCC, characterised by a relatively good prognosis and a good response to chemoradiotherapy, has been discovered. These are often young patients, affected by HPV-related oropharyngeal carcinoma. HPV-positive tumours often show a particular biochemical signature characterized by less frequent p53 mutations and a lower EGFR expression, if compared with their HPV-negative counterpart *(Cattani et al., 1998; Lassen et al., 2009)*. This can account for their relatively high chemosensitivity and radiosensitivity.

There are cellular mechanisms, which support increased radiosensitivity in HPV positive cancers. These include altered DNA repair, differences in activated repopulation signalling pathways and down regulated cell cycle control mechanisms.

One of the mechanisms of cell death post irradiation is p53-mediated apoptosis. Even though HPV E6-oncoprotein down regulates p53, there is enough wild type p53 that remains to induce apoptosis after irradiation *(Mirghani et al., 2015)*. Kimple et al.

(2013) supported this hypothesis as they demonstrated cells became less responsive to irradiation, when p53 was inhibited by RNA interference in HPV positive cell lines and human tonsillar epithelial cells transfected by E6. Rieckmann et al. *(2013)* demonstrated an increased response of HPV positive cells to irradiation. There was a significant association between residual double strand breaks and cellular radiosensitivity for HPV positive HNSCC cell lines.

The EGFR pathway is the most up regulated pathway in HNSCC and correlates with therapeutic resistance and a poor prognosis *(Temam et al., 2007; Mirghani et al., 2014)*. Interactions exist between fibroblast growth factor receptors (FGFR), phosphatidylinositol 3-kinases-AKT-mTOR (PI3K) and RAS pathways resulting in cell proliferation, growth and survival. An in vitro study however found evidence of enhanced EGFR activation in HPV-positive cell lines, and that loss of the HPV E6 and E7 oncoproteins in these cells decreased phospho-EGFR and modulated β–catenin activity *(Hu et al., 2014).*

Studies have shown that HPV-positive tumours are more likely to be seropositive for antibodies against HPV virus like particles E6 and E7. The presence of these antibodies correlates with improved survival *(Kreimer et al., 2005; Smith et al., 2009 and Cleary et al., 2016)*. Another study has shown radiation therapy decreases surface expression of CD 47, which is a self-marker. This is frequently overexpressed in HNSCC; and radiation induces a decrease of CD 47 in a dose-dependent manner, resulting in improved immune-mediated tumour clearance i*n vivo (Vermeer et al., 2013)*. These immune mediated mechanisms make HPV positive tumours increasingly radiosensitive and subsequently have a better overall prognosis.

Irradiation induced DNA damage will produce double stranded breaks and single stranded breaks. These in turn activate the family of checkpoint kinases 1/2 through ATM and ATR and arrest the cycle to allow DNA repair. Over expression of p16 impairs recruitment of RAD51 to the site of DNA damage and therefore decreases

DNA repair pathways *(Mirghani et al., 2015)*.

Given these characteristics, it is possible to treat them more conservatively, avoiding radical surgery in favor of chemoradiation or choosing the association of concomitant cetuximab and radiotherapy, rather than the standard cisplatin and radiotherapy *(Pajares et al., 2013; Kofler et al., 2014; Perri et al., 2015)*.

1.2 Epidemiology of Head and Neck Cancer

It is the sixth most common cancer in the world, associated with low survival and high morbidity; with more than 500,000 patients worldwide being given the diagnosis each year *(Haddad and Shin, 2008)*. Head and neck cancers accounted for approximately 140,000 new cases and 63,500 deaths in Europe in 2012 *(Ferlay et al., 2012)*. The incidence of HNSCC arising from different subsites varies according to age and gender, subsite (table 1.1).

Table 1-1 A table demonstrating the differences in incidences, age, gender, subsites and trends in time with different head and neck subsites *(www.cancerresearch.org.uk)*, unless otherwise specified).

Site of cancer	Incidence	Variation by age and gender	Variation by subsite	Variation by time
Larynx	6/100,000 for males; and 2/100,000 for females	Males mainly, and over the age of 60	Supraglottis and glottis, followed by subglottis	Decreased in males and remained stable in females since the 1970's
Oropharynx	11/100,000 for males	Increase in both males and females, affecting younger adult groups	Mainly palatine tonsil	Overall increase, especially from 1990 to 2010 due to HPV and is expected to continue *(Mehanna et al., 2010)*
Oral cavity	16/100,000 for males and 8/100,000 for females	Increases from 45 years of age, peaks at 60-69years in males; and peaks at over 80years in females	Tongue	Overall increase in the incidence since the 1970's
Sinonasal	3.7/100,000 for males and 2.8/100,000 for females	Increases with age, men more affected than women *(Robin et al., 1979)*	Mainly maxillary sinus	General worldwide decrease

1.3 Anatomy of the Upper Aero Digestive Tract (UADT)

1.3.1 Oropharynx

The oropharynx is the middle part of the pharynx that connects with the nasopharynx superiorly, oral cavity anteriorly and hypopharynx inferiorly. Anteriorly, its boundary is

the anterior faucial pillars (figure 1.1) (otherwise known as the palatoglossal folds, which are made from the palatoglossus muscle, originating from the soft palate and the overlying mucosa) and the base of tongue. The soft palate and the uvula form the superior border of the oropharynx; whereas the inferior border of the oropharynx is formed by the vallecula. The epiglottis is located at the posterior aspect of the vallecula. The posterior oropharyngeal wall is formed by the mucous membrane overlying the overlapping superior and middle pharyngeal constrictor muscles. Histologically, it is lined by stratified squamous epithelium (non keratinizing type).

In between the pillars lie the paired palatine tonsils, these are lymphoid tissue masses that form part of Waldeyer's ring; and are said to play a role in local immune responses to oral pathogens. The oropharynx itself plays a role in the second (pharyngeal) phase of swallowing *(Beasley, 2008)*

1.3.2 Oral Cavity

The oral cavity is divided into the oral vestibule and oral cavity proper. The oral vestibule is bounded externally by the lips and cheek mucosa and internally by the teeth and alveolar processes. The oral cavity proper is bound superiorly by the hard palate (which separates it from the nasal cavities), inferiorly by the floor of the mouth, posteriorly by the oropharynx and antero-laterally by the posterior/medial aspects of the teeth. Histologically, it is lined by stratified squamous epithelium (non keratinizing type).

The tongue is the major organ that occupies the oral cavity. It plays a role in the oral phase of swallowing, mastication, speaking and taste sensation. Saliva is secreted into the cavity from paired salivary glands (parotid, submandibular and sublingual) as well as multiple minor salivary glands located throughout the cavity. The saliva plays a role in digestion as well as lubrication of food when placed in the cavity *(Berkovitz, 2008)*

1.3.3 Larynx

The larynx consists of a framework of cartilages, supported by various muscles and ligaments; it is located in the lower part of the pharynx and connects to the trachea. Anatomically, it is divided into the supraglottis, glottis and subglottis. The supraglottis extends from the tip of the epiglottis superiorly to the laryngeal ventricles inferiorly. It includes the epiglottis (lingual and laryngeal surfaces), aryepiglottic folds, arytenoids and false cords. The glottis extends from the ventricle superiorly to 5mm below the inferior surface of the true cords. The subglottis extends from the inferior border of the glottis to the inferior edge of the cricoid cartilage. The cartilages include the cricoid, thyroid, epiglottis, arytenoids, corniculate and cuneiforms. The ligaments consist of the extrinsic (thyrohyoid and hyoepiglottic) and intrinsic (conus elasticus and quadrangular membrane) ligaments; and the muscle groups are the cricothyroid, cricoarytenoid and arytenoids muscles (figure 1.1). Histologically it is lined by stratified squamous epithelium (non keratinizing type) and pseudostratified ciliated columnar epithelium *(www. histology.med.umich.edu/medical; www.pathologyoutlines.com; Junqueira et al., 1995)*

Its role is to protect the airway when a stimulus takes place (e.g. during swallowing) to prevent aspiration from occurring. Other functions include voice production, coughing and ventilation control *(Beasley, 2008)*.

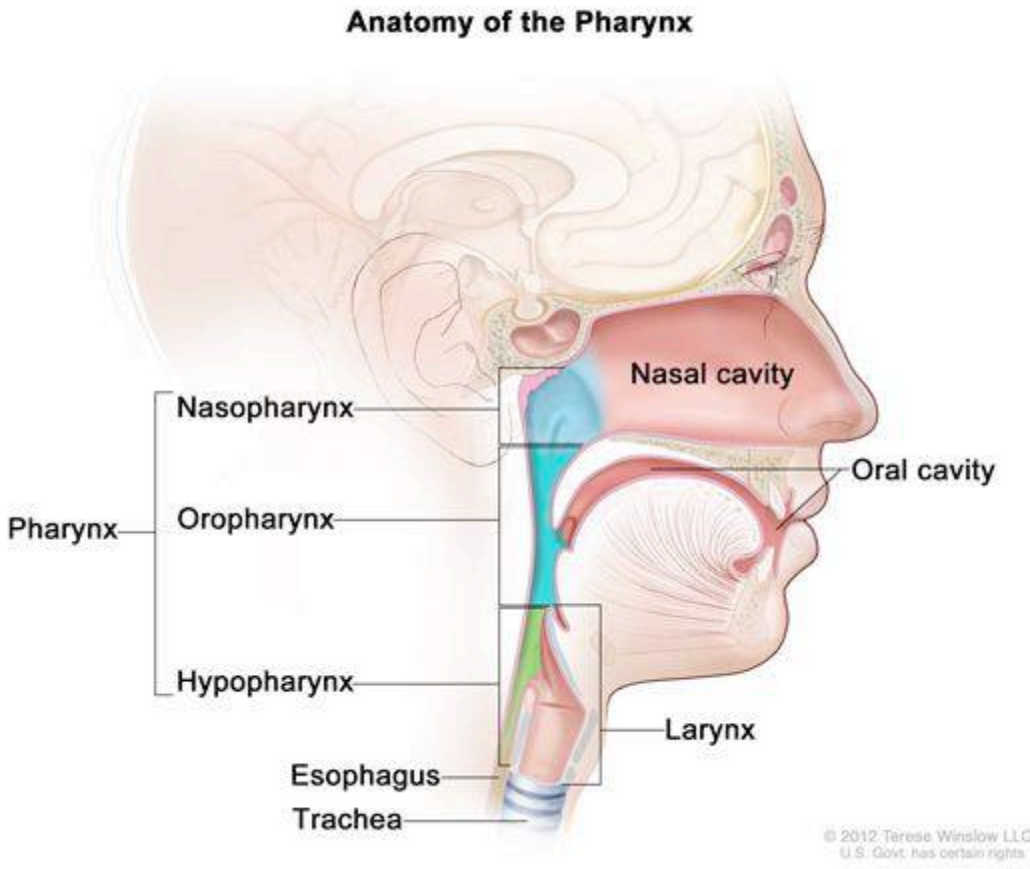

Figure 1-1 Diagram showing the head and neck subsites *(www.teresewinslow.com)*.

1.3.4 Maxillary sinus

It is the largest paranasal sinus and lies in the maxillary bone. The roof of the maxillary sinus forms most of the orbital floor and anteriorly, it is covered with kin, fat and facial musculature. Inferiorly there are the upper dentition and the hard palate; and posteriorly there are the pterygopalatine and infratemporal fosa *(Stammberger and Lund, 2008)*. The roles of the maxillary sinus include reducing the relative weight of the front of the skull, increasing the resonance of the voice and playing a role in immunological defence (figure 1.2)

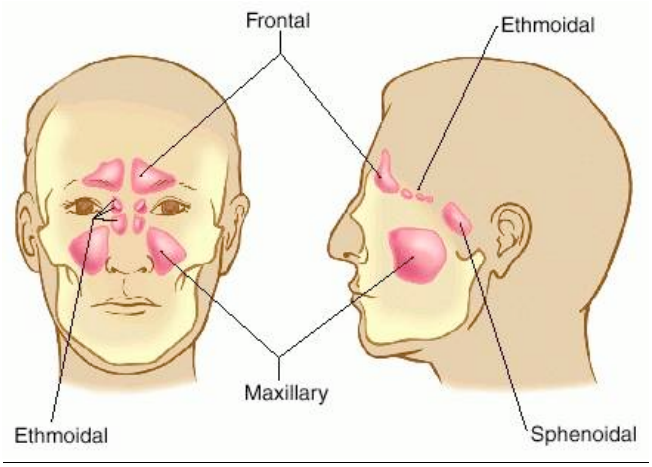

Figure 1-2 Diagram of maxillary sinus *(www.infovisual.info)*.

1.3.5 Lymphatic Drainage of the Upper Aero Digestive Tract

The lymphatic system consists of lymphatic fluid, vessels that transport it and organs that contain lymphoid tissue, as well as organized collections of lymph nodes. Its function is to return excess interstitial fluid to the blood, absorb fats and fat-soluble vitamins from the gastrointestinal system and transport them to the venous circulation; and is involved in defence against invading organisms and the spread of tumour cells. The superficial vessels originate in the tissue just beneath the skin and drain into deep vessels located adjacent to blood vessels. The lymphatic ducts (right lymphatic duct and thoracic duct) are the final step before lymph joins the venous system.

Malignancies in sub sites of the UADT can metastasize to various head and neck lymph node groups. Therefore, not only is knowledge of lymphatic drainage patterns of the head and neck important so we can understand where a potential tumour might be situated, the status of the cervical lymph nodes is the most important prognosticator in head and neck squamous cell carcinoma. Ultimately, lymph node involvement will play a role in treatment planning, whether surgical or non-surgical.

The Sloan-Kettering Memorial group established the lymph node regions and their subgroups. Their description is shown in figure 1.3 and table 1.2.

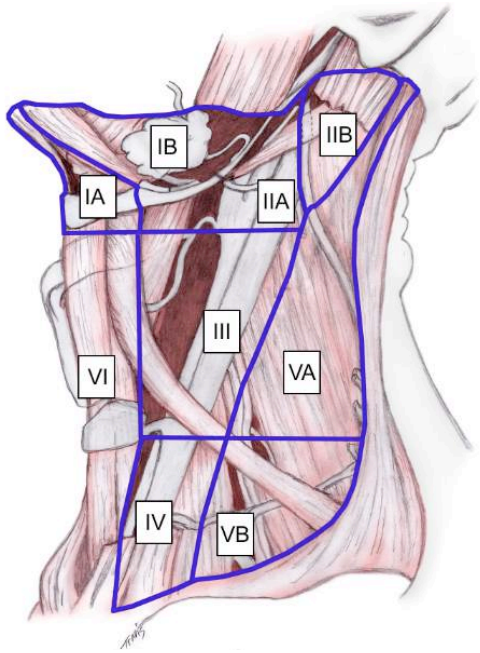

Figure 1-3 Lymph node levels in the neck *(www.emedicine.com)*.

Table 1-2 Lymph node levels in the neck and their corresponding locations.

Level of lymph nodes	Location of lymph nodes
Ia and Ib	Submental and submandibular region
IIa, IIb, III and IV	Internal jugular vein
Va and Vb	Posterior triangle
VI	Prelaryngeal, pretracheal and paratracheal

1.4 Aetiology of Head and Neck Cancer

As the majority of head and neck cancers are SCC, this section focuses on the causes / risk factors for HNSCC, which include: tobacco (with or without betel quid), marijuana, alcohol, viruses, dietary factors, gastro-oesophageal reflux and genetics.

1.4.1 Tobacco

Tobacco exposure is the most important risk factor for the development of HNSCC. The risk of developing a cancer depends on the amount of tobacco consumed (smoked or chewed) per day, the duration, the starting age of tobacco consumption and second hand exposure to smoke.

The link between tobacco and head and neck cancer was made in 1915 *(Abbe, 1915)*; it wasn't until 1957 however, that this association was first investigated with a case control study *(Wynder et al., 1957)*. In 1986, the International Agency for Research on Cancer (IARC) stated that tobacco was carcinogenic. Confirmed associations included the oral cavity, oropharynx, hypopharynx and larynx; and nearly two decades later, the association was extended to the remaining sites in the UADT *(IARC, 1987)*.

The main carcinogens in tobacco smoke are tobacco-specific N-nitrosamines (TSNA's) which cause DNA alkylation and hence mutations and when taking place in key target genes, cancer development can be initiated *(Hoffmann et al., 1994)*.

The IARC considered various studies and Table 1.3 provides an indication of the average relative risk for different head and neck sites *(Sasco et al., 2004)*, with the strongest association being with laryngeal SCC.

Table 1-3 Head and neck cancer sites associated with tobacco smoking *(Sasco et al., 2004)*.

Cancer Site	**Average Relative Risk**
Oral cavity	4-5
Oro/hypopharynx	4-5
Larynx	10
Nasal cavity, paranasal sinuses	1.5-2.5
Nasopharynx	1.5-2.5

Smokeless tobacco contains 28 known carcinogens; and the most harmful of these (TSNA's) are formed during the curing and aging of tobacco. Lesions appear at the site of application (e.g. oral cavity or nasal cavity) and although risk quantification is difficult, one systematic review from India has consistently shown that there is a significant risk of oral cancer with smokeless tobacco. Studies from the Western world however have been less conclusive *(Critchley and Unal, 2003)*.

1.4.2 Viruses

Human papilloma virus in head and neck cancer was recognized over 3 decades ago *(Syrjanen et al., 1982)*; and it is now accepted as a risk factor for oropharyngeal squamous cell carcinoma (OSCC) *(Mehanna et al., 2010)*. The incidence of HPV positive OSCC varies worldwide and is predicted to rise in the future. A retrospective study from Sweden showed increased detection of HPV in OSCC biopsies over three decades (23.3% in 1970s, 29% in 1980s, 57% in 1990s, 68% between 2000 and 2002, 77% between 2003 and 2005, and 93% between 2006 and 2007) *(Nasman et al., 2009)*. It is being seen in a younger cohort of patients aged 40 to 55 years, in males and patients without environmental risk factors *(Zaravinos, 2014)*. Changes in sexual practice may reflect the increasing proportion of HPV positive OSCC's *(Chaturvedi et al., 2011)*. A pooled analysis of eight multinational observational studies that compared 5642 cases of head and neck cancer with 6069 controls found that the risk of developing oropharyngeal carcinoma was associated with a history of six or more lifetime sexual partners (odds ratio 1.25, 95% confidence interval 1.01 to 1.54), four or more lifetime oral sex partners (3.36, 1.32 to 8.53), and for men an earlier age at first sexual intercourse (2.36, 1.37 to 5.05) *(Heck et al., 2009)*.

It is also important in the role of carcinomas of an unknown primary. In a recent study *(Axelsson et al., 2017)*, the prognostic factors for curatively treated head and neck carcinoma of the unknown primary were investigated. The majority of their tumours (69%) were positive for HPV by p16 immunostaining. The overall survival for these patients was significantly higher and the recurrence risk significantly lower for patients positive for p16. Their findings were in keeping with other studies showing

better survival for HPV positive carcinomas of the unknown primary *(Vent et al., 2013, Jensen et al., 2014)*.

The sinonasal tract compared to other head and neck sites has the lowest fraction of SCC; but some of the most significant histological variation and the increasing recognition of HPV in a subset of tumours *(Ansa et al., 2013; Lewis, 2016)*. Studies have suggested that high risk HPV may be important for the growth of carcinogenesis within inverted papillomas but does not drive the growth of established sinonasal tract tumours *(Alos et al., 2009; Bishop et al., 2013)*. Two groups compared transcriptionally active high risk HPV and examined survival outcomes; and the trends suggested favourable but not conclusive effects of HPV in sinonasal SCC *(Bishop et al., 2013; Larque et al., 2013)*.

HPV positive HNSCC patients are a younger group presenting at a later stage however they show an improved survival. Hence they may even be different tumour entities.

1.4.3 Alcohol

Alcohol is the second most important global risk factor for head and neck cancer, being involved in at least 75% of HNSCC, especially those in the oral cavity, oropharynx, larynx and hypopharynx *(Kufe et al., 2003)*. Extensive studies have shown that it has a multiplicative carcinogenic effect rather than an additive one *(Murata et al., 1996)*, and that SCC in the hypopharynx has the strongest association with alcohol (Table 1.4).

Table 1-4 Relative risks for various head and neck sites in individuals with an alcohol consumption of 12.5-20 units/day *(Talamini et al., 2002)*.

Cancer Site	Relative Risk (adjusted for tobacco)
Hypopharynx	28.6
Oropharynx	15.2
Oral Cavity	13.5

A study has shown that while there was a strong association between beer and spirit consumption and UADT cancer, those who consumed similar amounts of wine were at a lower risk; while moderate wine drinkers had an overall degree of protection compared with those who did not drink alcohol *(Gronbak et al., 1998)*.

In summary, tobacco and alcohol consumption are 2 major risk factors for head and neck cancer, not only in the UK but worldwide as well. There is evidence to suggest they act independently and synergistically *(Olsen et al., 1985, Merletti et al., 1989, Hashibe et al., 2007)*.

1.4.4 Other aetiological factors in head and neck cancer

Betel quid

Chewing of Betel quid (an areca nut) is an important risk factor for oral cancer. It is a very common habit in parts of Asia and Africa; and typically, it is made up of areca nut, betel leaf and slaked lime (calcium hydroxide). In association with tobacco betel quid was designated a carcinogen by the IARC in 1985 *(IARC, 1986)*. More recently betel quid on its own has been branded a carcinogen *(IARC, 2002)* and it is independently associated with oral cancer *(Merchant et al., 2000; Chen et al., 2002)*.

Marijuana

The carcinogenicity of tetrahydrocannabinol (THC), the major psychoactive ingredient in marijuana is still not clear *(Majchrzak et al., 2014)*. It has also been difficult to establish marijuana as an independent risk factor for HNSCC. This is because most users are long-term consumers of tobacco and alcohol anyway; and that typical marijuana users aren't consuming it at the same intensity as tobacco. One case controlled study demonstrated a suggestion of a dose-response relationship *(Zhang et al., 1999)*. Recent studies however have shown that there is no association between marijuana use and oral cavity SCC risk *(Rosenblatt et al.,*

2004) and that marijuana use modified the interaction between alcohol and tobacco, resulting in a decreased HNSCC risk amongst tobacco and alcohol consumers *(Liang et al., 2009)*.

Gastro-oesophageal reflux (GORD)

Reflux can cause irritation in the laryngopharynx and inspection can reveal findings such as an erythematous larynx, pharyngeal mucosal erythema, vocal cord granulomas and in some cases the development of laryngeal cancer. One case control study of laryngeal and pharyngeal SCCs has shown that GORD is associated with the development of both *(El-Serag, 2001)*.

Dietary Factors

Diet has a small but significant role to play in UADT SCC. Deficiencies associated with an increased risk of HNSCC are vitamins A, C, E, B-carotene, riboflavin with iron, selenium and zinc *(Maier and Tisch, 2001)*. Tomatoes are said to have a protective effect (De Stefani et al., 2000) and reduced meat and fat consumption seems to be associated with reduced risk of cancer *(Oreggia et al., 2001)*. There is a link between salted fish and nasopharyngeal carcinoma in Southern China; however, this relationship has not been repeated in other populations *(Knekt et al., 1999)*.

1.5 Genetics and the molecular basis for tumour development

The initiation and progression of head and neck cancer is a complex process that entails a progressive acquisition of genetic and epigenetic alterations (figure 1.4), which may result in a malignant phenotype. The molecular model proposed by Fearon and Vogelstein *(1990)* for colorectal tumourigenesis can be used for other tumours including those of the head and neck. Further work has allowed the model (figure 1.5) to be proposed for progression of HNSCC.

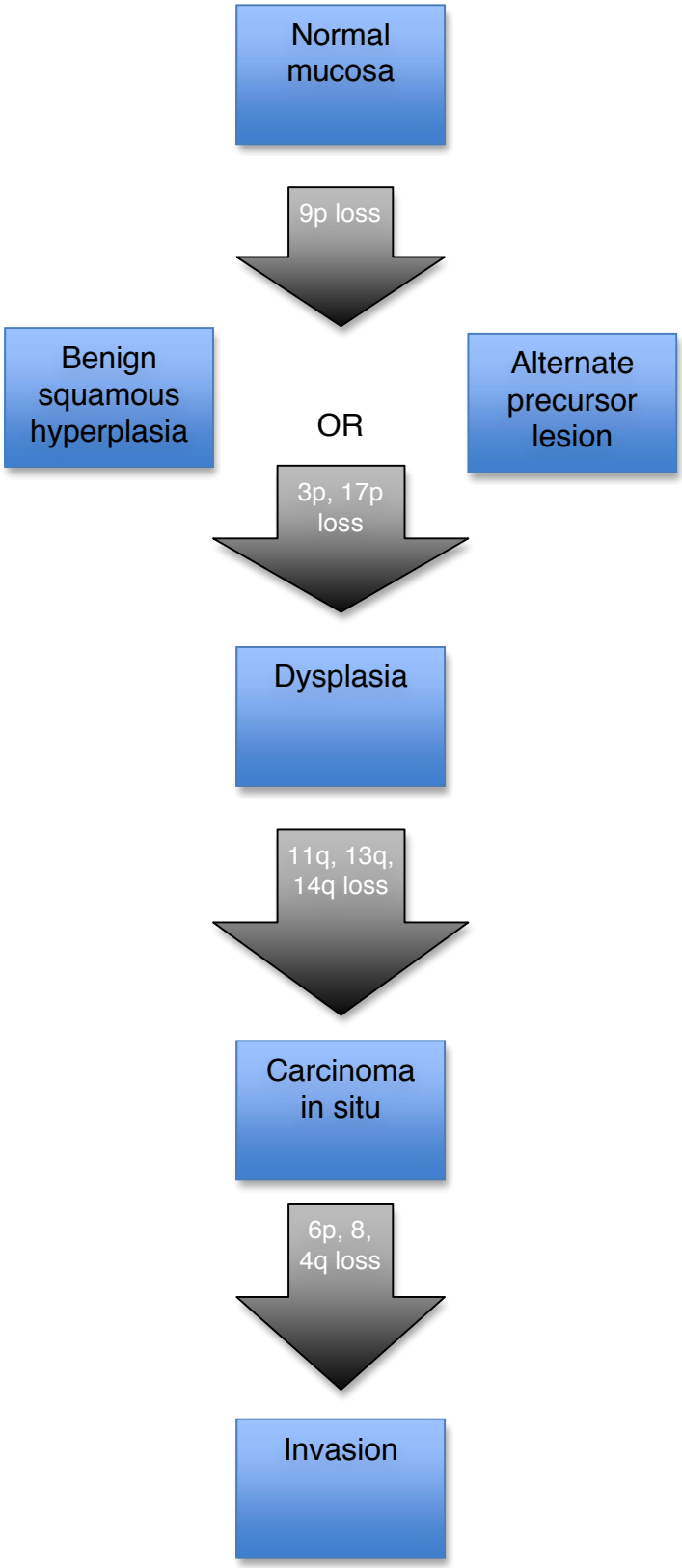

Figure 1-4 Genetic progression of HNSCC. Genetic changes associated with the histopathological progression of HNSCC based on loss of chromosomal material (allelic loss). Genetic alterations have been placed prior to the lesion where the frequency of the particular event plateaus. It is the accumulation and not necessarily the order of genetic events that determines progression. A small fraction of benign

squamous hyperplastic lesions contain 9p2l or 3p2l loss, suggesting that an unidentified precursor lesion (or cells) may also give rise to dysplasia. Candidate tumour suppressor genes include p16 (9p2l), p53 (lip), and retinoblastoma (13q), and a candidate proto-oncogene includes cyclin D1 (I 1q13) *(Califano et al., 1996)*.

The TP53 and retinoblastoma (Rb) pathways are almost universally disrupted in HNSCCs, indicating the importance of these pathways in head and neck cancer progression. The TP53 pathway controls cell growth by regulating cell-cycle progression and responses to stress via apoptosis. Over 50% of HNSCCs harbor inactivating *TP53* gene mutations *(Califano et al., 1996; Poeta et al., 2007)*, and over 50% demonstrate chromosomal loss at 17p—the site where the *TP53* gene resides. The most-targeted component of the Rb pathway is the $p16^{INK4A}$ tumor-suppressor gene. Its gene product prohibits cells from entering the cell cycle by inhibiting the cyclin-dependent kinases 4 and 6. Inactivation of $p16^{INK4A}$ can occur by any combination of promoter hypermethylation, gene mutation, and loss of heterozygosity (LOH). Indeed, LOH at chromosomal region 9p21 (where $p16^{INK4A}$ resides) occurs in up 80% of HNSCCs *(Pai and Westra, 2009)*. HPV positive HNSCC's consistently express the wild-type p16 protein, such that immunohistochemical detection of p16 can be used to assess the HPV status of HNSCC's *(Pai and Westra, 2009)*.

There is evidence to support the fact that genetic factors play a role in head and neck cancer development, as not all individuals exposed to the major carcinogens proceed to develop HNSCC.

To explain the genetic aspect, it is first of all important to appreciate that cell cycle homeostasis is kept under regulation by approximately 40 proteins that are produced by proto-oncogenes and tumour suppressor genes; so that under normal conditions, a balance is maintained between cell proliferation and cell death. However, a buildup of genetic alterations can result in carcinogenesis. These alterations are due to genetic mutations, which can be point mutations, deletions, amplification of DNA segments and chromosomal rearrangements. These genetic alterations can in turn

lead to proto-oncogene activation and tumour suppressor gene inactivation, so the cell cycle homeostasis is lost resulting in a malignant phenotype.

There are differences in inherited DNA repair systems that can make a person susceptible to carcinogenesis. Examples include the enzymes called glutathione S-transferases (GST's) whose activity has found to be suppressed in patients with HNSCC *(Konig-Greger et al., 2004)*. Another detoxifying enzyme UDP-glucuronyl transferase 1A7 (UGT1A7) has been shown to be associated with an increased risk of HNSCC development if their activity is low *(Zheng et al., 2001)*.

Alteration of p53 leads to an inability to arrest the cell cycle and inhibit apoptosis. As a consequence, the TP53 mutations are less sensitive to radiation-induced cell death and several genetic mutations accumulate leading to increased tumour heterogeneity and resistance to conventional therapy *(Ganci et al., 2015; Perri et al., 2015)*. TP53 mutations also cause cellular senescence inhibition by reduction or radiation-induced reactive oxygen species, thereby increasing resistance to radiotherapy *(Skinner et al., 2011; Ganci et al., 2015)*. The cell cycle and mechanisms involved in resistance to irradiation shall be discussed in more detail in section 1.9.3.

1.6 Squamous Cell Carcinoma of the Upper Aero Digestive Tract (Classification)

The majority of malignancies (>90%) in the UADT are squamous cell carcinomas *(Grégoire et al., 2010)*. The histological spectrum ranges from normal to hyperplasia, dysplasia, carcinoma *in-situ* and finally invasive carcinoma.

Transformation from normal epithelium to hyperplastic epithelium involves a thickening of the epithelium. The three grades of dysplasia are mild, moderate and severe. In the mild form, changes consisting of cellular disruption, mitotic figures, nuclear pleomorphism and a raised nuclear/cytoplasmic ratio are limited to the lower third of the squamous epithelium. In the moderate form, it covers the lower two-thirds of the epithelium; and in the severe form, it extends through the full thickness of the squamous epithelium (figure 1.5).

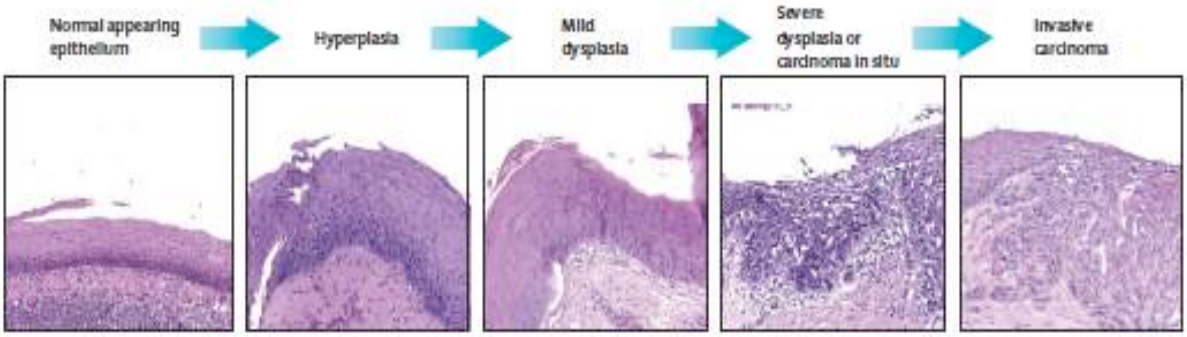

Figure 1-5 A modified diagram representing histological progression in head and neck carcinogenesis *(Califano et al., 1996; Argiris et al., 2008)*.

1.7 Head and Neck Cancer Staging

The objectives of head and neck cancer staging are to aid the clinician in treatment planning and to give an indication of the prognosis. It allows the extent of the disease to be assessed and can assist in evaluating the results of treatment.

The TNM system is used to describe the anatomical extent of the disease and has three components to it:

T – Extent of primary tumour
N – Absence or presence and extent of regional lymph node metastases
M - Absence or presence of distant metastases (table 1.5)

Table 1-5 Outline of the TNM system.

T – Primary Tumour	
Tx	Primary tumour can not be assessed
T0	No evidence of primary tumour
Tis	Carcinoma in situ
T1, T2, T3, T4	Increasing size and/or local extent of the primary tumour
N – Regional Lymph Nodes	
Nx	Regional lymph nodes cannot be assessed
N0	No evidence of regional lymph node metastases
N1, N2, N3	Increasing involvement of regional lymph nodes
M – Distant Metastasis	
M0	No distant metastasis
M1	Distant metastasis

All cases need histological confirmation. Pre-treatment clinical classification is termed cTNM and post surgical histopathological classification is pTNM.

The histological grading of squamous cell carcinoma performed by the examining histopathologist is an indication of the biological behaviour of the neoplasm (Table 1.6)

Table 1-6 Histopathological Grading.

GX	Grade of differentiation cannot be assessed
G1	Well differentiated
G2	Moderately differentiated
G3	Poorly differentiated
G4	Undifferentiated

After these classifications and grading, malignancies are assigned a stage grouping to show that each group is homogenous in respect of survival and that survival rates are distinctive for each cancer site.

1.8 Treatment of HNSCC

Radiotherapy and surgery are the two most frequently used modalities in the treatment of HNSCC. For advanced disease, a single modality treatment is associated with poorer outcomes hence the combined use of surgery and post-operative radiotherapy or the use of combined chemoradiotherapy offers the highest chance of achieving cure *(Paleri and Roland, 2016)*. Table 1.7 shows a summary of the treatment methods on offer in the UK for the different stages and subsites in HNSCC.

Table 1-7 A table showing a summary of the treatment methods on offer for the different stages and subsites in HNSCC studied in the current project.

	Site and stage	**Treatment**
Primary	Early Laryngeal and hypopharyngeal disease	Radiotherapy or transoral surgery
	Advanced laryngeal and hypopharyngeal disease	Chemoradiotherapy or radical surgery
	Oral Cavity & Maxillary sinus	Surgery (unless unfit for surgery) +/- postoperative radiotherapy
	Oropharynx	Transoral surgery (+/- radiotherapy) or radiotherapy or chemoradiotherapy
Lymph nodes	Node negative	Selective neck dissection of relevant levels if chance of micrometastases is 15-20% or elective radiotherapy
	Node positive	Comprehensive neck dissection (levels 1 – 5 (1a +/- 1b omitted if not oral cavity) with postoperative radiotherapy if adverse histological features present; or radiotherapy/chemoradiotherapy

1.9 Radiotherapy

1.9.1 Background

Radiation therapy or radiotherapy is an approach utilising ionising radiation to allow treatment of malignant disease. This all started after the German physicist, Wilhelm Röntgen discovered electromagnetic radiation in a wavelength range know as Röntgen rays or X-rays, in November 1895 *(Reisz, 1995)*. By 1896 X-rays were being used as a treatment modality; however there was no prior understanding of the beams' physical or biological characteristics *(Slater, 2012)*, nor was there any concept of accurate dosimetry, treatment planning and reduced ability to determine prognosis *(Webb and Evans, 2006)*. The driving force for improvements came from patients' needs for effective disease control and maintaining quality of life. Henri Coutard, a French Radiologist working at the Curie Institute (Paris) presented evidence that laryngeal cancer could be treated without disastrous side effects. By 1934 he developed a protracted fractionated process that remains the basis for cancer treatment today *(Coutard, 1934)*.

Radiation therapy has progressed through the eras of discovery, orthovoltage, megavoltage (which began with higher-energy linear accelerators for therapy in the 1950's) and intensity-modulated X-ray therapy (IMXT or IMRT) *(Slater, 2012)*. Radiation therapy can also be divided into external beam radiation therapy, brachytherapy and systemic radioisotope therapy, the differences of which are due to the position of the radiation source.

Currently, external beam radiation therapy is predominantly delivered in the way of linear accelerator X-rays or IMRT, for the treatment of head and neck SCC *(Paleri and Roland, 2016)*.

1.9.2 Radiation Physics

Radiation therapy uses ionising radiation in the treatment of malignancies. This can be electromagnetic (X-rays) or particulate (electrons) radiation. In the clinical setting, X-rays are produced by a linear accelerator (linac) (figure 1.6), which uses a device called a magnetron. It is an electron tube that provides high radio-frequency electromagnetic waves to accelerate electrons to relativistic speeds inside a structure called a waveguide. The electrons collide with a tungsten target and the majority of the electrons' energy becomes heat.

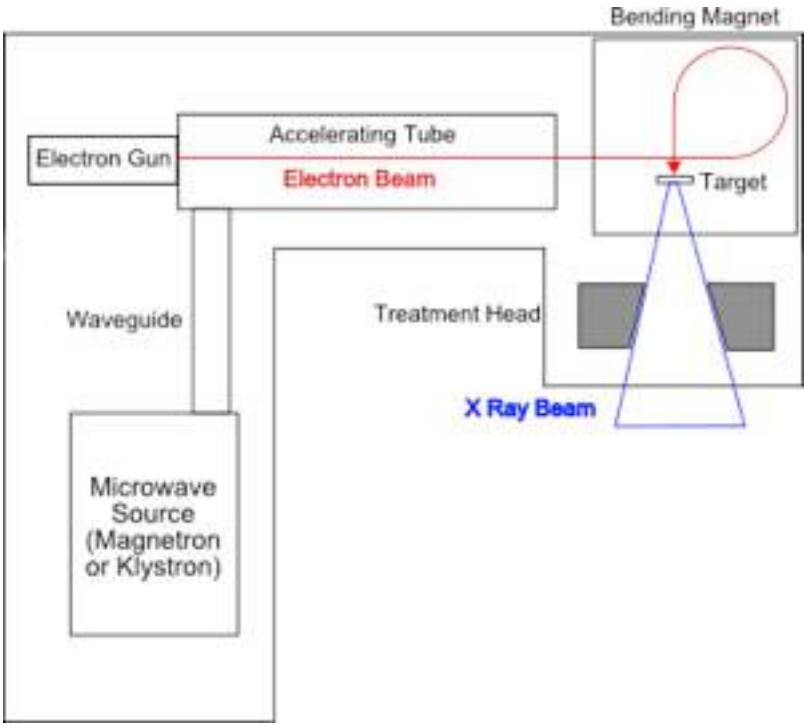

Figure 1.6 A diagram showing a medical linear accelerator used in radiation therapy *(www.peninsulacancercenter.com)*.

The remaining fraction results in two types of X-rays named Bremsstrahlung and characteristic X-rays. Bremsstrahlung X-rays are produced by the sudden deceleration of electrons due to Coulomb interactions with nuclei in the tungsten target; whereas characteristic X-rays result from Coulomb interactions between incident electrons and atomic orbital electrons of the target material *(Podgoršak, 2005)*. Bremsstrahlung X-rays are used in radiotherapy.

X rays produced by electrons with kinetic energies between 10 kilo electronvolts (keV) and 100 keV are called superficial X rays, those with electron kinetic energies between 100 keV and 500 keV are called orthovoltage X rays, while those with electron kinetic energies above 1 mega electronvolts (MeV) are called megavoltage X rays *(Podgoršak, 2005)*. In radiotherapy treatment of HNSCC, megavoltage X-rays with a nominal energy of 6 megavolts are utilised *(Beyzadeoglu, 2010)*. The same energy value was used in this study.

Radiation therapy damages dividing cells by destroying the genetic material that controls how cells grow and divide. The goal of radiation therapy is to destroy the cancerous cells and as few normal, healthy cells as possible. In the following section, the effects of irradiation on the cell cycle shall be discussed.

1.9.3 Radiobiology

Cell cycle

The basic function of the cell cycle is to duplicate the amount of DNA and pass them into two genetically identical daughter cells. The cell exhibits a longer phase in which no division occurs (interphase) and a shorter phase (mitosis) in which division occurs. The most radiosensitive stages during the cell cycle are the early G2 and M stages; whereas radioresistance is high in the S, late G1 and G0 phases. The resistance of the S phase is due to the large amounts of synthesis enzymes present, which have the ability to rapidly repair DNA *(Beyzadeoglu, 2010)*.

Interphase is the preparatory phase prior to entering cell division. It is divided into G_1 (Gap_1), S (Synthesis) and G_2 (Gap_2) phases. The gap_1 phase is the longest phase during which dividable cell growth occurs. In the synthesis phase, DNA replication takes place and at its completion the chromosomes have been replicated. The gap_2 phase ensures the cell grows and that the contents are ready for the mitosis phase. The G_0 phase is a resting phase where cells transiently stop their cellular activities.

The mitotic (M) phase consists of mitosis (nuclear division) and cytokinesis. This produces two identical daughter cells during prophase, prometaphase, metaphase, anaphase and telophase (figure 1.7).

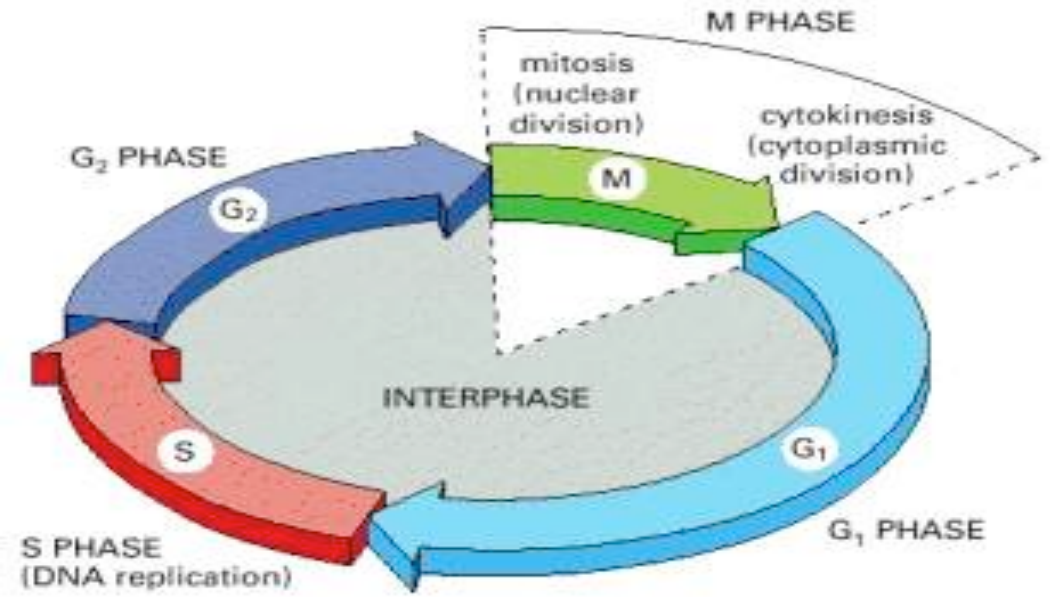

Figure 1.7 A diagram showing the phases of the cell cycle *(Alberts, 2002)*.

Cancer cells

Carcinogenesis can simply be defined as the origin of cancer, where normal cells are changed into cancer cells. The fundamental concept and the molecular basis for tumour development have been explained above (section 1.5). Ultimately there is an imbalance between the excessively proliferating cancer cells, normal cell loss and a deficiency in recognizing and destroying the cancer cells. Cancer cells have unique features in that most can originate from just one abnormal cell, they can undergo an unlimited number of divisions (immortality), genetically they are unstable and they have the ability to metastasize *(Bignold 2006; Beyzadeoglu, 2010).*

Genetic instability is due to defects in the DNA repair process and DNA mismatch recognition, resulting in tumour heterogeneity. Cancer cells form clones that with time respond less to the proliferation control mechanism but can also metastasize.

1.9.4 Effects of Radiation

Damage to mammalian cells via radiation can be classified into three categories. The first is lethal damage, which is irreversible, irreparable and results in cell death. This is observed in high LET (linear energy transfer) radiation. The second is sub lethal damage, which can be repaired in hours unless additional sub lethal damage is added and eventually leads to lethal damage (and hence cell death). This is observed in low LET radiation. Repair of sublethal damage is evident between dose rates of 0.01 – 1 Gy/minute. The third category is potentially lethal damage, which can be manipulated by repair when cells are allowed to remain in a non-dividing state. Cell survival is greater for a delivered radiation dose if the dose rate is decreased. This effect is important in brachytherapy applications and the dose rate in external therapy is 100 cGy/minute *(Podgoršak, 2005; Beyzadeoglu, 2010)*.

Radiation can have direct and indirect effects at a molecular level. In the direct method, ionization of the atoms in the DNA molecules occurs; and can result in a single DNA strand break (which can be repaired by the cell) or a double strand break (which can result in cell death). If cell DNA is damaged by radiation, the cell cycle is stopped by p53 and the DNA is repaired (this shall be discussed in further detail later). Thereafter, the cell re-enters the cell cycle and continues with proliferation. If at higher radiation doses however the damage to the DNA caused cannot be repaired, the cell will undergo apoptosis *(Beyzadeoglu, 2010; Desouky et al., 2015)*.

Most of the damage at the molecular level is caused by the indirect method. Radiation interacts with water molecules, resulting in the formation of free radicals, which in turn reacts with DNA and results in molecular damage via the breakage of chemical bonds. These changes result in biological effects *(Podgoršak, 2005)***.** As part of this reaction, hydrogen peroxide is formed. This oxidises the surrounding tissues and prevents the nutrition of neighbouring cells *(Hall, 2000)*.

Target theory and the linear quadratic model

Target theory is an essential concept in radiation biology. The fundamental principle is that inactivation of the target inside an organism by radiation results in the organism's death. The target considered is a unit of biological function e.g. DNA *(Nomiya, 2013)*. Whatever the radiation dose received by the tissue, there is always a chance of 'hitting' DNA or cells and producing harmful effects. This is known as the 'stochastic effect'. The target theory is based on the principles of probability of survival. This includes the 'single target single hit' and 'multiple target single hit' mechanisms. In the former, one hit on one target is sufficient to inactivate the target. In the latter, there is more than one target per cell and one hit of any of these targets is sufficient for cell death *(Beyzadeoglu, 2010)*.

A cell survival curve describes the relationship between the radiation dose and the fraction of cells that can survive once the dose has been absorbed. The linear quadratic equation is used to describe the cell survival curve; and it models the number of cells killed following exposure to a varying amount of radiation.

$$S(D)=e^{-(\alpha D+\beta D^2)}$$

Figure 1.8 The linear quadratic equation.

S(D) is the fraction of cells surviving a dose D. α is a constant describing the initial slope of the cell survival curve and corresponds to the cells that can not repair themselves after one radiation hit. Apoptosis and mitotic death are dominant here. β is a smaller constant describing the quadratic component of cell killing and corresponds to cells that stop dividing after more than one radiation hit (but can repair the damage caused by radiation). Mitotic death is dominant here (figure 1.9).

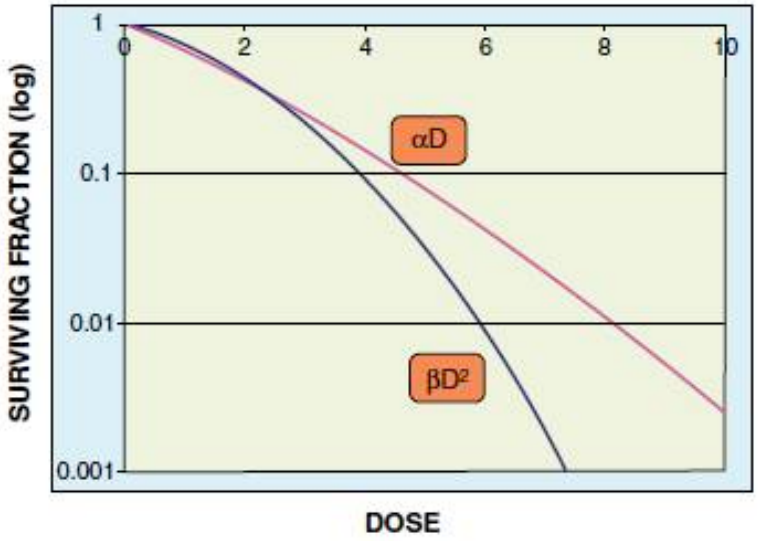

Figure 1.9 A diagram showing the relationship between dose and surviving fraction in the linear quadratic model (αD is the product of the linear coefficient (α) and the fraction of cells surviving a dose (D). βD^2 is the product of the quadratic coefficient (β) and the square of the fraction of cells surviving a dose (D^2) *(Beyzadeoglu, 2010)*.

The α/ β ratio gives the dose at which the linear and quadratic components of cell killing are equal (the number of acutely responding cell deaths is equal to the number of late-responding cell deaths). For early effects (tissues that respond early to irradiation and are radiosensitive), the α/ β ratio is large and α dominates at low doses. These die linearly. Whereas for late effects, (tissues that respond late to radiation and are radioresistant) α/ β is small and β has an influence even at low doses *(Podgoršak, 2005)* (figure 1.10).

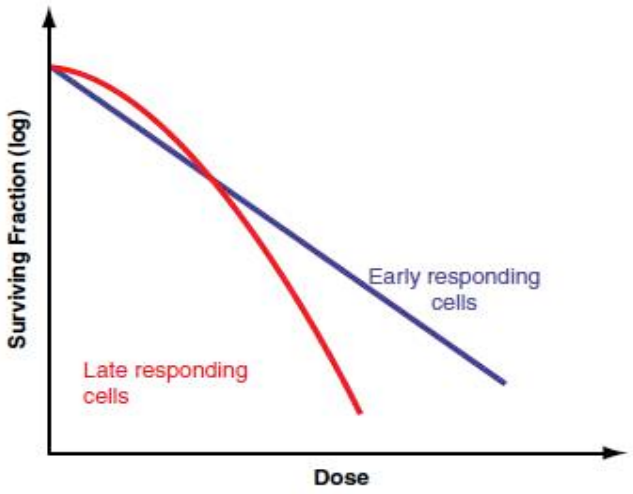

Figure 1.10 A diagram showing the relationship between surviving fraction and radiosensitivity *(Beyzadeoglu, 2010)*.

The α/ β ratio may be as high as 20Gy in the case of advanced head and neck cancer, which is an early responding tissue with an extremely aggressive rate of cell proliferation. Signs of radiation-induced damage can be seen days to weeks after exposure. This can be explained by the short lifespan of their cells *(O'Rourke, 2009)*.

Time – dose fractionation

Fractionated radiotherapy is the delivery of a radiation dose divided and given over a number of treatments. Fractionation was introduced not because of the understanding of radiobiology; but it was due to the technological limitations of the early machines in use *(Williams, 2006)*. Coutard applied fractionated radiotherapy to head and neck cancers; and the subsites treated included the palatonsillar region, larynx, pharynx and the maxillary sinus. Treatment was considered successful if five-year survival was attained. The results achieved were 32%, 24%, 11% and 50%. He noted that skin and mucosal reactions seen during radiotherapy of the pharyngeal and laryngeal cancers depended on the dose and duration of radiotherapy *(Coutard, 1937)*.

1.9.5 The major factors in radiobiology

Clinical practice in radiotherapy is based on the five R's of radiobiology, which are repair, repopulation, redistribution, reoxygenation and radiosensitivity *(Williams et al., 2006)*. However, 3 major biological factors have been defined that determine the response of solid tumours to fractionated radiotherapy. These are intrinsic radiosensitivity of tumour cells, tumour hypoxia and repopulation of tumour cells during gaps in treatment. More recently, other factors have been implicated, including various signal transduction pathways, HPV status, cancer-initiating stem cells and epithelial mesenchymal transition *(Begg, 2012)*. These will be discussed later.

Repopulation

Proliferation of surviving cells in both tumours and normal tissues will occur during the course of fractionated treatment. Repopulation is when there is an increased rate of cell proliferation, which occurs in response to cellular damage and cell death during the course of treatment *(*Podgoršak, 2005*)*. It is the time required for the tumour cell number to double and is also known as the tumour doubling time. It is slow at the beginning of radiotherapy but speeds up after the first doses of irradiation. This increase in repopulation rate is termed accelerated repopulation and is an important concept as it allows for normal tissues to repopulate so the acute side effects of irradiation can be repaired *(Beyzadeoglu, 2010)*.

During a conventional course of radiotherapy, it is an important factor influencing tumour control in patients with HNSCC. Local control is reduced by 0.5% for every day treatment time is prolonged. Repopulation provides the biological basis for accelerated radiotherapy *(*Podgoršak, 2007*)*; and a Cochrane review in 2010 supports altered fractionation radiotherapy over conventional radiotherapy for HNSCC *(Baujat et al., 2010)*. The Cochrane review showed a statistically significant reduction in total mortality (hazard ratio (HR) 0.86, 95% confidence interval (CI) 0.76 to 0.98). In addition, a statistically significant difference in favour of the altered fractionation was shown for the outcome of locoregional control (HR 0.79, 95% CI 0.70 to 0.89). No statistically significant difference was shown for disease free survival.

This is likely due to the rapid repopulating capacity of HNSCC cells during gaps in treatment; and shortening the overall time reduces the opportunity for such repopulation, allowing increased cell kill for a given radiation dose *(Begg, 2012)*.

Studies have been undertaken utilising markers to predict the tumour repopulation rate, so patients with slowly repopulating tumours can be spared the extra toxicity associated with accelerated fractionation regimen. Ki-67 is a monocloncal antibody that binds to a protein that is expressed during the G1, S and G2 phases of the cell

cycle (Lothaire et al., 2006). It has been used as a marker of tumours with more advanced TNM stage disease *(Fumic-Dunkic et al., 2003)*.

Three studies *(Kropveld et al., 1998; Raybaud et al., 2000 and Couture et al., 2002)* utilized Ki-67 as a marker of repopulation. The largest study comprised 304 patients *(Couture et al., 2002)*; and they found that low Ki-67 expression was a bad prognostic indicator. One explanation is that slowly proliferating tumours before treatment may have the capacity for rapid repopulation during treatment. This hypothesis is supported by 2 studies *(Eriksen et al., 2005; Bentzen et al., 2005)* of accelerated fractionation. This showed patients with high epidermal growth factor receptor (EGFR) expressing tumours and more differentiated tumours benefitted from accelerated fractionation regimens. The theory is that these tissues act in a similar manner to normal epithelial tissues and respond to damage by accelerated repopulation *(Begg, 2012)*. Bentzen et al. *(2005)* however demonstrated that there was no significant association with Ki-67 index or Ki-67 pattern. Eriksen et al. *(2005)* had not utilised Ki-67 in their study.

Repair

The three types of damage that ionizing radiation can cause to cells are lethal, sublethal and potentially lethal. Lethal damage is fatal whereas sublethal damage can be repaired before the next fraction of radiation is delivered. Potentially lethal damage can be repaired under certain circumstances, usually when the cell is paused in the cell cycle. The amount of damage repaired depends on the ability of the cell to recognize the damage and activate the repair pathways and cell cycle arrest. Normal tissue cells with intact repair pathways can repair the sublethal damage prior to the next fraction, compared with tumour tissue cells *(McMillan, 2002)*.

Redistribution

Redistribution is where given time, tumour cells in the resistant phase of a cycle may progress into the sensitive phase at the next fraction and hence the probability of exposure to radiation during a sensitive phase increases. This probability will increase over the course of the treatment and the benefit of radiation shall increase *(Beyzadeoglu, 2010)*.

Reoxygenation

Reoxygenation is the process by which cells that are hypoxic during irradiation become oxygenated afterwards. Hypoxic cells are more resistant to radiation; but given time, the vascularity of the tumour tissue and oxygenation improves and their radiosensitivities increase (figure 1.11) *(Podgoršak, 2005, Beyzadeoglu, 2010)*

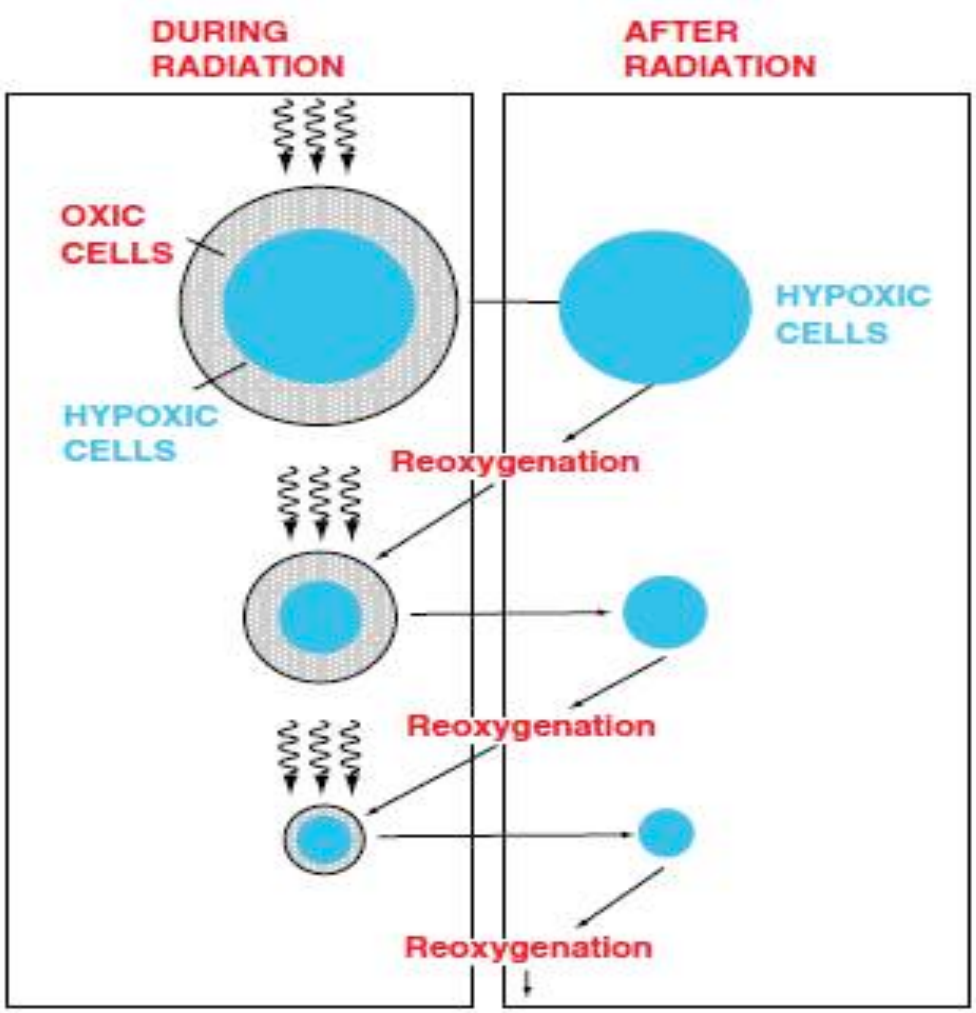

Figure 1.11 A diagram showing what happens to hypoxic cells during radiation and reoxygenation *(Beyzadeoglu, 2010)*.

Radiosensitivity

Radiosensitivity (intrinsic radiosensitivity) is the relative susceptibility of cells, tissues, organs or organisms to the harmful effect of ionizing radiation. Evidence to support the significance of intrinsic radiosensitivity in head and neck cancer was shown by Bjork-Eriksson et al. *(2000)* when cell suspensions from head and neck tumour biopsies were assayed for radiosensitivity in vitro using clonogenic assays. Their study showed that tumour radiosensitivity measured as SF_2 (surviving cell fraction after a dose of 2Gy) was a significant prognostic factor for local control of HNSCC

and that intrinsic radiosensitivity is a significant factor in determining the outcome in HNSCC treatment. There is also evidence that certain genes can act as potential markers in radiation-induced DNA damage response and hence determine the tumour's intrinsic radiosensitivity e.g. KU70 protein, X-ray repair cross complementing 5 protein (XRCC5), DNA protein kinase (DNA-PK), ataxia telangiectasia mutation (ATM), RAD51 and XRCC3 proteins *(Silva et al. 2007)*.

Tumour hypoxia

Studies have shown that hypoxia is a negative prognostic indicator in the treatment of HNSCC, utilizing radiotherapy, surgery and chemotherapy *(Höckel et al., 1993, Vaupel et al., 2001)*. Radiosensitisers such as oxygen and nitroimidazoles can increase the damaging effects of radiation. Hypoxia is associated with radioresistance *(Overgaard J, 2011)* and there are various mechanisms that can account for this in the tumour microenvironment. Ionising radiation produces DNA radicals with the help of oxygen; and DNA damage if unrepaired can undergo cell death. In the hypoxic environment, DNA damage is reduced *(Barker et al., 2015)*. Radiotherapy leads to tumour reoxygenation, an increase in reactive oxygen species and hypoxia inducible factor 1α (HIF- 1α). The latter is stabilized under hypoxic conditions leading to up regulation of genes promoting cell survival *(Semenza GL, 2004)*. Vascular endothelial growth factor A is increased in the presence of hypoxia that leads to abnormal vessel formation, which in turn contributes to hypoxia *(Barker et al., 2015)*.

Studies using oxygen electrodes in patients with HNSCC, have shown a worse outcome after radiotherapy *(Brizel et al., 1997, Nordsmark et al., 2005)*. Brizel et al. showed the disease free survival was 78% for patients with a median tumour of pO_2 > 10mmHg but only 22% for patients with a median tumour of pO_2 < 10mmHg. Nordsmark et al showed the 5-year survival for patients with pO_2 < 2.5mmHg ranged from 0% to 20%. Hypoxia acts as a trigger for changes in gene expression to stimulate angiogenesis, glucose transport, pH regulation and erythropoiesis *(Semenza, 2003)*. Toustrup et al. *(2011)* developed a 15-gene hypoxia gene

expression classifier with prognostic impact as well as predictive impact for the hypoxia modifying therapy with nitroimidazole in conjunction with radiotherapy. It was capable of predicting which tumours would and would not benefit from the addition of hypoxic modification. Harris et al. *(2015)* performed a systematic review of gene expression signatures as biomarkers of tumour hypoxia. They concluded that there is no current gold standard to derive hypoxia signatures and tumours from different tissues are too variable in their hypoxia responses for such generalisation *(Harris et al., 2015)*.

Signal transduction pathway

Pathways that have been shown to affect radiosensitivity include the phosphatidylinositol 3 kinase/protein kinase B (PI3K/AKT), nuclear factors of kappa light polypeptide gene enhancer in B-cells 1 (NKB1), mitogen activated protein kinases (MAPK) and transforming growth factor beta (TGF ß) pathways *(Begg et al., 2011)*. In particular, the PI3K/AKT pathway has been associated with radioresistance; and its inhibition can radiosensitize cells *(Kim et al., 2005)*. The AKT activation in HNSCC has also been shown to have a worse outcome post radiotherapy *(Gupta et al., 2002)*. EGFR has a high expression in HNSCC and correlates with a poor response to treatment *(Ang et al., 2002; Chung et al., 2006)*. Hence this has lead to the use of EGFR inhibitors such as cetuximab (a monocloncal antibody drug) in combination with radiotherapy and has resulted in improved locoregional control and a reduction in mortality. Bonner et al. *(2006)* demonstrated in their study the median duration of locoregional control was 24.4 months among patients receiving combined therapy, versus 14.9 months in those receiving radiotherapy alone (hazard ratio for locoregional progression or death was 0.68; $p = 0.005$) *(Bonner et al., 2006; Begg, 2012)*.

Human papilloma virus (HPV) status

It has become evident that HPV positive patients with HNSCC, especially those with oropharyngeal tumours, have a better outcome *(Leemans et al., 2011)* and includes those patients treated with radiotherapy *(Lassen et al., 2009; Ang et al., 2010)*. Testing for p16 has shown to be sensitive for predicting HPV status, however gene expression signatures have been developed such that a high expression of genes associated with HPV positivity predicts a better outcome in HNSCC *(Slebos et al., 2006; Lohavanichbutr et al., 2009; de Jong et al., 2010)*. It has been suggested that patients who are HPV positive have less hypoxia and hence respond better to radiotherapy *(Lassen et al., 2010; Brockton et al., 2011)*.

There are however numerous accounts for the mechanism of HPV mediated response to radiotherapy. One explanation is that HPV infection via E6 and E7 subsequently leads to p53 and retinoblastoma proteins' degradation. In turn, there is compromise with DNA repair, repopulation signaling and cell cycle redistribution, which increase the radiosensitivity of the HPV positive tumour (*Dok et al., 2014, Chen et al., 2017*). Huang et al. (*2015*) showed that pretreatment high circulating neutrophil and monocyte counts independently predicted inferior outcome survival and recurrence free survival; whereas a high circulating lymphocyte count predicted better recurrence free survival and marginally better outcome survival in HPV positive OPSCC patients. This suggests that the adaptive immune system contributes to the suppression of tumour progression (*Chen et al., 2017)*.

Radiotherapy is a key modality in the treatment of head and neck cancer. It traditionally offered higher rates of organ preservation; and for some cancers where function is important, it is the treatment of choice (*Paleri and Roland (ed), 2016*). However, when radiotherapy fails or the patient has a recurrence, salvage surgery is an option for further management. It is unfortunately associated with high complication rates, morbidity (*Paleri and Roland (ed), 2016*) and mortality. The Radiation Therapy Oncology Group (RTOG) 91-11 study reported a complication rate of 59%, 19% of which were classified as major complications (*Weber et al.,*

2003). Those who had a salvage laryngectomy post chemoradiotherapy experienced a fistula rate of 30% but only 15% if they had been treated with radiotherapy. Zafereo et al. (*2009*) showed a complication rate of 48% for patients having salvage surgery for OPSCC. Their series also showed considerable functional deficits, with reports on return to oral intake varying from 44% to 68%. A meta-analysis (*Paydarfar and Birkmeyer, 2006*) revealed that performing a neck dissection was a significant risk factor for pharyngocutaneous fistula after laryngectomy, in the salvage setting.

There is a difference between radioresistance and failure of loco-regional control with the modality of radiotherapy. There are molecular mechanisms that underlie the resistance to radiotherapy to cellular proliferation, apoptosis, DNA repair and angiogenesis. These are hypoxia, alterations in the EGFR – PI3K/Akt pathway, the epithelial mesenchymal transition process, deregulation in p53 signaling cascades, alterations in expression of angiogenic factors and the presence of cancer stem cells in tumour tissue (*Ganci et al., 2015; Perri et al., 2015*).

Locoregional failure includes patients who seemingly initially respond to radiotherapy clinically and radiologically but proceed to develop proven recurrences 1 to 2 years later. It is the most common cause of death in patients with HNSCC (*Lambrecht et al., 2009*). Recurrence may arise from residual neoplastic cells that survive treatment or from underlying field cancerisation. The latter is explained by preneoplastic processes at multiple sites in the mucosa (*Ganci et al., 2015)*. When analysed at a histological level no tumour is present; however at a molecular level, genetic alterations are present (*Braakhuis et al., 2003; Ha and Califano, 2003*).

Epithelial mesenchymal transition

Tumour cells' invasive and metastatic behaviour can be influenced by a change in their morphology from an epithelial to a mesenchymal phenotype. Gene signatures containing EMT genes have been found to be associated with response to radiation of HNSCC. Whether it is useful in determining outcome and as a predictor isn't clear at this stage *(Begg, 2012)*.

Tumour heterogeneity and cancer-initiating stem cells

Tumour heterogeneity describes how different tumour cells can show distinct morphological and physiological profiles *(Maruysk and Polyak, 2010)* and occurs between tumours (inter-tumour heterogeneity) and within tumours (intra-tumour heterogeneity). This has been observed in the field of HNSCC *(Califano et al., 1996)*. Two models exist to explain the heterogeneity of tumour cells, which are the cancer stem cell theory and the clonal evolution model.

According to the cancer stem cell concept, only a minor fraction of tumour cells, termed 'tumour stem cells' is responsible for the maintenance and progression of tumours because they can self-renew and differentiate into the majority of 'nonstem' cells. Only some tumour cells will be capable of limited proliferation *(Maruysk and Polyak, 2010)*. Phenotypic plasticity is the ability of an organism to change its phenotype in response to its environment. With this concept, the majority of tumor cells can be viewed as stem cells with varying degrees of 'stemness', where the 'stemness' is influenced by micro environmental cues and perhaps some stochastic cell autonomous mechanisms *(Hill, 2006)*. Interactions of tumour cells with the microenvironment both shape malignant behavior and promote tumor progression *(Park et al., 2000)*. The microenvironment within a tumor is not completely homogeneous. Different regions of a tumor can have different densities of blood and lymphatic vasculature, numbers and types of infiltrating normal cells and the composition of the extracellular matrix can differ as well *(Maruysk and Polyak, 2010)*.

The clonal evolution was first proposed in 1976 *(Nowell, 1976)*. Tumours arise from a single mutated cell; and as they accumulate, so do additional mutations and increased genomic instability, ultimately being 'tested' by Darwinian selection. As its progression is influenced by the tumour microenvironment, it is stated that tumour evolution is likely to be non-linear *(Maruysk and Polyak, 2010)*. Clonal heterogeneity has been documented for head and neck malignancies *(Califano et al., 1996)*.

Intra-tumour heterogeneity has been hypothesized to lead to a worse clinical outcome. One particularly important type of intra-tumor heterogeneity arises from differences among cancer cells that are inherited during cell division, which we refer to as genetic heterogeneity. Differences can result from unrepaired copy-number aberrations (CNAs) (amplification or loss of chromosomes, chromosome arms, or large genome segments) or smaller somatic mutations (single-nucleotide variants or short genomic insertions or deletions) that are passed on to a cell' s lineage during tumor development *(Ciriello et al., 2013)*.

It is thought that tumours with a higher fraction of stem cells are more difficult to treat with radiotherapy. This is not due to radioresistance but if there is a greater tumour volume, then there will be a greater stem cell fraction meaning there are more tumour cells to kill. The concept of stem cells has meant assays to monitor stem cell number would help in predicting outcome post radiotherapy *(Begg, 2012)*. In one study, early stage laryngeal cancer treated with radiotherapy, expression of the stem cell marker CD44 predicted local control using both microarray technology to monitor mRNA expression and immunohistochemistry in another series to monitor protein expression *(de Jong, 2010)*. Therefore, a high stem cell count appeared to be a factor in determining treatment outcome post radiotherapy in HNSCC.

1.10 Mechanisms of radiation-induced cell death

Clarke *(1990)* stated there are 3 types of cell death. Apoptosis *(Kerr et al., 1972)*, also termed type I cell death, is defined by characteristic changes in the nuclear morphology, including chromatin condensation and fragmentation, overall cell shrinkage, blebbing of the plasma membrane and formation of apoptotic bodies that contain nuclear or cytoplasmic material *(Schweichel and Merkel, 1973)*. Autophagic cell death, also known as type II cell death, is characterized by a massive accumulation of double-membrane containing vacuoles known as autophagosomes, which subsequently fuse with lysosome vacuoles. Type III cell death, better known as necrosis, is often defined in a negative manner as death lacking the characteristics of the type I and type II processes *(Clarke, 1990)*. Necrosis is morphologically defined by cytoplasmic swelling, dilation of organelles, which causes

cellular vacuolation, and rupture of the plasma membrane, resulting in the proinflammatory leakage of the intracellular content *(Rode, 2008)*.

The Nomenclature Committee on Cell Death (NCCD) has in keeping with the latest developments in cell death research, have proposed a novel systematic classification of cell death based on biochemical features. The terms include: anoikis, autophagic cell death, caspase-dependent and caspase-independent intrinsic apoptoses, cornification, entosis, extrinsic apoptoses by death receptors and dependence receptors, mitotic catastrophe, necroptosis, netosis, parthanatos and pyroptosis *(Galluzzi et al., 2012)*.

Radiation induced cell death occurs via apoptosis, mitotic catastrophe, senescence *(Eriksson and Stigbrand, 2010)* and necroptosis *(Orth et al., 2014)* (figure 1.12). Apoptosis plays a modest role in the treatment response of most solid tumours; however if irradiation doesn't induce apoptosis, other mechanisms are in place such as mitotic catastrophe and radiation-induced senescence. The latter two are involved in the response of HNSCC to radiotherapy. In contrast to early apoptosis, p53 inactivation seems to promote rather than repress the induction of mitotic catastrophe *(Ianzini et al., 2006)*.

P53 is a transcription factor with control of target genes that influence cell cycle arrest, DNA repair, apoptosis, and senescence. Following irradiation, activation of p53 promotes cell survival by growth arrest and DNA damage repair. However, depending on the extent of damaged DNA and cell type, p53 can also activate elimination routes for damaged cells by apoptosis or senescence *(Helton and Chen, 2007)*. The amount of activated p53, its duration of activation, the availability of p53 co-factors and different sets of p53-responsive genes will dictate the final outcome *(Das et al., 2007; Tanaka et al., 2007)*. There are some cells having been exposed to genotoxic damage, will have impaired activation of p53-dependent DNA damage checkpoints and can ultimately facilitate the development of cancer *(Storchova and Pellman, 2004; Erenpreisa and Cragg, 2007; Ganem and Pellman, 2007; Ganem et al., 2007)*.

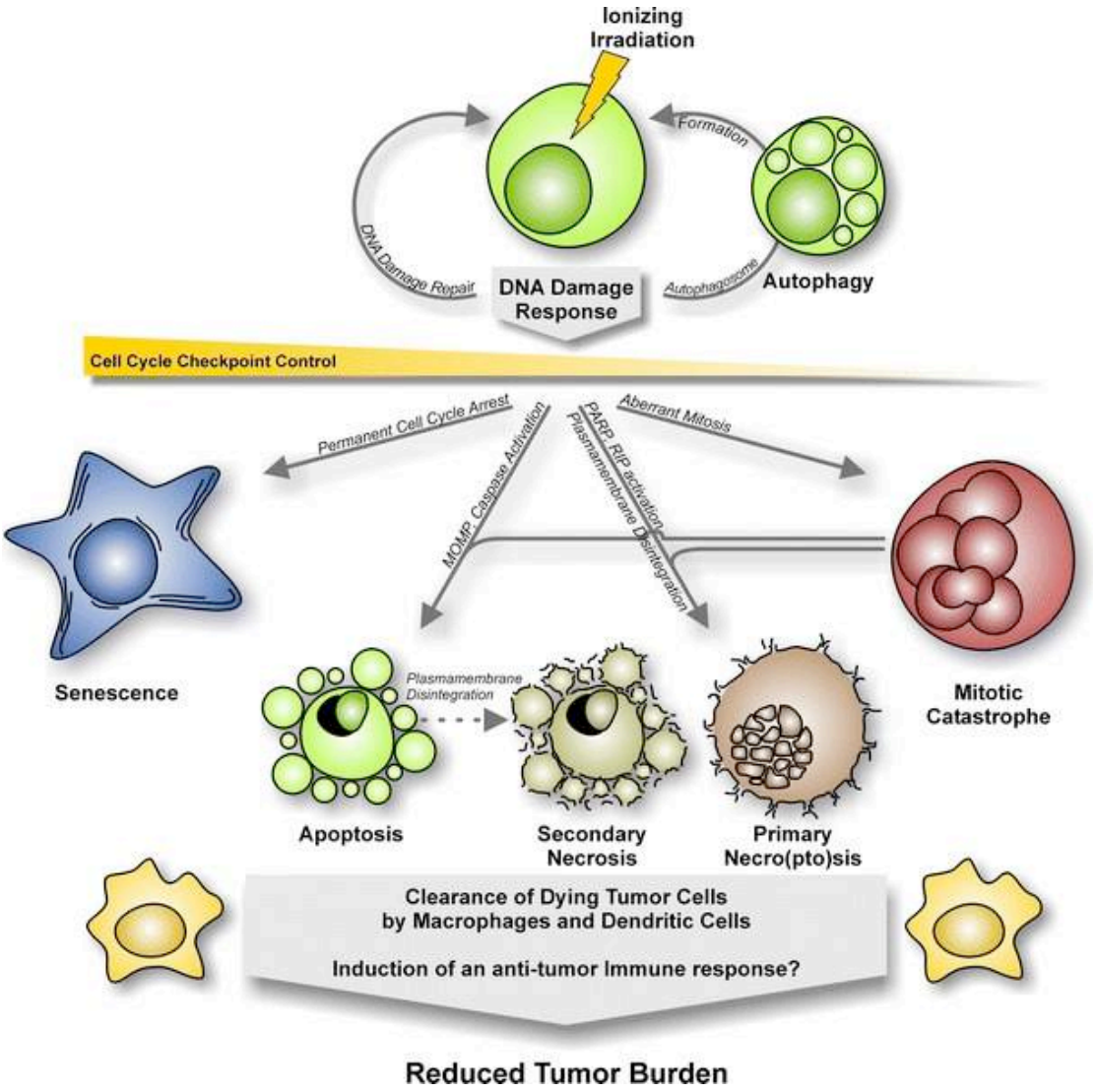

Figure 1.12 A diagram representing mechanisms of cell death by ionizing radiation *(Orth et al., 2014)*.

1.10.1 Radiation-induced apoptosis

In response to irradiation, apoptosis is predominantly observed in cells of the haematopoietic system *(Orth et al., 2014)*; but also in HNSCC in which it plays a modest role *(Eriksson and Stigbrand, 2010)*. This is due to most tumours including HNSCC losing their pro-apoptotic mechanism during progression; and p53 is impaired in more than half of all human malignancies *(Soussi and Beroud, 2001; Soussi and Lozano, 2005)*. Even though tumours can retain a functional p53

pathway, resistance to apoptosis can be acquired through enhanced expression of anti-apoptotic proteins such as Bcl-2 and survivin or inactivation of pro-apoptotic genes like Bax and apoptotic protease activating factor 1 (Apaf 1) *(Igney and Krammer, 2002)*.

Radiation-induced apoptosis can activate the intrinsic and extrinsic pathways.

The intrinsic pathway, also called the mitochondrial pathway, involves mitochondrial outer membrane permeabilization (MOMP) that disrupts the mitochondrial function. MOMP is mainly controlled and mediated by members of the Bcl-2 family. This family is divided into pro-apoptotic members and anti-apoptotic members. The pro-apoptotic members comprise two subfamilies, the Bax-like family (Bax, Bak, Bok) and the BH3-only proteins (Bid, Bad, Bim, Bik, Bmf, Noxa, Puma, Hrk), which both seem to be required to promote induction of apoptosis by formation of Bax–Bak pores in the mitochondrial outer membrane *(Jin and El-Diery, 2005)*. Following exposure to radiation, p53 activates transcription of pro-apoptotic genes, the most important being pro-apoptotic members of the Bcl-2 family. Bax *(Zhan et al., 1994; Findley et al., 1997; Kobayashi et al., 1998; Alvarez et al., 2006)* as well as members of the BH3-only subgroup appear to play a critical initiating role in radiation-induced apoptosis.

The anti-apoptotic members (Bcl-2, Bcl-XL, Bcl-W, Mcl1, Bcl2A1, Bcl-B) conversely block apoptosis. P53 can mediate transcriptional repression of anti-apoptotic genes including the Bcl-2 gene *(Haldar et al, 1994; Miyashita et al., 1994)* and the inhibitor of apoptosis protein-family member survivin *(Hoffman et al., 2002)*.

MOMP releases several potentially lethal proteins from the intermembrane space into the cytoplasm, the most important of which is cytochrome c. This binds and activates APAF1 and changes its conformation to allow binding of ATP/dATP *(Jiang and Wang, 2000; Wang, 2001)*. This formation is referred to as the apoptosome, and it will mediate the activation of caspase-9 *(Rodriguez and Lazebnik, 1999)*. Caspase-9, as an initiator caspase, subsequently cleaves and activates effector caspases,

which in turn cleave cell death substrates that collectively produce the phenotypic changes in the cell characteristic of apoptotic cell death *(Eriksson and Stigbrand, 2010)* (figure 1.13).

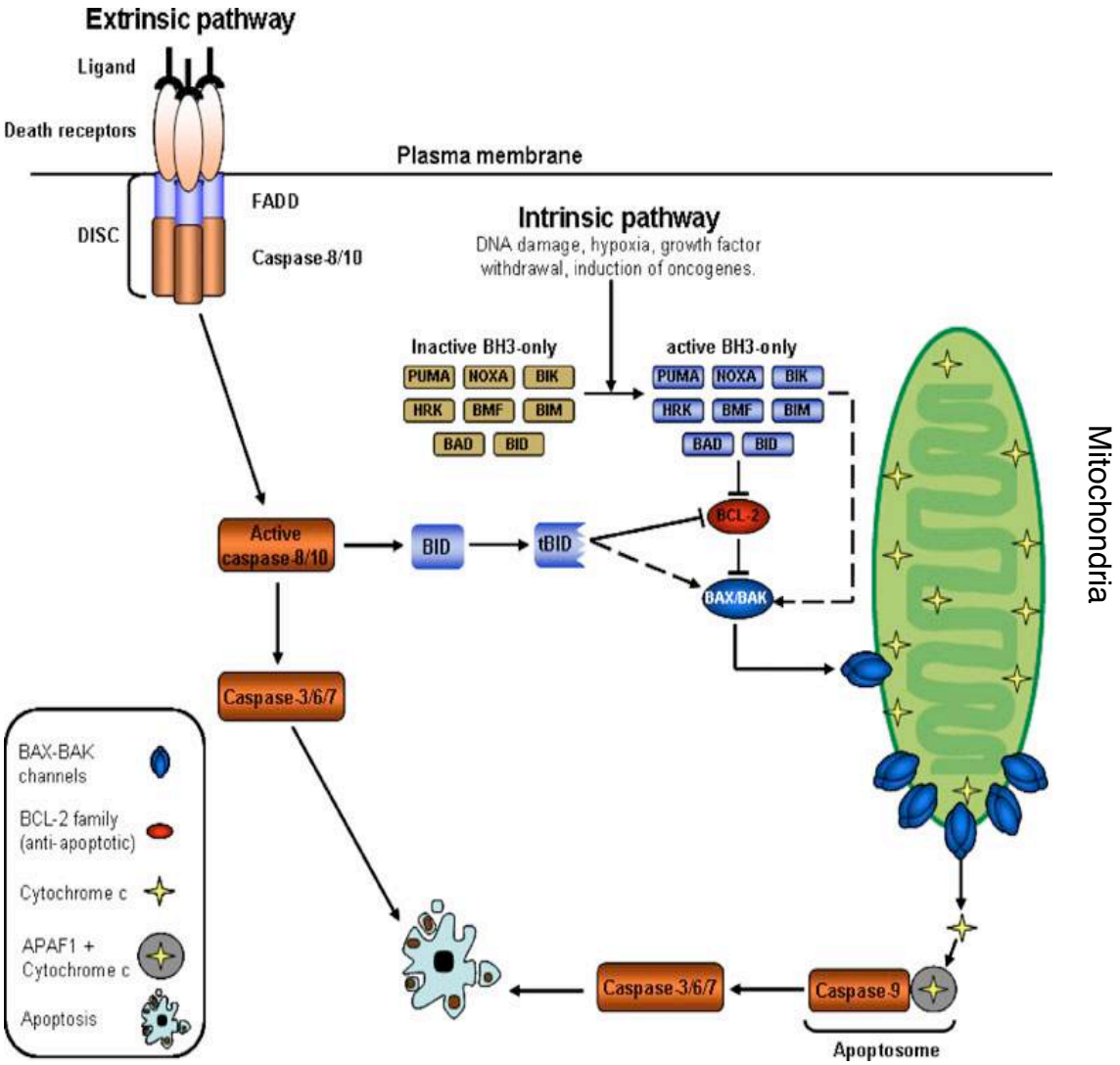

Figure 1.13 A diagram representing mechanisms of the extrinsic and intrinsic apoptosis signaling pathways *(Eriksson and Stigbrand, 2010)*.

The extrinsic pathway is often referred to as the death receptor pathway and requires ligand-dependent activation of plasma-membrane receptors from the TNF receptor superfamily. The expression of TNF death receptor family members (Fas/CD95 *(Sheard et al., 1997; Kobayashi et al., 1998; Embree-Ku et al., 2002; Sheard et al., 2003)*, DR5/TRAIL receptor 2 *(Wu et al., 1997; Sheikh et al., 1998; Burns et al., 2001; Alvarez et al., 2006)* can be upregulated by radiation and activate caspases by mitochondria-dependent and independent mechanisms *(Kastan et al., 1997; Scaffidi*

et al., 1998).

Interaction between specific ligands and the death receptors induces receptor-proximal recruitment of the death-inducing signaling complex. The resulting activation of caspase-8/10 leads to cleavage and activation of effector caspase-3, caspase-6, caspase-7, which subsequently cleave cell death substrates *(Taylor et al., 2007)*. In cells in which the initial level of caspase-8/10 activation is low, an amplification loop is triggered *(Scaffidi et al., 1998)*. In this amplification loop, caspases-8/10 cleave and activate the pro-apoptotic Bcl-2 family member Bid, which triggers cytochrome c release from the mitochondria and subsequent activation of caspase-9 and caspase-3, strongly amplifying the initial apoptotic signal *(Luo et al., 1998)*.

1.10.2 Radiation-induced mitotic catastrophe

Mitotic catastrophe is a term used for cell death that occurs during or as a result of an aberrant mitosis *(Galluzzi et al., 2007)*. It is a consequence of premature or improper entry of a cell into mitosis and can be induced by a multitude of DNA-damaging agents including radiation. The mitotic catastrophe is a delayed type of cell death executed days after treatment initiation, which can explain why clinical regression of solid tumours is slow. It is the main mode of cell death in HNSCC post irradiation *(Vakifahmetoglu et al., 2008)*. The latest study to show radiation-induced mitotic catastrophe in HNSCC *(Maalouf et al., 2009)*, demonstrated an early p53 independent apoptotic process and mitotic catastrophe occurred. This was performed in two p53 mutated HNSCC cell lines after exposure to different types of irradiation.

Two important mechanisms for the induction of the mitotic catastrophe have been proposed. First, a mitotic catastrophe has been suggested to occur as a consequence of DNA damage and deficient cell cycle checkpoints. In cells with impaired p53, a premature entry into mitosis, due to a compromised G2/M checkpoint, will occur. The G2/M checkpoint includes both p53-independent and p53- dependent mechanisms, with p53 playing a critical role in the maintenance of

the arrest. Cells entering mitosis prematurely as a consequence of a failure to activate p53 will contain unrepaired DNA damage *(Eriksson and Stigbrand, 2010)*.

The second mechanism is hyperamplification of centrosomes *(Kawamura et al., 2004; Kawamura et al., 2006; Eriksson et al., 2007; Bourke et al., 2007; Dodson et al., 2007)*. This can result in multipolar mitotic spindles, which cause abnormal chromosome segregation and generate cells with multiple micronuclei or binucleated giant cells followed by mitotic catastrophe *(Eriksson et al., 2008; Wang et al., 2009)* (figure 1.14)

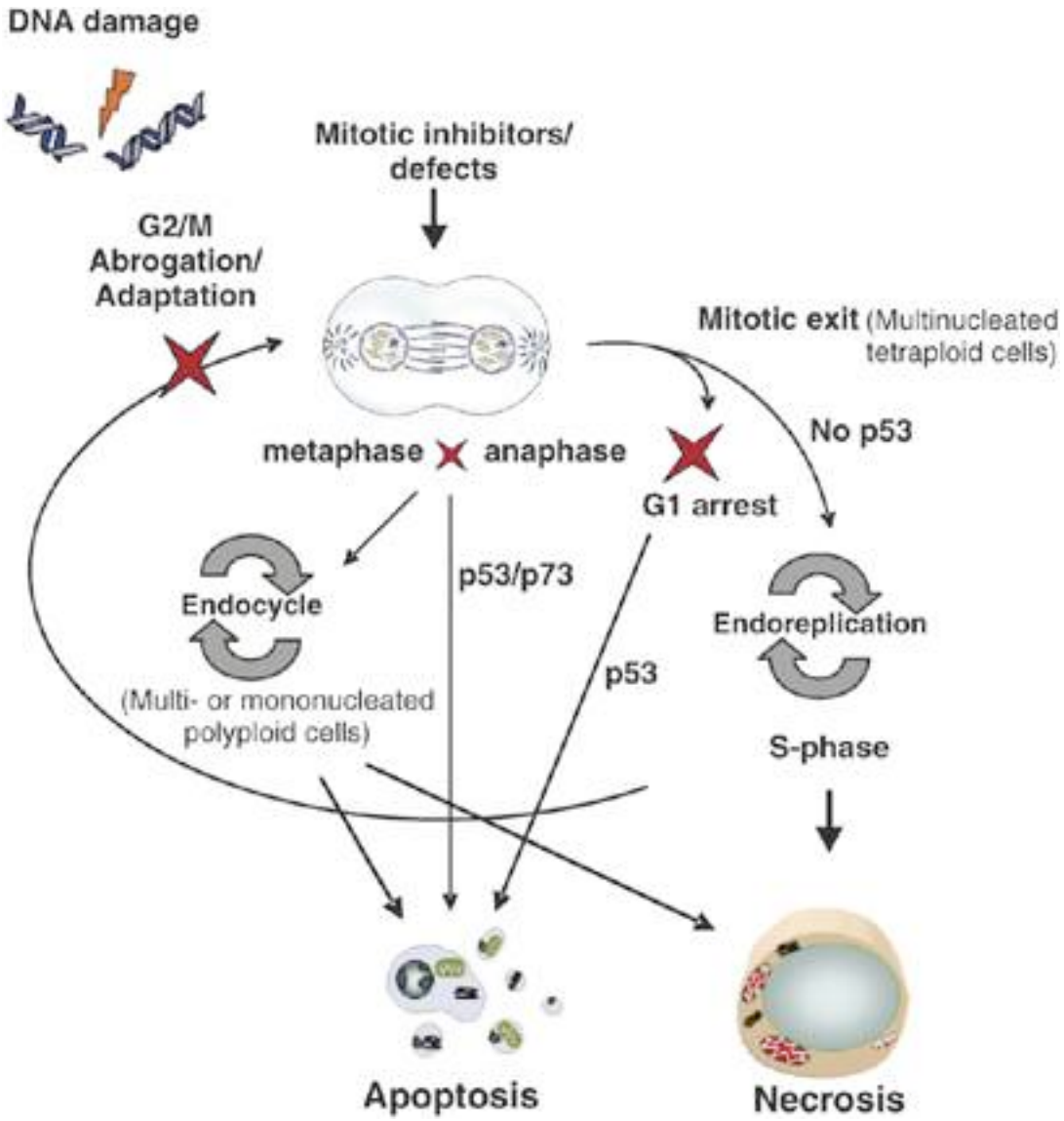

Figure 1.14 A schematic illustration of the pathways leading from mitotic catastrophe to cell death *(Vakifahmetoglu et al., 2008)*.

The type and dose of radiation along with the molecular profile of the cells influences the mode of cell death *(Abend, 2003)*. Consistent for all cell deaths that follow mitotic catastrophe is that they are delayed, occurring 2–6 days following irradiation *(Ruth and Roninson, 2000)*.

However, often, cells adapt to the mitotic checkpoint and consequently do not die by apoptosis in metaphase. These cells will exit the arrest but fail cytokinesis and enter the next G1 phase with a tetraploid DNA content *(Weaver and Cleveland, 2005; Yamada and Gorbsky, 2006)*. As a result, giant polyploid cells will be generated with aberrant nuclear morphology *(Eriksson et al., 2003; Castedo and Kroemer, 2004; Eriksson et al., 2007)*, multiple nuclei *(Eriksson et al., 2003; Erenpreisa et al., 2005)*, and/or several micronuclei *(Roninson, 2001)*. These cells can survive for days, but in the end, they die either by delayed necrosis, delayed apoptosis, or induced senescence *(Rieder and Maiato, 2004)*.

1.10.3 Necroptosis/necrosis

When activation of caspases is prevented, DNA damage can induce necroptosis. Necroptosis depends on hyperactivation of the poly-ADP-ribose-polymerase (PARP), a protein involved in DNA excision repair, and subsequent activation of receptor-interacting protein (RIP)—kinases as a response to depletion of intracellular ATP (figure 1.6). Necroptosis, once triggered by a structure called the necrosome, is characterized by the appearance of reactive oxygen species (ROS), lipid peroxidation, failure in calcium homeostasis, organelle swelling, and plasma membrane rupture *(Vandenabeele et al. 2010)*. It is important in cancer cells of epithelial origin which reveal a limited apoptosis induction capacity in response to ionizing radiation *(Mantel et al., 2010; Schildkopf et al., 2010)*. High doses of ionizing radiation can also stimulate necrosis, an accidental, uncontrolled type of cell death, which is predominantly characterized by rupture of the plasma membrane and a resulting release of intracellular contents, including danger signals, which can potently alert the immune system *(Orth et al., 2014)*.

1.10.4 Radiation-induced senescence

The term ‘senescence’, originally defined as a series of cellular changes associated with aging, now refers more commonly to a signal transduction program leading to irreversible arrest of cell growth, accompanied by a distinct set of changes in the cellular phenotype *(Shay and Roninson, 2004)*. Senescence has been reported to occur in tumour cells in vitro and in experimental tumours in vivo following extensive cellular stress induced by a number of DNA damaging agents including radiation *(Lehmann et al., 2007; Gewirtz et al., 2008)*. Cellular senescence remains of significance as a radiation-induced mechanism to inhibit tumour cell growth *(Eriksson and Stigbrand, 2010)*. Skinner et al. *(2012)* demonstrated in their series of HNSCC cell lines obtained from patients who had been treated with surgery and radiotherapy, that the main response to radiation affected by TP53 status was cellular senescence. Radiation induced senescence has also been reported in breast and prostate cancers *(Jones et al., 2005; Lehmann et al, 2007)*, glioblastoma multiforme cells *(Quick and Gewirtz, 2006)* and human solid tumour derived cell lines expressing wild type p53 *(Mirzayans et al., 2005)*.

Senescence commonly occurs in normal cells that have reached their proliferative limit as a consequence of telomere shortening *(Deng et al., 2008)*. Telomere attrition is recognized as damaged DNA and initiate growth arrest referred to as replicative senescence. In response to radiation, a DNA damage response (DDR) is induced. The DDR senses DNA damage and transmit a signal amplification cascade, which activates a transient cell cycle arrest during which DNA damage is repaired. DNA damage that is hard to repair and/or more severe will induce cell death (apoptosis (p53-dependent) or mitotic catastrophe (p53-independent)) or activate a persistent, chronic DDR signaling and senescence *(Rodier et al., 2009)*.

Replicative senescence has been reported to depend on the activation of two major tumor suppressor pathways controlled by p16/pRB and p53/p21 *(Sugrue et al., 1997; Dai and Enders, 2000; Steiner et al., 2000; Zhang, 2007)*.

Senescence induced in tumor cells in response to radiation treatment is promoted by p53 and is generally accompanied by expression of p21. When p53 signaling is impaired, radiation-induced senescence may be abolished *(Eriksson and Stigbrand, 2010)*.

Senescent cells do not divide but may remain metabolically active. Senescent cells have been shown to overexpress and secrete factors that can be not only tumor suppressing but also tumor promoting. These secreted factors include a number of cytokines that may strengthen the growth arrest and allow communication between senescent cells and their microenvironment *(Rodier et al., 2009; Coppe et al., 2010; Novakova et al., 2010)*.

Summary

So far, the background to HNSCC, the theory involved in radiation physics, the major factors that play a role in radiobiology and the various modes of radiation induced cell death have been composed. The different tissue culture devices and techniques used in HNSCC shall be discussed next.

1.11 Tumour Culture models

1.11.1 Introduction

Primary human tumour culture models allow for individualised drug testing and ultimately aim to achieve personalised treatment for patients with HNSCC. Cell lines derived from HNSCC tumours have been an asset in investigating molecular, biochemical, genetic and immunological properties of head and neck cancer. There are now numerous cell lines available for in vitro experiments as summarized by Lin et al. *(2007)*. A number of HNSCC cell lines were established through the explant technique as has been described by Carey in 1994. Fresh tumour specimens were mechanically split into fragments, dispersed enzymatically and the resulting cell suspension placed into a culture medium such as DMEM with additional fetal bovine

serum (FBS) and transferred into culture flasks. Bacterial and fungal overgrowths were prevented using antibiotics and antimycotics; and fibroblast overgrowth was managed through trypsinisation or cell scraping. Cells were then cultured at 37^{o} C in an air mixture with 5% CO_2. When cells grew to confluency, they were passaged; and according to Carey, a cell line is established after the 20th passage *(Carey, 1994; Dohmen et al., 2015)*.

Although advantageous as mentioned previously, a major disadvantage of using HNSCC cell lines is that cell culture is a selective process and tumour heterogeneity in HNSCC is well established. The cells that outgrow from an explant or attach following proteolytic dissociation of a primary tumour have the potential to grow in culture. Also, cells that survive and adapt to both the culture medium and culture techniques have the potential to grow *(Sacks, 1996)*. Other limitations of tissue culture are summarised in table 1.8 *(Freshney, 2010)* and existing tissue culture techniques are summarised in table 1.9.

Table 1.8 A table representing the limitations of tissue culture *(Freshney, 2010)*.

Category	**Examples**
Necessary expertise	Sterile handling Avoidance of chemical contamination Detection of microbial contamination Awareness and detection of mis-identification
Environmental control	Isolation and cleanliness of workplace Incubation, pH control Containment and disposal of biohazards
Quantity and cost	Capital equipment for scale-up Medium, serum Disposable plastics
Genetic instability	Heterogeneity, variability
Phenotypic instability	Dedifferentiation Adaptation

	Selective overgrowth
Identification of cell type	Markers not always expressed Histology difficult to recreate and atypical Geometry and microenvironment changes cytology

Table 1.9 A table representing an outline of different HNSCC culturing techniques.

Type of culture	**Assay**
Single cell culture	Cell adhesive matrix assay Soft agar clonogenic assay
Histocultures	Histoculture drug response Spheroids Squamospheres Organoids
Others	Flow cytometric analysis Tumour slices in test tubes Microfluidic devices Micronucleus assay

1.11.2 Single cell cultures

This technique has been used in HNSCC to assess radiosensitivity *(Brock et al., 1990; Girinsky et al., 1994; Eschwege et al., 1997).* The cell adhesive matrix (CAM) assay is a monolayer culture that uses a fibronectin and fibrinopeptides coated dish for cell adhesion. Cell growth was achieved using supplemented media and tumour biopsies were mechanically and enzymatically digested and plated as single cells. After a short period of incubation, the cells were either administered with drugs or

irradiation *(Baker et al., 1986; Dohmen et al., 2015)*. Radiosensitivity was determined by comparing the cell-covered surface to the total surface of the plates after irradiation with 2 Gray (surviving fraction at 2 Gray, SF2). Girinsky et al. *(1994)* demonstrated that SF2 values were not predictive for long term local control but a significantly higher local control rate was obtained for patients with higher values (which demonstrates the increased rate of cell kill by a single dose of irradiation). Eschwege et al. *(1997)* demonstrated however that SF2 and alpha values were not prognostic factors for local control and overall survival *(Girinsky et al., 1994; Eschwege et al., 1997; Dohmen et al., 2015)*.

The main feature with soft agar clonogenic assays is its selection for stem cells or transformed cells. HNSCC samples were processed as in the 'explant' technique described by Carey *(1994)*. This technique has been used to assess radiosensitivity in HNSCC *(Rofstad et al., 1987; Stausbol-Gron et al., 1999; Bjork-Eriksson et al., 2000)*. Rofstad discovered the SF2 differed considerably amongst individual tumours that were the same histologically. Stausbol-Gorn showed neither tumour cell SF2 nor overall SF2 predicted locoregional tumour control probability. Bjork-Eriksson et al. *(2000)* showed that tumour SF2 was found to be an independent prognostic factor for local control *($p = 0.036$)* but not for overall survival *($p = 0.20$)*.

1.11.3 Histocultures

This technique of culturing involves leaving the tumour tissue intact so the interactions occurring within the tumour would occur as if in vivo.

The histoculture drug response assay (HDRA) was a method developed to preserve the three dimensional (3D) tumour's histological structure, maintaining cell heterogeneity and cell-cell interactions *(Sherwin et al., 1980)*. Robbins et al. *(1994)* described HDRA in HNSCC for the first time. They investigated inhibition of tumour proliferation by using cisplatin; and they described a positive predictive value of 83%. More recently *(Freudlsperger et al., 2014)* in their cohort of 120 patients, used HDRA to evaluate the prognostic value of the phosphorylation status of AKT on Ser473 and

Thr308 for the clinical outcome of patients with advanced HNSCC treated with radiotherapy. Their data showed pharmacological interference of the phosphorylation pathway significantly induced a decline in cellular proliferation.

Spheroids

This culture technique was developed to allow the tumour specimen to grow as *in vivo*, maintaining tissue heterogeneity and 3D tissue architecture. They are composed of an outer later of proliferating cells with inner layers of quiescent and necrotic cells. Kross et al. *(2005)* used this model to describe the number of epithelial cells, fibroblasts and macrophages in HNSCC and benign spheroids. In 2008 they found increased IL-6 cytokine production *in vitro* to be predictive for recurrence and survival. Leong et al. *(2014)* described improved chemoresistance of spheroids when treated with chemotherapeutic agents or irradiation. The drawback of this study was the ex vivo results were not correlated with the clinical outcomes.

Squamospheres

Lim et al. *(2011)* reported the isolation of squamospheres from culturing mechanically and enzymatically digested biopsies from HNSCC patients. Single cells were incubated to assess sphere forming ability but also tumour-initiating capabilities. They asserted that primary HNSCC driven squamospheres possess cancer stem cells properties whose functional analysis can be used to investigate the tumourigenic process of HNSCC.

Organoids

Kopf-Meier and Kolon *(1992)* are the only group that has described the organoid culture assay in HNSCC. This involved use of xenografted HNSCC in mice, so they could achieve 3D in vitro tumour growth. Their study showed a model for testing chemotherapeutic agents in vitro; and the organoid culture assay seemed suitable for defining the patterns of drug sensitivity and resistance of individual human cacrinomas in vitro within a few days.

1.11.4 Other techniques

Garozzo et al. *(1989)* disaggregated HNSCC specimens into cell suspensions and exposed them to various chemotherapeutic agents. The major end point was determined by flow cytometry. Their assay predicted sensitivity to several drugs, with a positive predictive value of 85%. Elprana et al. *(1989)* described a study where cell suspensions and tumour slices of HNSCC specimens were placed in test tubes with or without chemotherapeutic agents. These in vitro assays were compared with in vivo tests in mice. The outcomes were quantified using incorporation of (3H) thymidine as a parameter. No data was obtained from the cell suspensions due to a reduction in cell viability; however in 6 out of 7 cases, the cytotoxic effects were similar between the tumour slices and the in vivo tests in mice. Champion et al. *(1997)* described a micronucleus assay to identify micronuclei, by establishing a monolayer culture of primary HNSCC specimens that were immunohistochemically stained after irradiation. Three established cell lines and 10 primary cell cultures were used in this study. However, no relationship between micronucleus frequency at 2 or 6 Gy and patient clinical outcome 12 months following surgery and radiotherapy was seen.

Summary

There are a variety of tissue culture techniques that exist (table 3.2); however they have their disadvantages. Monolayer cell culture requires a long period of time to establish the cell line. Also there can be low culture success rates *(Carey et al., 1994; Sacks, 1996)* and a state is reached when the cells can no longer divide *(Rheinwald and Beckett, 1981; Dohmen et al., 2015)*. The soft agar clonogenic assay can lead to a low population of HNSCC stem cells; and as they are mechanically digested, this can be traumatic but can also lead to altered results when comparing in vitro to in vivo sensitivity *(Miller et al., 1984; Kobayashi et al., 1993; Dohmen et al, 2015)*. The HDRA technique has advantages over the monolayer cell culture and soft clonogenic assay and has been confirmed by several research groups to show good correlation with clinical response *(Robbins et al., 1994; Singh et al., 2002; Ariyoshi et al., 2003; Hasegawa et al., 2007; Pathak et al.,*

2007). However these studies tested chemosensitivity in vitro while practically patients often received chemotherapy in combination with radiotherapy.

1.12 Microfluidic Technology

Microfluidics is the science and technology of systems that process or manipulate microliter to nanoliter volumes of fluids in purpose-built devices fabricated from glass or other biocompatible polymers. Laboratory procedures are integrated onto a single device and it's therefore known as 'lab-on-a-chip' or a 'micrototal analysis system' *(Tanweer et al., 2012)*. The device offers an environment in which pseudo *in vivo* tissue studies can be carried out under *in vitro* conditions. Microfluidic technology is increasingly being explored and validated for use in the detection, diagnosis and treatment of cancer *(Chaudhuri et al., 2015)*.

Tanweer et al. *(2012)* described the different types of microfluidic systems (MFS), which are the continuous-flow MFS, droplet-based MFS and the integrated MFS (continuous or droplet). In the continuous-flow type, a central well is used to keep the specimen alive for analytical purposes. Inlet channels constantly supply fresh media, with or without test reagents, and the outlet channels remove waste products and provide effluent for biochemical analysis. Droplet-based MFS allow rapid degeneration of monodispersed aqueous microdroplets up to 1pL volume in immiscible carriers such as oil *(Huebner et al., 2007)*. Flow focusing of oil and aqueous cell suspension, perpendicular to each other, produces droplets containing single cells for analysis. This technique has been used for genomic and proteomic analysis on single cells *(Chung et al., 2007; Mazutis et al., 2009; Schaerli and Hollfelder, 2009; Konry et al., 2011)*. Integrated MFS use either continuous or droplet=based flow systems that are coupled to different purpose-built analysis units for simultaneous operation *(Tanweer et al., 2012)*. For this research, the continuous flow type (a bespoke University of Hull device) has been used.

In vitro cancer models have been used extensively to study cancer proliferation and

key genetic events, however, it has been noted by many that these models do lack the complex *in vivo* structure and dynamic kinetics of nutrients and signaling molecules *(Hattersley et al., 2011)*. Under normal physiological conditions the flow within vascular capillaries and tissues is known to have Reynolds numbers <100, resulting in predominantly diffusion based characteristics, over spatial distances of approximately 100 µm, *(Kim et al., 2007; Ling et al., 2007)* conditions under which cellular metabolite uptake, gaseous exchange and waste removal occur *(Nevill et al., 2007)*.

As the flow and spatial parameters in tissue are very similar to those of the microfluidic environment, the opportunity to carry out continuous perfusion of tissue samples *(Kim et al., 2006; Nevill et al., 2007)* offers an experimental approach that may overcome some of the limitations of current standard batch culture systems *(Yu et al., 2007)*. The benefits of microfluidic techniques for cell/tissue culture that have been demonstrated previously include laminar flow conditions, small length scales, large surface to volume ratios, diffusion dominant transport, portability, reusability or disposability and reduced cost *(El-Ali et al., 2006, Meyvantsson and Beebe 2008)*. In addition, by exploiting the flow conditions present in a microfluidic device, unprecedented spatial and temporal control over materials entering and leaving an experimental system can be achieved (*Takayama et al., 2003; Hattersley et al., 2008; Zhang et al., 2008)*. Accordingly the ability to place a viable tissue biopsy in a microfluidic device will offer the opportunity to control, probe and monitor complex cell functions in diseased and healthy tissue whilst maintaining in vivo architecture *(El-Ali et al. 2006; Weibel and Whitesides 2006; Puleo et al., 2007; Nakanishi et al., 2008)*. The microfluidic environment can facilitate the continuous perfusion of fresh media at a scale that enables the contents of the microchannels to be continually replaced and analysed without disturbing individual cell dynamics *(Kim et al., 2006; Nevill et al., 2007)*.

Many of the cell lines used in cell culturing both in traditional and microfluidic systems have been immortalized or are tumour-derived, which are genetically unstable, have intrinsic changes in gene expression, loss of proliferative regulation

and signaling transduction pathways. These cells therefore are not a replicate of the typical in vivo cell *(Balis 2002)*. It has also been shown lately the importance of the ECM and its components. ECM is composed of structural proteins such as collagen and elastin, specialized proteins such as fibrillin, fibronectin, and laminin and proteoglycans *(Hattersley et al., 2011)*.

Overall, the main benefits of the microfluidic devices are automated operation, portability, short analysis time, reproducibility, and relatively low cost *(Tanweer et al., 2012)*.

Other studies have used microfluidic devices to investigate HNSCC cell behaviour (table 1.10). However, one study has been found, assessing the response to irradiation of HNSCC biopsies in the continuous flow type microfluidic device *(Carr et al., 2013)*.

Table 1.10 A summary of the latest studies utilising microfluidic devices in the assessment of HNSCC tissue.

Title	Summary of results	Author
Ultrasensitive microfluidic array for serum pro-inflammatory cytokines and C-reactive protein to assess oral mucositis risk in cancer patients.	Accuracy and diagnostic utility of four biomarkers (TNF-α, IL-6, IL-1β, CRP) in serum from oral cancer patients were demonstrated and correlated with results from standard ELISA	Krause et al, 2015
Nanoparticle-based sorting of circulating tumor cells (CTC's) by epithelial antigen expression during disease progression in an animal model.	There was an increase of CTC's during tumour progression and correlated with radiological measurements of tumour volume. The levels dropped post tumour resection and the MF device could accurately monitor disease progression.	Muhanna et al, 2015
Paired single cell co-culture microenvironments isolated by two-phase flow with continuous nutrient renewal.	UM-SCC-1 (HNSCC) cells and endothelial cells were co-cultured to simulate tumour proliferation enhancement in the vascular endothelial niche.	Chen et al, 2014
On-line protein capture on magnetic beads for ultrasensitive microfluidic immunoassays of cancer biomarkers.	The MF system allowed detection of IL-6 and IL-8 in conditioned media from oral cancer cell lines, showing good correlation with standard ELISA's.	Otieno et al, 2014
Analysis of radiation-induced cell death in head and neck squamous cell carcinoma and rat liver maintained in microfluidic devices.	A glass MF device was used and M30 was a superior method compared with soluble markers in detecting low-dose radiation-induced cell death, in laryngeal, and oropharyngeal SCC and metastatic cervical lymph nodes.	Carr et al, 2013
Real-time and non-invasive impedimetric monitoring of cell proliferation and chemosensitivity in a perfusion 3D cell culture microfluidic chip.	Human oral cancer cells (OEC-M1) were encapsulated in 3D agarose scaffold and cultured The measured impedance magnitude directly correlated with the cell viability and proliferation.	Lei et al, 2014
A microfluidic chip-based fluorescent biosensor for the sensitive and specific detection of label-free single-base mismatch via magnetic beads-based "sandwich" hybridization strategy.	Detection of oral cancer-related DNA in saliva and serum samples, without sample labelling, preseparation or dilution.	Wang et al, 2013
Desmolein 3 (DSG3) as a biomarker for the ultrasensitive detection of occult lymph node metastasis in oral cancer using nanostructured immunoarrays.	DSG3 was highly expressed in al HNSCC lesions and their metastatic cervical lymph nodes but absent in non-invaded lymph nodes.	Patel et al, 2013

Ultrasensitive detection of cancer biomarkers in the clinic by use of a nanostructured microfluidic array.	Detection of four biomarkers (IL-6, IL-8, VEGF and VEGF-C) in diluted serum from oral cancer patients, which correlated with results from ELISA.	Malhotra et al, 2012
Probing the role of mesenchymal stem cells in salivary gland cancer on biomimetic microdevices.	Using MF devices for 2D and 3D assays, it was demonstrated mesenchymal stem cells could be recruited by salivary gland cancer cells, whose effect was potentially mediated by TGF ß.	Ma et al, 2012
A microfluidic system for testing the responses of head and neck squamous cell carcinoma tissue biopsies to treatment with chemotherapy drugs.	The greatest level of cytotoxicity was achieved using a combination of cisplatin, 5-FU and docetaxel.	Hattersley et al, 2012
Interdigitated microelectrode-based microchip for electrical impedance spectroscopic study of oral cancer cells.	Impedance change at given frequencies was found to be linearly increased with increasing cell number of oral cancer cell lines, compared with non-cancer oral epithelial cells.	Mamouni and Yang, 2011
Oral cancer diagnosis by mechanical phenotyping.	The compliance of cells from oral cell lines and primary samples of healthy donors and cancer patients were measured using a MF optical stretcher. The cancer cells showed significantly different mechanical behaviour and were confirmed by histopathology.	Remmerbach et al, 2009
Cell-based sensor for analysis of EGFR biomarker expression in oral cancer.	There was a significant increase in EGFR expression in three oral cancer cell lines above control cells, the results of which also correlated well with flow cytometry.	Weigum et al, 2007
Identification of a gene signature for rapid screening of oral squamous cell carcinoma.	A 25-gene signature for oral SCC was generated and could classify normal and oral SCC specimens. It was 96% accurate on cross-validation, averaging 87% accuracy using three independent validation test sets	Ziober et al, 2006
Detection of picomolar levels of interleukin-8 in human saliva by biacore surface plasmon resonance (SPR).	Diagnostic sensitivity for oral cancer could be achieved by pre-concentrating the saliva samples 10 fold prior to SPR analysis, making the target levels 300pM for healthy individuals and 860 pM for oral cancer patients.	Yang et al, 2005

Aims

The initial objective is to use rat liver in the microfluidic device, so the conditions can be optimized. Soluble markers (lactate dehydrogenase - LDH) released by the tissue will be measured to assess cell death. Once the tissue has been maintained in the microfluidic device, the tissue will be cryosectioned. Haematoxylin and eosin (H&E) staining and immunohistochemical staining of 5-bromo-2'-deoxyuridine (BrdU), which detects proliferating cells in the S phase of the cell cycle, will be performed. The media being used to maintain the tissue will have the constituents varied and the flow rates altered with the aim of optimizing the conditions for the microfluidic device.

The next objective is to maintain the HNSCC samples in the microfluidic device; subject them to differing doses of irradiation and analyses of the tumour response to irradiation performed. The tissue morphology appearance will be evaluated by H&E

staining; cell death assessed by measuring LDH and immunohistochemical staining of cleaved cytokeratin-18 and BrdU will be performed.

Using a microfluidic approach, the ultimate goal is to predict the radiotherapeutic response of a patient's biopsy prior to starting treatment. By doing so, the patient can be given the appropriate treatment with the highest chance of a successful outcome. This could avoid patients with radioresistant tumours receiving primary radiotherapy and having to return for another modality of treatment with a higher rate of morbidity and mortality *(Tanweer et al., 2012)*.

Chapter 2

Materials and Methods

2.1 Head and Neck Tissue Sample Collection

Local Research Ethics (10/H1304/6) and NHS Trust Research and Development (R0987) approvals were in place before recruitment commenced.

Patients were identified at both the Otolaryngology and Maxillofacial departments at Castle Hill Hospital and Hull Royal Infirmary respectively. Samples were collected from patients with head and neck squamous cell carcinomas, undergoing initial biopsies and resection surgery following written informed consent. Once the operating surgeon dissected the sample, it was transported to the laboratory in cooled (5°C) complete tissue culture medium (Dulbecco's Modified Eagle's Medium (DMEM); Lonza, Slough, UK) with 10% (v/v) foetal bovine serum (Biosera, East Sussex, UK), 30mM HEPES (hydroxyethyl piperazineethanesulfonic acid; PAA Laboratories, Yeovil, Somerset), penicillin/streptomycin (10000 U Penicillin and 10000 U Streptomycin; Lonza), L - glutamine (PAA Laboratories,), 1% non essential amino acids (PAA Laboratories,) and amphotericin B (250μg/ml, Life Technologies Corporation, Renfrewshire, UK). Under sterile conditions in a Class II laminar flow hood (ESCO Airstream E series cabinet, Wiltshire, UK), the tissue was divided into multiple specimens (approximately 3mm^3) using scalpels and minimal slicing action to minimize tissue damage and placed into cryovials (Sarstedt, Leicester, UK); and thereafter snap frozen in liquid nitrogen before long term storage at -80°C.

2.2 Patient exclusion criteria

Patients were excluded from the recruitment process if they conformed to any of the following:

1) A history of previous cancer
2) Previous treatment for cancer, either chemotherapy, radiotherapy or surgery
3) Non-squamous cell carcinoma or mixed tumour histopathology
4) An inability to sign or understand the consent form/process

2.3 The Microfluidics System

Each microfluidic device was fabricated from glass using photolithography and wet etching techniques. Access holes (1.5mm diameter) and a central chamber (3mm diameter) were drilled (using traditional glass drilling techniques) in the top plate (3mm thickness) and then thermally bonded with the etched bottom plate in a furnace at 590°C for 3 hours. The channel network was etched into the bottom (1mm) glass layer to produce channels of 190-µm width and 70-µm depth, which diverged into three channels *(Broadwell et al., 2001; Hattersley et al., 2011)* as shown in figure 2.1.

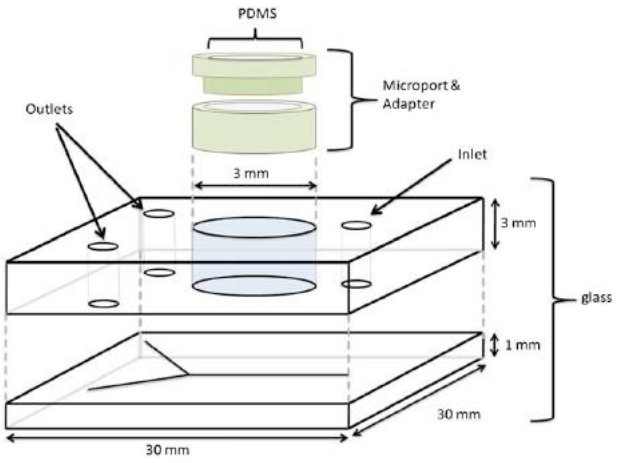

Figure 2.1 Schematic diagram of the microfluidic chip used. **(**PDMS **–** Polydimethylsiloxane) (*Hattersley et al., 2012)*.

The microfluidic device had an adaptor base (IDEX Health and Science, USA) component glued (Araldite Resin and Hardener, Huntsman Corporation, UK) to the surface of the top glass layer surrounding the 3mm diameter cavity to form a tissue

chamber. The adapter base was secured using a bulldog clip for 24 hours prior to use. The central distal outlet channel was also glued, as it was not used.

Multiple lengths of tubing (Tefzel (ETFE), 0.010IN x 1/16IN x 50 FT, IDEX Health and Science, USA) were prepared to a length of approximately 38cm. Multiple pipette tips (200µl, Sarstedt) were cut to size and glued to the end of the tubes and allowed to set for 24 hours prior to use (Figure 2.2).

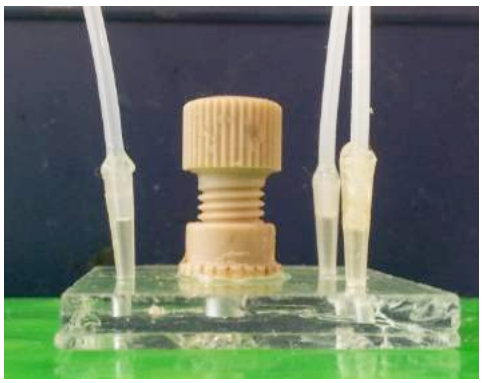

Figure 2.2 A photograph showing pipette tips glued to the tubing and placed in the microfluidic device.

The narrow end of each pipette tip was trimmed to ensure a tight fit in the inlet channel and two outlet channels to prevent fluid leakage.

2.4 Priming and maintenance of the microfluidic device

Once the inlet and outlet tubes were in place, a 10ml syringe (Luer slip Plastipak syringe, Becton Dickinson, Oxford, UK) filled with 70% ethanol (VWR Chemicals, Lutterworth, Leicestershire) was attached to the inlet tube using a one piece plug (1/16 IN, Mengel Engineering, Denmark,) and a Luer-lock adaptor (Mengel Engineering). The inlet tube was flushed to ensure adequate flow to the centre well which was then filled with ethanol.

A threaded bung (Anachem, UK) was pre-filled with polydimethylsiloxane (PDMS; Dow Corning, UK) to allow gaseous exchange to occur. Polytetrafluoroethylene (PTFE, 50mm x 12mm x 0.075mm, Homebase, UK) thread seal tape was wrapped around the thread of the bung. This bung along with the PTFE tape was used to seal the adaptor base and prevent any leakage (Figure 2.3).

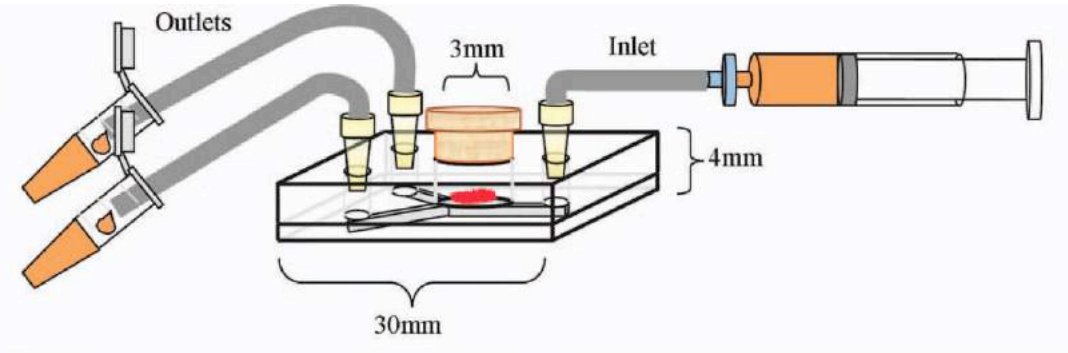

Figure 2.3 A schematic diagram showing the microfluidic setup including the syringe, tubing, adaptor and eppendorfs *(Tanweer et al., 2012)*.

Further flushing of the device with 70% ethanol (VWR Chemicals) was performed to ensure flow through the complete system and no leakage was from the inlet and outlet channels, the adaptor base and bung. The microfluidic device was placed in an incubator (Covatutto 24 Eco semi automatic incubator, Novital, Varese, Italy) and the syringe attached to the syringe pump (Harvard PHD 2000 Syringe Pump, Harvard Apparatus, Kent, UK). The microfluidic device was primed with 70% ethanol at a rate of 10ml/hr for 15 minutes, followed by sterile distilled water for a further 15 minutes. Under sterile conditions in a laminar flow cabinet (ESCO), the syringe was then replaced with a syringe containing medium and an in-line 0.2 micron filter (Sarstedt, Numbrecht, Germany) was used to prevent contamination and reduce air bubbles. The syringe and filter were reattached to the pump and the device primed for a further 30 minutes at a rate of 20µl/min.

During the priming process, the stored tissue was removed from the -80°C freezer. In the laminar flow cabinet, the tissue was allowed to thaw for 5 minutes in 5ml of

phosphate buffered saline (Oxoid Limited, Hampshire, UK) with penicillin streptomycin (final concentration 10000 U each, Lonza) and amphotericin B (250µg/ml, Life Technologies Corporation). The tissue was dissected in a petri dish using a slicing action of two scalpels (size 11, Swann-Morton, Sheffield, England) and weighed on an electronic scale (Sartorius, Surrey, UK). An ideal weight between 5mg to 10mg was achieved for each piece of tissue, which equated to approximately 3mm^3.

Post priming, the microfluidic system was returned to the laminar flow cabinet (ESCO) and the pre-weighed tissue placed into the central well. Any air bubbles were removed; and once the bung was replaced, a small amount of pressure was exerted on the syringe to ensure there was no blockage to flow in the device. The device and syringe were reconnected to the pump and the flow rate was set to 2µl/min. Effluent was collected every 2 hours in 0.5 ml polypropylene tubes (Fisher Scientific, Loughborough, UK). At each collection, effluent was aliquoted for further assays and stored in (depending on the assay conducted) the cold room (4°C) or the -80°C freezer. The temperature in the microfluidic incubator was digitally measured and maintained between 36°C and 37°C (Checktemp, HANNA Instruments, Rhode Island, USA).

The microfluidic system was checked at regular intervals and any problems, such as blockages or leaks, were promptly dealt with by returning the microfluidic device to the laminar flow cabinet before the tissue was removed and placed in a 1.5 ml polypropylene tube (Fisher Scientific) containing complete DMEM. If there was a blockage, the device was flushed (with the equivalent medium); and/or if there was any leakage, this was addressed by adjusting the inlet/outlet tubes or bung. If necessary, further glue (Araldite Resin and Hardener) was applied to prevent future leaks. Thereafter the tissue was returned to the central well, the bung replaced and the syringe given a further push to ensure there was no resistance to flow.

A maximum of three collections were taken before running the device overnight. Two hourly collections continued into the next day. After a period of approximately 24

hours, the microfluidic device was placed in a custom made Perspex block in the incubator and the syringe pump connected to a portable battery pack (Riello UPS Ltd, Wrexham County Borough, UK). The Perspex block was specifically constructed by the medical physics department at Castle Hill Hospital. It consisted of an upper part, which had 3 holes to allow the inlet and outlet tubes to be placed; and a lower part, which had an indent to allow the microfluidic device to be placed. A milling machine was used to index and cut the indent and edges, whereas the holes were indexed and drilled. They were transported to the radiotherapy suite in the Oncology department at Castle Hill Hospital (Hull), where the tissue was irradiated. On return to the laboratory, two further collections of effluent were taken prior to a further overnight flow. On the second day after the second effluent collection had taken place, the syringe was replaced with another syringe containing medium with a concentration of 10μM BrdU (5-Bromo-2'-deoxyuridine, Sigma-Aldrich Company Ltd, Dorset, UK). The microfluidic device was run for a further 6 hours and regular effluent collections were taken. Once completed, the tissue was embedded in OCT embedding matrix (Fisher Scientific), on a cork board (pre-labelled for future identification), and snap frozen by placing it in liquid nitrogen cooled 2-methylbutane (Sigma-Aldrich) before being stored in the -80°C freezer.

The microfluidic device and tubing were flushed with 70% ethanol and distilled water to remove residual medium and minor debris from the central well. The bung had the PTFE tape removed and was immersed in 70% ethanol. Otherwise the rest of the microfluidics system was steam sterilised for 30 minutes at a temperature of 121°C using an autoclave (Boxer Laboratory Equipment Ltd, Hertfordshire, UK).

If the microfluidic chip was blocked when primed for further use, it was placed in concentrated HCL (Fisher Scientific) for 72 hours in a laminar flow cabinet (ESCO) and flushed thereafter with 70% ethanol to ensure flow through the complete system. If this was not successful, the microfluidic chip was placed in a high temperature furnace to ensure all blockages were removed.

2.5 Irradiation Protocol

In the radiotherapy suite, the Perspex block containing the microfluidic device was closed and removed from the incubator. The incubator lid was closed ensuring other microfluidic devices were kept at the required temperature. The microfluidic device containing the tissue to be irradiated was placed in line with the head of the Linear Accelerator (Clinac iX, Varian Medical Systems, California, USA). Laser beams emitted from the Linear Accelerator allowed the microfluidic device to be accurately positioned. The irradiation field was focused by magnets in the treatment head and shaped by collimation and set to an 8 x 8 cm^2 field.

The departmental radiation physicist performed operation of the Linear Accelerator. The irradiation dose administered was given to either side of the tissue and was achieved by rotating the head of the Linear Accelerator through 180^0 (Figure 2.4).

Figure 2.4 Photographs showing the linear accelerator (above) and the microfluidic device in the perspex block lined up with the head of the linear accelerator (below).

Once complete, the Perspex block was opened and the microfluidic device repositioned in the 37°C incubator. The setup was returned to the laboratory and the experiment continued (Section 2.4).

2.6 Tissue cryostat sectioning

The cork-mounted embedded tissue specimen was removed from the -80°C freezer and attached to a specimen disc ("chuck") using OCT Embedding Matrix (Fisher Scientific). This was then placed in the cryostat (Leica CM1100 cryostat chamber, Leica Microsystems, Buckinghamshire, UK) at -20°C and the OCT compound allowed to freeze. The rotary microtome was set at 8µm and a continuous series of sections were cut and collected on labelled Poly-L-lysine coated microscope slides (StarFrost, Scientific Laboratory Supplies, Hull, UK). All sections were dried at room temperature for 30 minutes, before being stored in the -20°C freezer ready for staining.

2.7 Haematoxylin and Eosin (H&E) Staining

The frozen tissue sections (Section 2.6) were placed in a metal staining rack and fixed with pre-cooled (30 minutes at -20°C) 100% methanol (VWR) for 10 minutes in the -20°C freezer. Thereafter, the slides were rinsed in running tap water for 1 minute, stained with filtered Harris Haematoxylin (Sigma-Aldrich Company Ltd, Dorset, UK) for 5 minutes before rinsing in running tap water for a further 1 minute. The slides were then transferred into 5% (w/v) eosin in 95% ethanol (Sigma-Aldrich Company Ltd, Dorset, UK) for 2 minutes and rinsed in running tap water for 1 minute. The sections were then dehydrated through graded ethanol (70%, 90% and 100%) for 2 minutes each before being cleared in three changes of Histo-Clear™ II (National Diagnostics, Hull, UK) for 2 minutes each. Finally the slides were mounted using Histomount™ (National Diagnostics) and glass cover slips (24mm x 50mm, Fisher Scientific) and left to dry overnight prior to microscopic examination using at x100 and x400 magnifications and analysis using a Nikon E800 microscope with

camera attachment and Image pro premier software (Media Cybernetics, Cambridge, UK). Details for this process is in section 2.10.

2.8 General Immunohistochemistry

Frozen tissue sections (section 2.6) were placed in a metal staining rack and fixed in pre-cooled (30 minutes at -20°C) 100% methanol (VWR) for 20 minutes at -20°C. The slides were then rinsed in 1 x Tris-buffered saline (TBS; Appendix 1) pH 7.6 for 5 minutes. Endogenous peroxidases were blocked by incubating the slides in 3% hydrogen peroxide (Fisher Scientific) in methanol for 15 minutes before rinsing for 2 minutes in tap water. The slides were transferred to a Sequenza rack and washed three times with TBS. To prevent non-specific binding of the secondary antibody the sections were incubated for 20 minutes with a diluted normal horse serum (Vectastain® Universal ABC Kit, Vector Laboratories, Peterborough, UK). The serum was prepared by adding one drop (50μl) of blocking serum to 5ml of 1 x TBS. Following incubation Avidin and Biotin binding sites on the sections were blocked using an avidin/biotin blocking kit (Vector Laboratories). Immediately following incubation with the horse serum, 3 drops of avidin solution were added to each slide, for 15 minutes before being washed three times with 1 x TBS followed by a further 15 minute incubation with 3 drops of biotin solution and three further washes with TBS. Primary antibody (100μl) at the appropriate dilution was added to each section and 100μl of isotype control antibody was added to the negative control slide and incubated for 1 hour at room temperature.

Three washes with 1 x TBS were performed and the sections were incubated with diluted horse secondary antibody (Vectastain® Universal ABC Kit) for 30 minutes. The secondary antibody was prepared adding 2 drops (100μl) of the normal horse serum and 2 drops (100μl) of biotinylated secondary antibody to 5ml of TBS buffer. During the incubation with the secondary antibody, the Vectastain® Elite ABC reagent (Vectastain® Universal ABC Kit) was prepared by adding 2 drops (100μl) of reagent A to 5ml of TBS followed by 2 drops (100μl) of reagent B before being mixed and allowed to stand for 30 minutes. Post incubation with the diluted secondary

antibody, three washes with TBS were performed and the sections then incubated for 30 minutes with the prepared Vectastain® Elite ABC reagent (Figure 2.5).

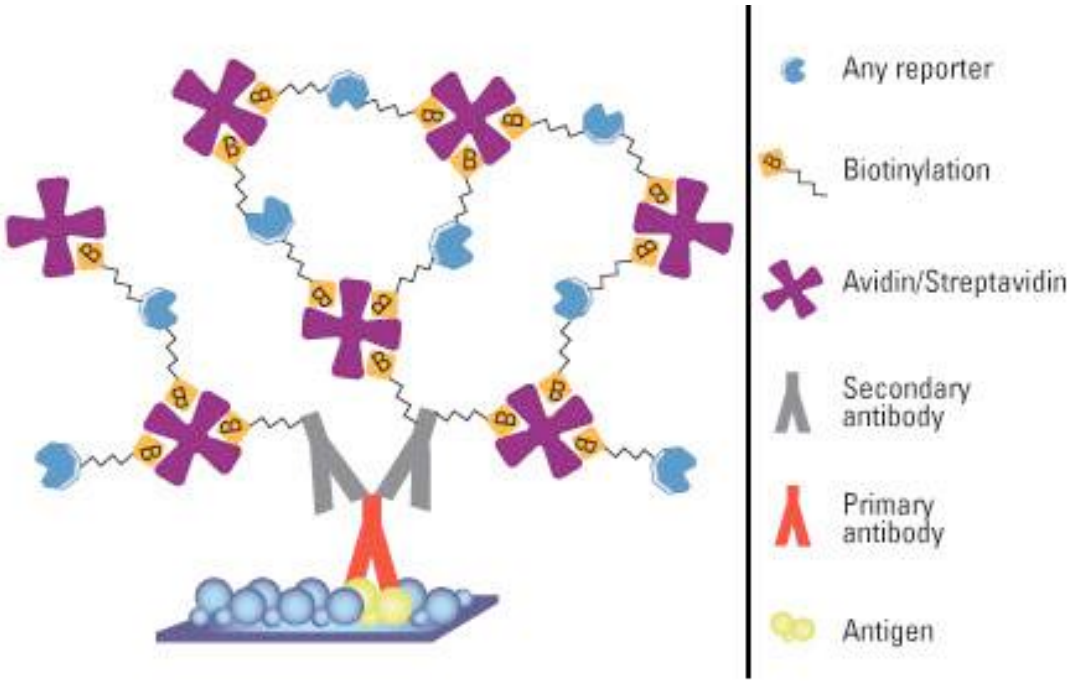

Figure 2.5 A diagram showing the avidin biotin complex method for IHC (www.lifetechnologies.com).

During this period, one gold tablet of 3,3' – diaminobenzidine (Sigma *FAST*™, Sigma-Aldrich) and one silver tablet of hydrogen peroxide (Sigma *FAST*™,) were added to 1ml of distilled water; vortex mixed and allowed to dissolve. Post incubation, three final washes with TBS were performed and the slides were removed from the Sequenza rack and dried around the periphery and the sections isolated with a wax pen (Vector Laboratories). The DAB solution (100µl/section) was applied to the sections until the colour had sufficiently developed (approximately 5 minutes). The sections were then rinsed under running water for 2 minutes and counterstained with pre-filtered Harris Haematoxylin (Sigma-Aldrich) for 20 seconds. They were rinsed in tap water for 2 minutes prior to being successively dehydrated through graded ethanol (70%, 90% and 100%) for 2 minutes each and then cleared in three changes of Histo-Clear™ II (National Diagnostics,) for 2 minutes each. Finally the slides were mounted using Histomount™ (National Diagnostics,) and glass cover slips (24mm x 50mm, Fisher Scientific) before microscopic evaluation

using a Nikon E800 microscope with camera attachment and Image pro premier analysis software (Media Cybernetics).

2.9 Lactate Dehydrogenase (LDH) Assay

To determine the amount of cell death occurring during the microfluidic incubation and following irradiation of the tissue a Cytotoxicity Detection Kit^{PLUS} for LDH (Roche Diagnostics, West Sussex, UK) was used according to the manufacturer's instructions.

LDH activity was determined by a coupled enzymatic reaction. In the first enzymatic reaction LDH reduced NAD+ to NADH and H+ by oxidation of lactate to pyruvate. In the second enzymatic reaction the catalyst (diaphorase) transfered H/H+ from NADH and H+ to the tetrazolium salt INT (2-(4-iodophenyl)-3-(4-nitrophenyl)-5-phenyl-2H-*tetrazolium), which* was reduced to formazan (Figure 2.6).

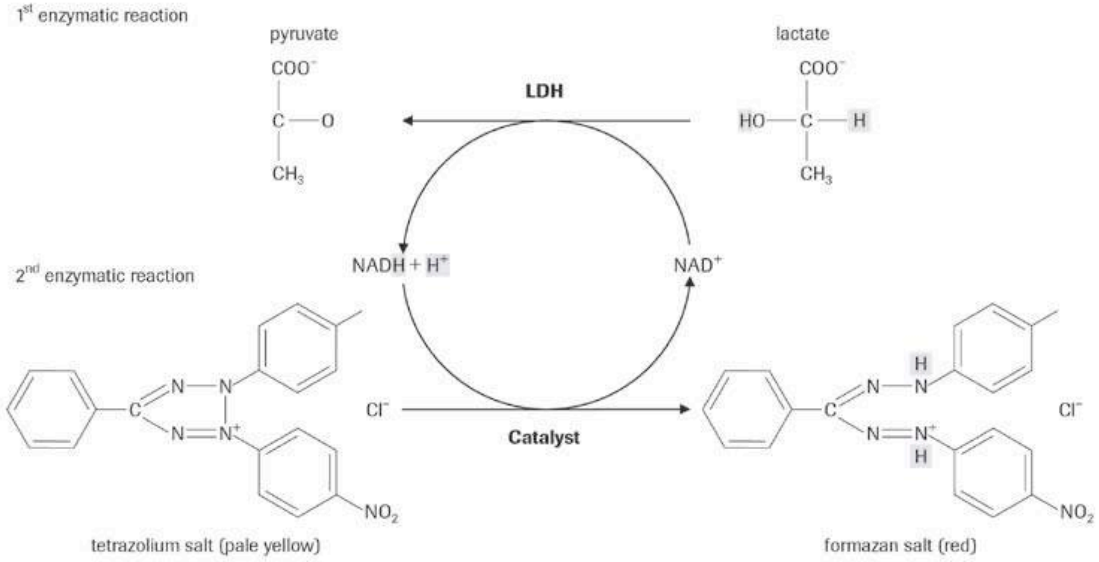

Figure 2.6 A schematic diagram showing the biochemistry of the Cytotoxicity Detection Kit^{PLUS} for LDH (Roche Diagnostics) (Rode *et al.*, 2008).

The release of LDH correlated with the amount of formazan formed, which was responsible for the colour development during the incubation and was quantified using a microplate photometer.

Briefly, the dye solution, catalyst and stop solution from the -20°C freezer were brought to room temperature and under sterile conditions 1ml of sterile distilled water was added to the catalyst and mixed to dissolve. For each two hundred tests (wells), 250µl of the catalyst was added to 11.25ml of the dye solution and mixed together. Effluent from all the time points (50µl) obtained from one microfluidic device (including 50µl of control medium used for that run) were placed in duplicate into separate wells of a 96 well plate (96 Well Cell Culture Cluster, Corning Incorporated, Sarstedt).

A multichannel pipette (Biohit Limited, Devon, UK) was used to add 50µl of the prepared catalyst/dye mixture to each well. The 96 well plate was covered and incubated at 37°C for 30 minutes before 25µl of the stop solution was added to each well. The absorbance at 492nm of each well was then measured in a microplate photometer (Multiskan^{TM} FC, Thermo Fisher Scientific, Loughborough, UK). The mean absorbance value for the control (medium alone) wells was determined and substracted from the mean absorbance for each sample before dividing the value by the specimen weight (mg) to standardize the readings to absorbance/mg for each sample (Equation 2.1). The mean of the duplicate values at each time point were plotted on a scatter graph against the respective time points.

$$\frac{\text{Mean absorbance} - \text{mean media absorbance (background reading)}}{\text{Specimen weight (mg)}}$$

Figure 2.7 The equation showing the method of calculating the absorbance/mg at each time point for which effluent was collected.

.

2.10 Calculation of the apoptotic labelling indices

Photographs were taken of a chosen section (magnification x100) using the Nikon E800 microscope and camera attachment; and they were amalgamated using the Image pro premier software (Media Cybernetics) (Figure 2.8)

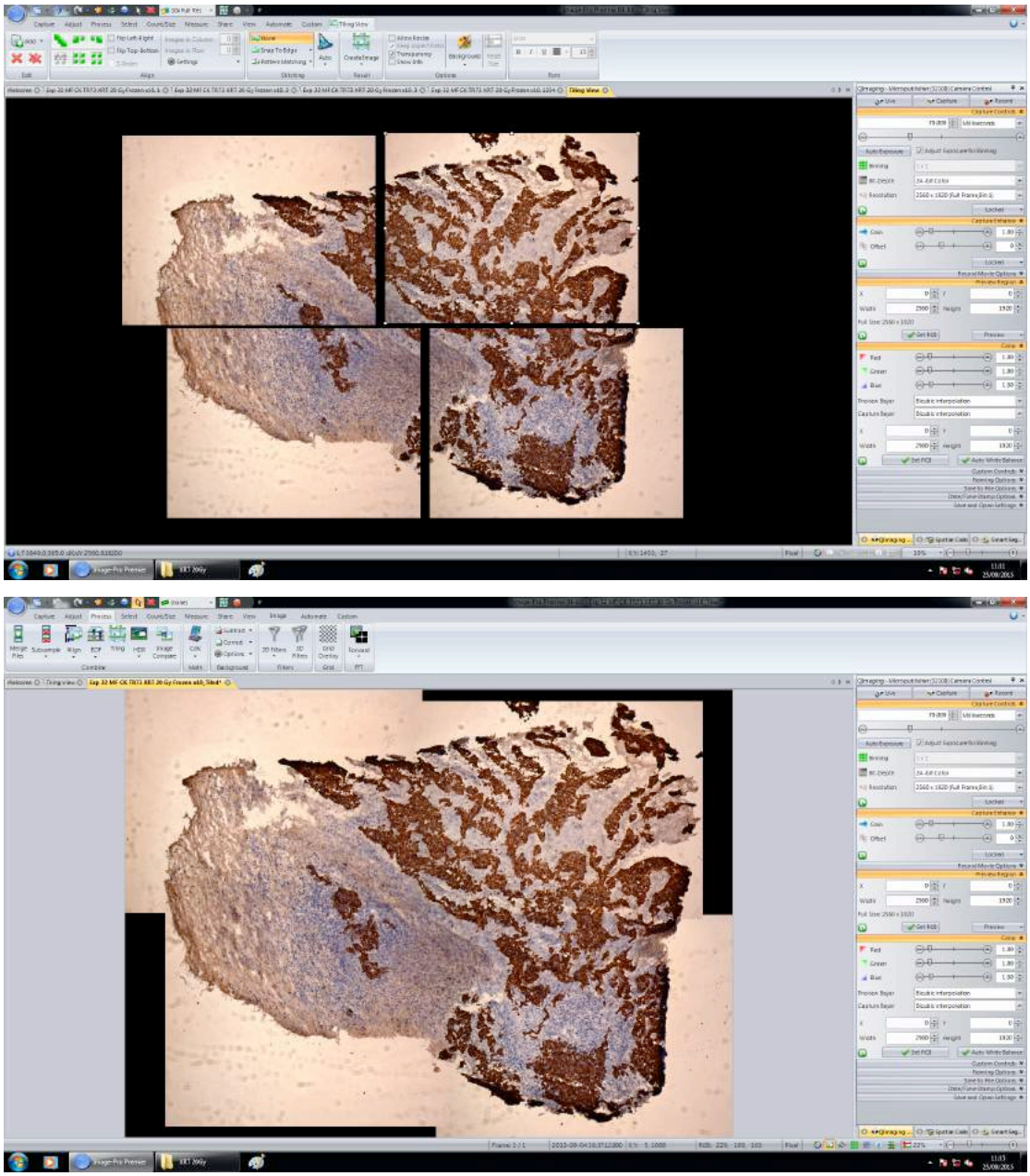

Figure 2.8 Photographs showing 4 separate images of a section (above) which were merged together to produce one image (below).

The apoptotic labelling indices (CK18-LI) were calculated by counting the cells that stained a positive brown colour for cytokeratin (CK) and the M30 *CytoDEATH™ antibody.* The Image pro premier software was used to count the cells using the automated counting function (Figure 2.8). The CK18-LI was obtained by expressing the percentage of apoptotic area (M30) over the total tumour area (CK).

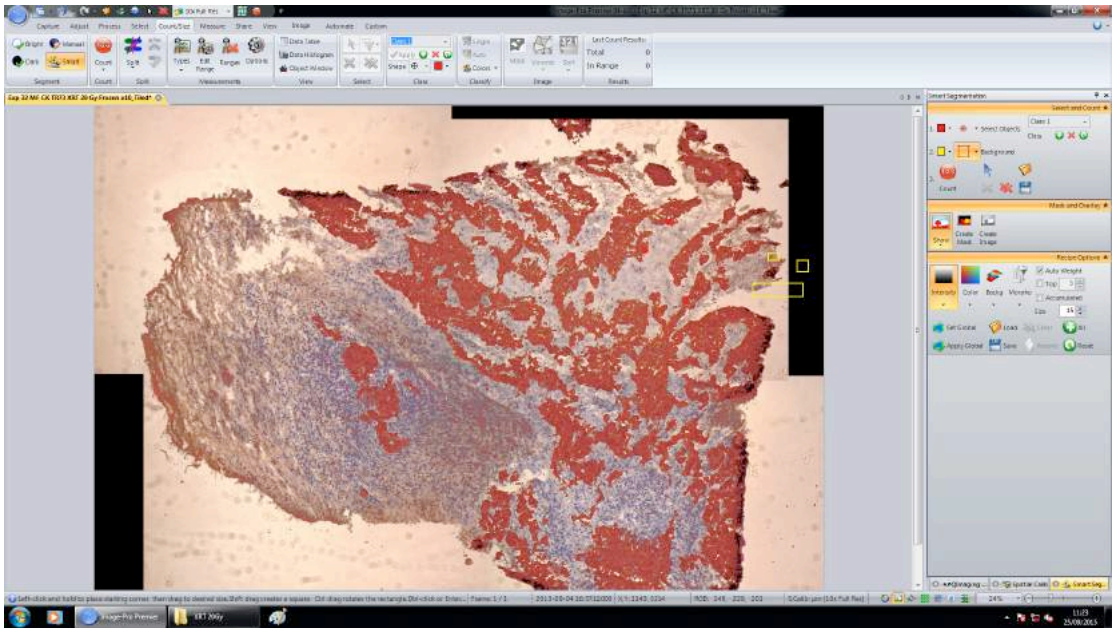

Figure 2.9 The photograph shows the positive areas (the cells counted and highlighted in red) marked against the background.

Chapter 3

The optimisation of the microfluidic device

3.1 Introduction

The aim of this part of this study was to optimise the conditions associated with the microfluidic system using rat liver prior to the use of HNSCC tissue biopsies. The parameters assessed are represented in table 3.1.

Table 3.1 A table representing the parameters that were assessed to optimise the conditions in the microfluidic system.

The maximum length of time the tissue could be maintained within the microfluidic system
The optimal length of time for the tissue to be perfused with BrdU during the microfluidic experiment, to show incorporation following immunohistochemical analyses
The concentration of serum in the medium
The different flow rates of medium supplying the microfluidic system
The use of HEPES (hydroxyethyl piperazineethanesulfonic acid) in the medium
The oxygen tension in the perfusion medium

Rat liver was used for optimisation because of its homogeneity, availability, high metabolic activity and it has a similar radiosensitivity to HNSCC *(Stryker, 2007)*. Previous studies produced similar results *(Hattersley et al., 2008, Carr et al., 2013)* and have shown rat liver tissue can be maintained in the same device. Hattersley et

al. *(2008)* revealed the LDH activity measured in the effluent remained at low levels for the 96 hour period of incubation. Carr et al. *(2013)* showed rat liver could be maintained for upto 15 days. Low LDH levels were detected throughout and upon addition of the lysis agent prior to termination of the experiment, LDH levels rose to show the tissue was still in a viable state. In this study, LDH was measured to assess the sustainability of rat liver tissue in the microfluidic device. To ensure the rat liver tissue was viable at the completion of the experiment, a lysis-inducing agent was added to the culture medium. This would allow the cells to break and release LDH, demonstrating the rat liver tissue is in a viable state with cells having intact membranes containing the enzyme.

The H&E staining technique was used to analyse the rat liver tissue histologically, so the tissue architecture and morphology could be assessed post incubation in the microfluidic device.

HEPES is a buffering agent used in tissue culture. Carbon dioxide produced in culture media can alter the pH and potentially alter cell growth. Bicarbonate buffer can be used because of its low toxicity and cost; but HEPES is a much stronger buffer in the pH 7.2 – 7.6 range *(Freshney, 2010),* due to its high buffer capacity, efficiency and appropriate temperature coefficient for control of pH in the physiologically important range at reduced temperatures *(Baicu and Taylor, 2002)*. HEPES was utilised in this study to assess if it had any effect on the outcomes of incubation in the microfluidic device.

BrdU is a synthetic analogue of thymidine. It is a common reagent used for cell proliferation assays. Prior to cell division and proliferation, DNA replication takes place and if BrdU is added to the cells, it will incorporate into the DNA during the S (synthesis) phase of the cell cycle substituting thymidine and acting as a marker for cell proliferation. The incorporated BrdU is then detected using monoclonal antibodies specific for BrdU and will indicate if cells are replicating their DNA and hence undergoing proliferation. Table 3.2 shows HNSCC studies that have used the BrdU assay whether *in vitro* or *in vivo*.

Table 3.2 A table representing a summary of studies that have utilized the BrdU assay and their incubation periods.

Author	Aim	Time of incubation for BrdU (hrs)
Lee et al., 1989	Detection of the labeling index of S-phase cells in normal and neoplastic tissues, In vitro	2
Cooke et al., 1994	Evaluation of cell kinetics in HNSCC, In vivo	3 - 16
Wilson et al., 1995	Tumour cell proliferation in head and neck cancer, In vivo	6
Corvo et al., 1996	Investigation of cell kinetics and tumour regression during radiotherapy in HNSCC, In vivo	4 – 6
Shapira et al., 1998	Investigation of the dynamics of BrdU incorporation into DNA of squamous carcinoma cells during mid and late logarithmic growth, In vitro	Daily incubation but time period not documented
Riedel et al., 1999	Evaluation of the expression of basic fibroblast growth factor protein and its down regulation by interferons in head and neck cancer	3
Corvo et al., 2000	Investigation of cell kinetics as a predictive factor of response to radiotherapy alone or chemoradiotherapy in patient with advanced HNSCC, In vivo	6
Masunaga et al., 2006	Evaluation of hypoxic cell radio-sensitisers, compared under aerobic and hypoxic conditions and a repair inhibiting effect following irradiation, HNSCC cell lines in mice	5 days and 7 days
Hass et al., 2007	Evaluation of DNA ploidy, proliferative capacity and intratumoural heterogeneity in primary and recurrent HNSCC	2
Erlich et al., 2008	Investigation of the efficacy of valproic acid as a therapeutic agent in HNSCC	6
Ijichi et al., 2008	Determining the cytotoxicity when using 5-FU and cisplatin in HNSCC cell lines, In vitro	0.5
Zheng et al., 2011	Evaluation of the effect of human keratinocyte growth factor gene transfer to murine salivary glands, on the prevention of radiation-induced salivary hypofunction, In vivo (mice)	2
Gyenge et al., 2012	Evaluation of photosensitisers on two different HNSCC cell lines	Not documented
Lenarduzzi et al., 2013	Evaluation of the expression of iron related genes in HNSCC cell lines, In vitro	24
Bertrand et al., 2014	Evaluation of cancer stem cells from a radioresistant HNSCC cell line against photon and carbon ion irradiation, In vitro	Not documented

Appropriate culture conditions are required to imitate *in vivo* physiological conditions if growth and maintenance of cells *in vitro* are to be successful. Animal sera of different origins are essential to supplement basal culture media to allow cell growth. The major functions of serum in culture media are: providing hormonal factors allowing cellular growth and proliferation, provision of transport proteins carrying hormones, minerals, trace elements and lipids; and stabilising and detoxifying factors needed to maintain pH or to inhibit proteases *(Gstraunthaler, 2003)*.

Foetal bovine serum (used at concentrations of 10%) is the standard supplement used in culture media. The advantages are it includes most factors required for cellular proliferation and differentiation and is an effective universal growth supplement *(Gstraunthaler, 2003)*. The disadvantages are variable shelf life and consistency, product availability, contamination and physiological variability due to the role of undetermined components *(Gstraunthaler, 2003, Freshney, 2010)*.

Cellular function and biological processes are affected by the partial pressure of oxygen, or oxygen tension, in the microenvironment. In standard cell culture, incubators maintain cells at 37 °C in 5% CO_2 so the pH of media can be buffered. The range of oxygen tensions found in cells and tissues in the human body does not reflect the 21% oxygen used in cell culture; and is normally well below the ambient atmospheric oxygen tension *(Brennan et al., 2014)*. In the liver, the normal levels of oxygen range from 10% – 13% *(Hung et al., 2012)*. If the oxygen tensions are below the physiological levels (hypoxia), this can promote alterations in hypoxia related gene expression, which rely on the transcriptional activity of the hypoxia inducible factors *(Rexius-Hall et al., 2014)* and ultimately promote tumourigenesis *(Philip et al., 2013)*.

3.2 Materials and Methods

3.2.1 Setup and maintenance within the microfluidic system

The rat tissue samples used for all the experiments as part of the optimisation process were taken from a single male rat (Wistar, B&K Universal Ltd, UK). The animal was fed and watered *ad libitum* until anaesthetized (10 ml kg–1 of 10 mM sodium thiopentone, intraperitoneal) and killed under a Schedule 1 procedure by a trained animal technician prior to liver extraction. The liver was immediately sectioned into 3mm^3 pieces, placed in cryovials, snap frozen in liquid nitrogen and stored at -80°C.

The microfluidic system was set up and maintained as previously described (Section 2.4). The medium used to perfuse the rat liver throughout the entire optimisation process was William's Medium E (Life Technologies Ltd, Paisley, UK). The effluent was collected as described in section 2.4 and LDH levels calculated as described in section as described in section 2.9. Termination of the experiment took place as described in section 2.4. The tissue cryostat sectioning and H&E staining were performed as described in section 2.6 and 2.7 respectively.

3.2.2 5-Bromo-2'-deoxyuridine (BrdU) perfusion

In order to determine the optimum perfusion time for bromodeoxyuridine into the rat liver tissue for immunohistochemical detection of proliferation (Section 2.8), the microfluidic system and stored liver tissue was set up and maintained as previously described (Section 2.4). After a period of 23 hours, the syringe containing the perfusion medium was replaced with another syringe containing medium with a concentration of 10µM BrdU (5-Bromo-2'-deoxyuridine, Sigma-Aldrich Company Ltd, Dorset, UK). The microfluidic device was run for a further incubation period of either 1, 6 or 24 hours before terminating the experiment.

The frozen tissue sections (section 2.6) were placed in a metal staining rack and fixed in pre-cooled (30 minutes at -20°C) 100% methanol (VWR) for 20 minutes at -

20°C. The cells were then subject to DNA denaturation and the histone proteins removed by placement in 2M HCl for 30 minutes followed by neutralisation in 2 x borate buffer (Appendix 1) pH 8.4 for 10 minutes. The slides were then rinsed in TBS and the experiment continued as described in section 2.8. The primary antibody used was mouse anti-BrdU antibody (IgG1; 0.5 mg/ml; AbD Serotec, UK) diluted in a ratio of 1:50; and the matched isotype control antibody was mouse IgG1 (AbD Serotec, UK) diluted in a ratio of 1:100. The immunohistochemistry was completed as described in section 2.8.

Positive staining with BrdU incorporation was seen as a brown colour change in the nuclei. Selected sections were analysed to show BrdU incorporation and was assessed visually (n=2).

3.2.3 Serum concentration in the medium

The different serum conditions investigated were: serum free medium, 0.1% bovine serum albumin (BSA), 1% foetal bovine serum (FBS; Biosera, East Sussex, UK), 5% FBS and 10% FBS. For each serum condition, the microfluidic system was maintained for 24 hours, 2 days and 4 days. The experiments were repeated (n=2) to show reproducibility of results.

3.2.4 Flow rates supplying the microfluidic system

The flow rates investigated were 2µl, 5µl, 7µl, 10µl, 12µl and 15µl/minute. The experiments were repeated to show reproducibility of results (n=2).

3.2.5 Hydroxyethyl piperazineethanesulfonic acid (HEPES) buffer

It was determined whether the addition of 30mM HEPES (hydroxyethyl piperazineethanesulfonic acid; PAA Laboratories, Yeovil, Somerset) was required to help the buffering capacity of William's Medium E with 10% FBS. The microfluidic system was set up with rat liver as described previously (section 2.4) and maintained for 4, 5 and 6 days. The experiment was repeated (n=2) to show reproducibility of results.

3.2.6 Oxygen tension in the medium

Under sterile conditions in a laminar flow cabinet (ESCO Airstream E series cabinet, Wiltshire, UK), William's Medium E with 10% FBS and 30mM HEPES was placed in a glass bottle. An oxygen cylinder (99.5 % purity, BOC Industrial Gases, UK) was connected to rubber tubing; and the end was placed in the laminar flow cabinet and attached to a sterile glass pipette. This pipette was placed in the bottle containing medium and covered with foil. Oxygen flow was commenced at a rate of 0.5l/minute and continued for 5 minutes. Once complete, the medium was used to perfuse the microfluidic system containing the rat liver and thereafter maintained as described in section 2.4. The experiment was repeated (n=2) to show reproducibility of results.

3.2.7 Summary

Parameters Assessed	Techniques Used	Number performed
Duration (1-9 days) rat liver could be maintained in the microfluidic device	LDH, H&E staining	LDH (n=9) H&E (n=9)
BrdU incorporation (1, 6, 24 hrs & negative control)	BrdU IHC	n=8
Serum concentration (serum free, 0.1%, 1%, 5% and 10%) at 1, 2 & 4 days	BrdU IHC	n=15
Varying flow rates (2, 5, 7, 10, 12 & 15ul/min) at 4 days	BrdU IHC, H&E staining	n=12
Effect of HEPES buffer at days 4, 5 & 6	BrdU IHC, H&E staining	n=6
Effect of oxygen tension at days 4, 5 & 6	BrdU IHC, H&E staining	n=6

Figure 3.1 A flow chart representing the parameters assessed, techniques used and the number of times the experiments were performed as part of the optimisation process of the microfluidic system (LDH – lactate dehydrogenase, BrdU – bromodeoxyuridine, IHC – immunohistochemistry, H&E – haematoxylin and eosin, n – number).

3.3 Results

3.3.1 Evaluation of the duration of maintenance of rat liver tissue

The levels of LDH release from rat liver maintained over one to nine days in a microfluidic device are shown in Figure 3.2.

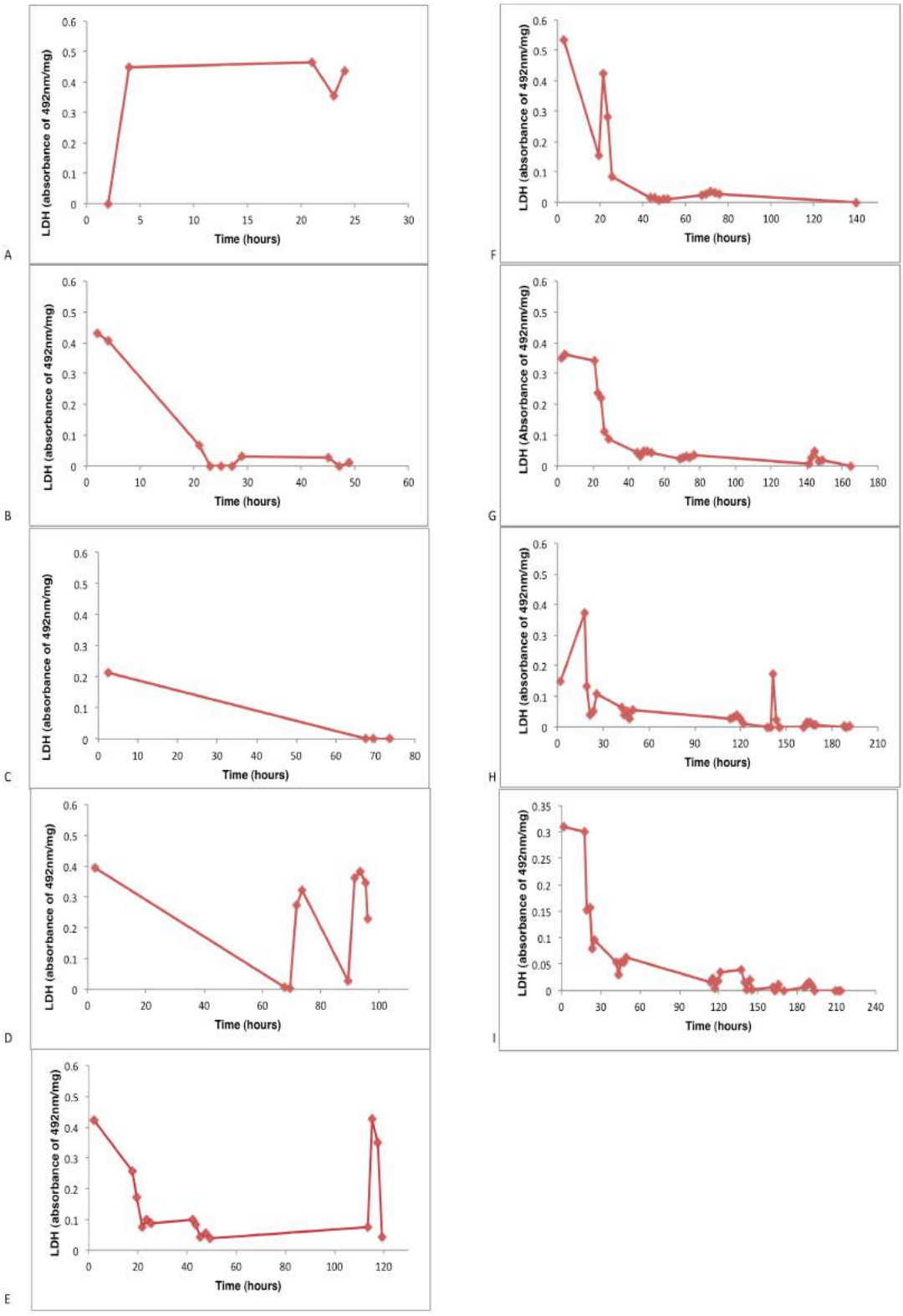

Figure 3.2 Graphs showing the absorbance of the formazan product formed following the enzymatic conversion of a tetrazolium salt catalysed by LDH. A) – I) show the different release patterns following different periods of incubation of rat liver tissue within the device. A) Day 1 - I) Day 9. Each graph represents separate experiments set up on different days. Each point on each graph represents an average of duplicate readings of the same sample.

In all of the experiments the LDH tended to be high from the offset. However, between 20 – 30 hours, the LDH levels generally decreased and remained relatively low throughout the remainder of the experiments. The rat liver tissue that had been in the microfluidic system for 4 and 5 days had LDH spikes in the final 26 hours and 6 hours of the experiments respectively; and the rat liver tissue that had been in the microfluidic system for 6 – 9 days, showed small LDH spikes in the latter part of the incubation in the microfluidic system.

An undergraduate colleague had undertaken the above study as part of their thesis and repeated the experiments three times. The study showed that LDH release was higher at the beginning of the experiment but gradually lowered throughout the incubation period (figure 3.3).

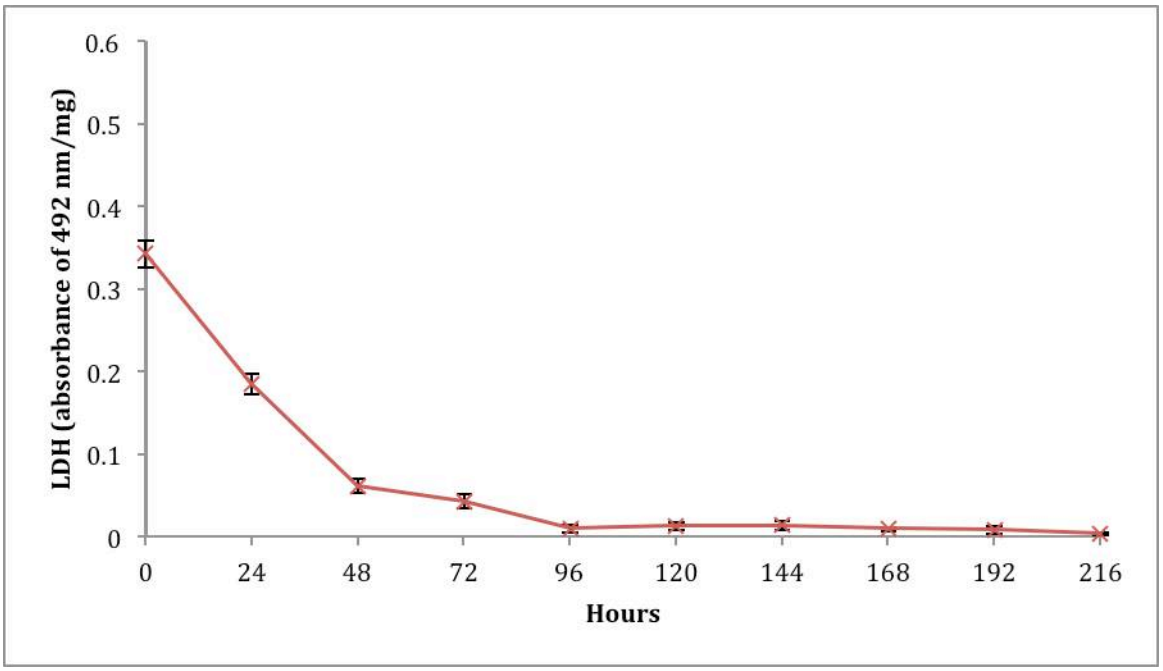

Figure 3.3 A graph showing the absorbance of the formazan product formed following the enzymatic conversion of a tetrazolium salt catalysed by LDH.

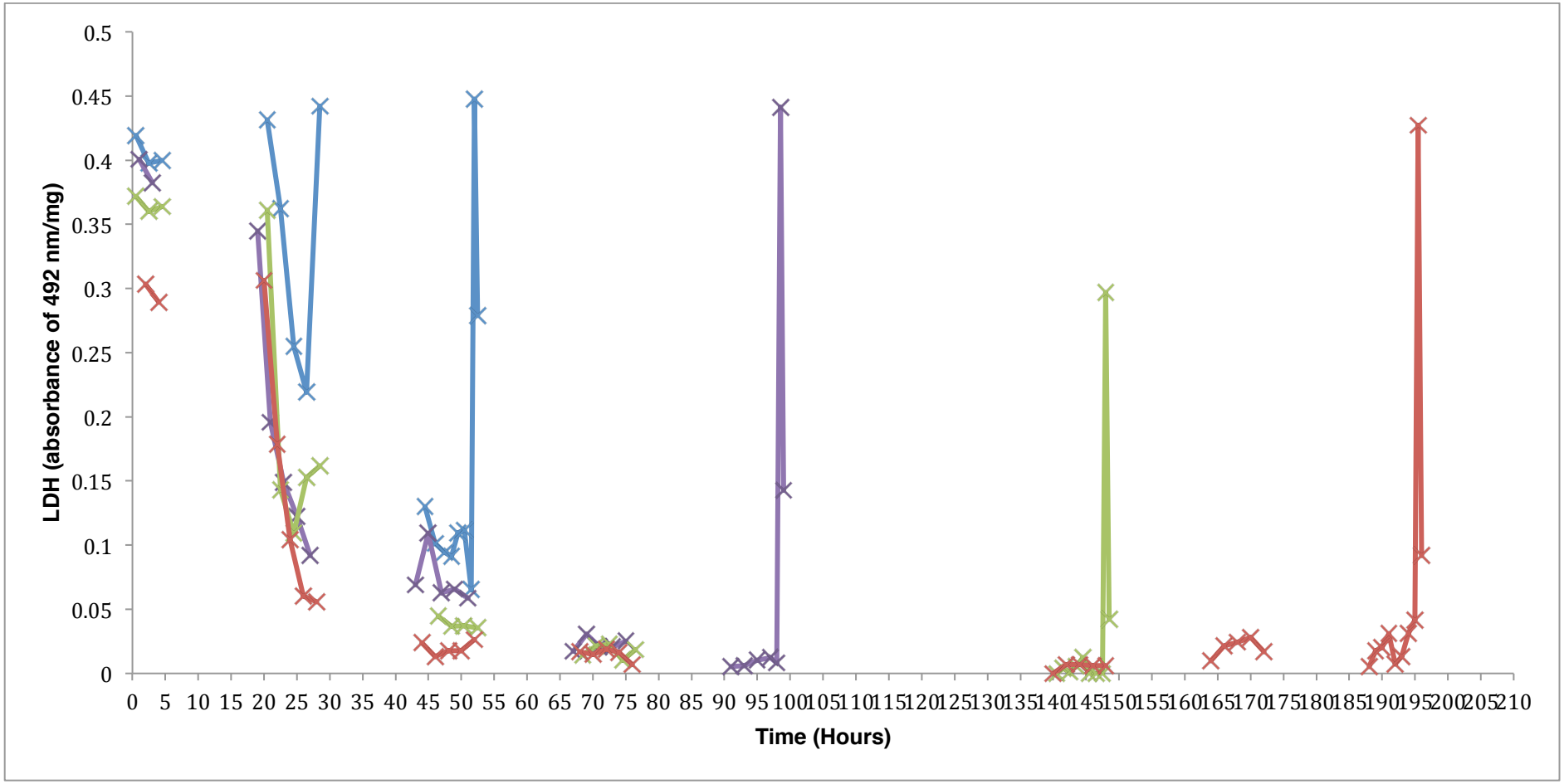

Figure 3.4 A graph showing the effect of addition of the lysis reagent and subsequent LDH release. Blue – day 2, purple – day 4, green – day 6, red – day 8.

As can be seen, LDH release was observed in all the tissues where lysis reagent had been added (figure 3.4).

Representative images of the haematoxylin and eosin staining of the rat liver following incubation for different lengths of time in the microfluidic device are shown in Figure 3.5.

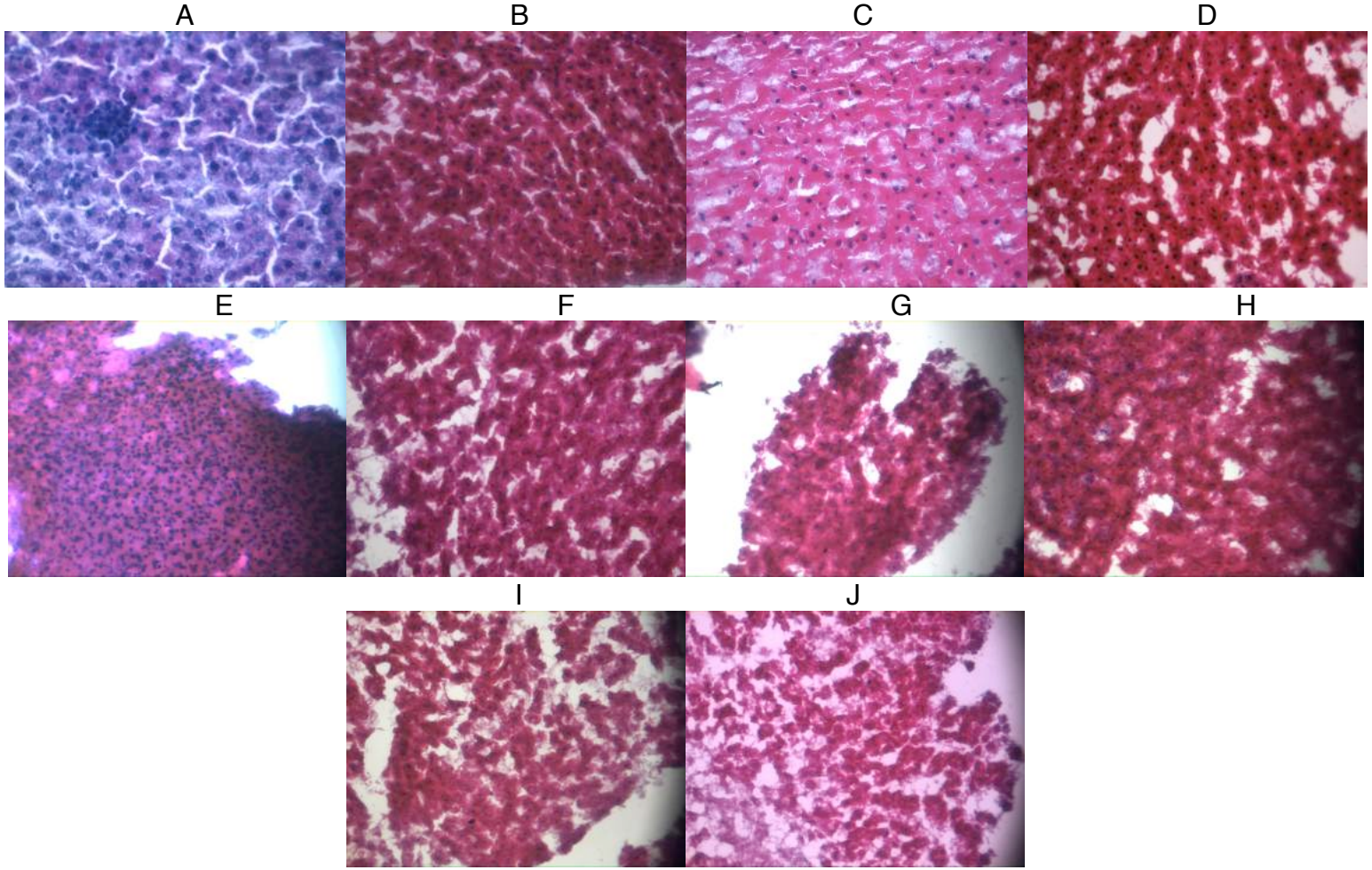

Figure 3.5 Haematoxylin (Blue) and eosin (Pink) staining of rat liver following different lengths of incubation in the microfluidic device and cryostat sectioning at 8μm. A) Control (not incubated in the microfluidic device), B) Day 1 – J) Day 9. Magnification x400.

Rat liver tissue in the microfluidic device at days 1,2 and 3 displayed some loss of cohesion of the tissue. The nuclei were visible and there was no change in their shape. At day 5 however there are signs of distortion of the architecture and the nuclei not being prominent. Thereafter however, the tissue architecture was not as well maintained and there was loss of nuclei with poorer evidence of haematoxylin staining of the nuclei.

3.3.2 Assessment of the optimal time for the BrdU asay

Positive BrdU incorporation was seen as the nuclei stained a brown colour. This was visually assessed at a higher magnification (x400). Incorporation was noted at 1 hour, 6 hours and 24 hours. However, it was most prominent with rat liver tissue that was perfused for 6 hours with BrdU (figure 3.6).

Although reproducibility of the results was proven (n=2) one problem that was encountered repeatedly was that of background staining. This was seen as a diffuse brown colour evident throughout the tissue section and made it difficult to analyse if true BrdU incorporation in the nuclei had occurred or not (figure 3.6, C, x400). In order to address this problem several parameters were changed as shown in table 3.3.

Fresh solutions once made were used 3 times only then disposed
Reducing the time (from 30 minutes to 15 minutes) the slides spent in 2M HCl to allow the DNA to be denatured and histone proteins removed
Thoroughly deep cleaning the equipment used throughout the experiments
Ensuring any materials used throughout the immunohistochemical staining were in date and not expired

Table 3.3 A table representing the parameters that were changed to address the problems with BrdU incorporation.

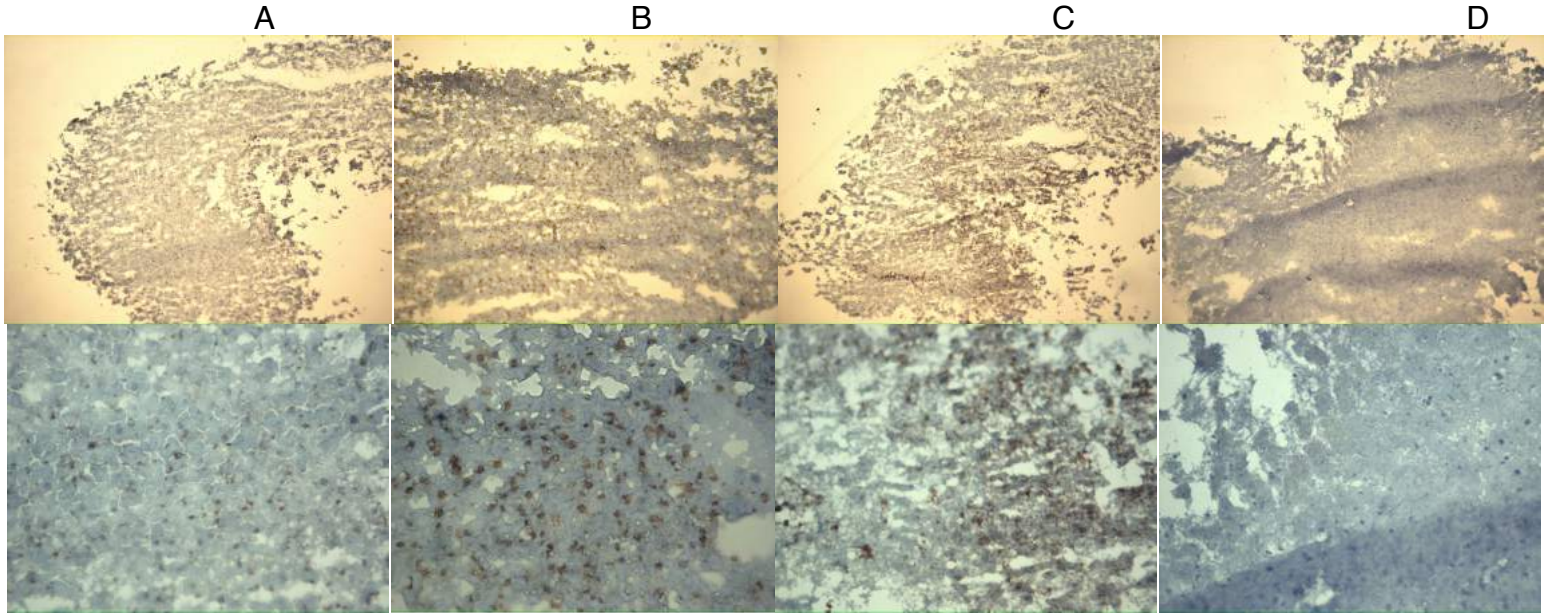

Figure 3.6 Photomicrographs of rat liver tissue which has been maintained in a microfluidic device for 23 hours followed by a further perfusion with medium containing 10μM BrDU for A) 1 hour, B) 6 hours and C) 24 hours. D) shows the negative control. Anti-BrdU immunohistochemistry identifies the incorporated BrdU (brown) indicating the proliferating cells. Blue haematoxylin counterstain. Magnification x100 (above) and x400 (below) (n=2).

3.3.3 Serum concentration in the medium

It was noted that for each serum concentration, BrdU incorporation was evident following both 24 and 48 hours of incubation in the microfluidic device (figure 3.7). At 96 hours however, BrdU incorporation was not evident (table 3.4) (n=2)

Concentration of Serum	**Incubation period in the microfluidic system (hours)**	**BrdU Incorporation**
Serum free	24	Yes
	48	Yes
	96	No
0.1% BSA	24	Yes
	48	Yes
	96	No
1% FBS	24	Yes
	48	Yes (nuclei few in number)
	96	No
5% FBS	24	Yes
	48	Yes
	96	No
10% FBS	24	Yes
	48	Yes
	96	No

Table 3.4 A table representing the outcomes of BrdU incorporation with varying sera and incubation periods of 24, 48 and 96 hours respectively.

A

B

C

D

E

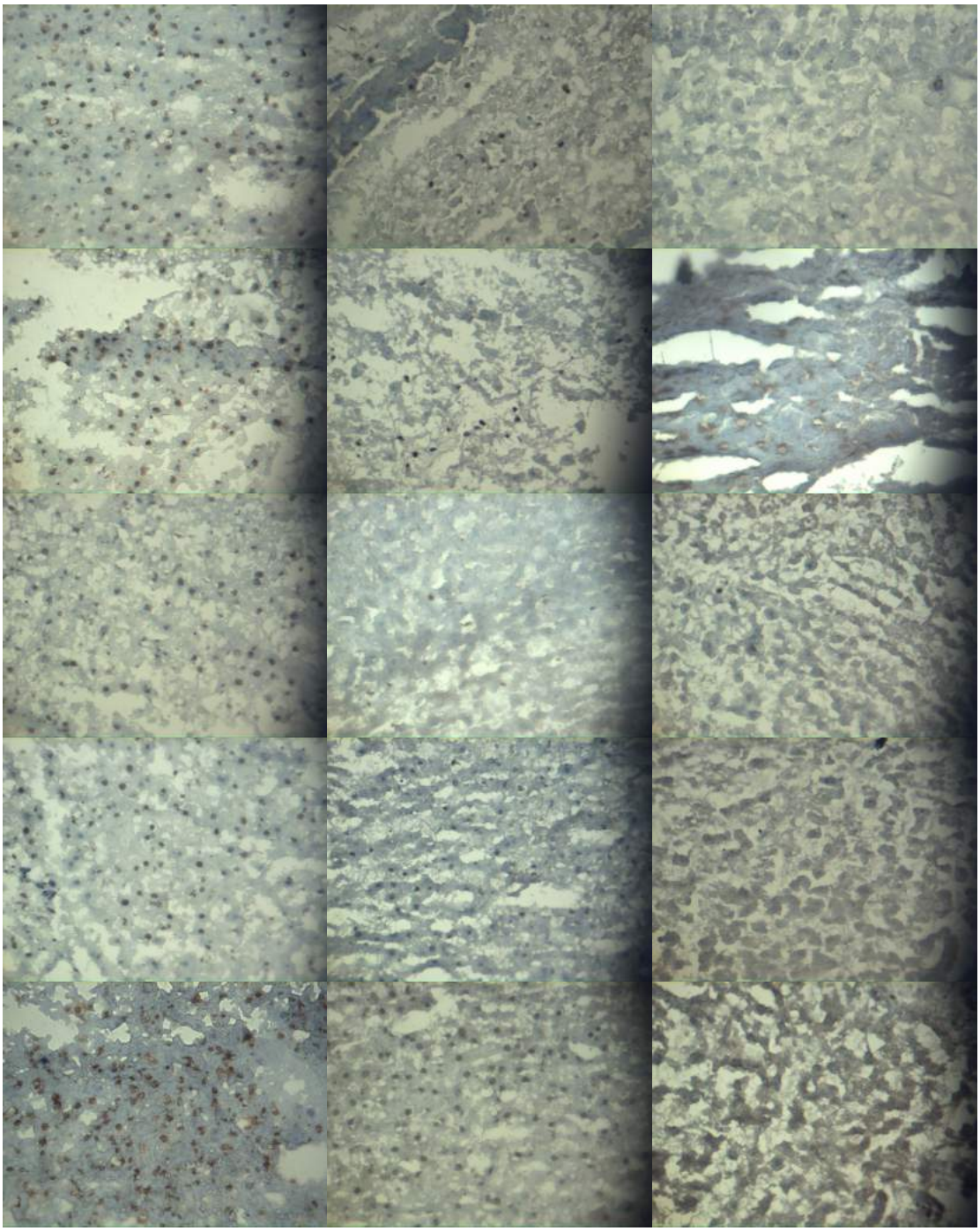

Figure 3.7 Photomicrographs showing rat liver maintained in a microfluidic device for 24 hours (left), 48 hours (middle) and 96 hours (right) with A) serum free medium, B) 0.1% BSA, C) 1% FBS, D) 5% FBS and E) 10% FBS in the perfusion medium, following 6 hours of BrdU incorporation and anti-BrdU immuohistochemistry (brown). Haematoxylin counterstain (blue). Magnification x400.

3.3.4 Flow rates supplying the microfluidic system

Figure 3.8 shows representative photomicrographs of rat liver tissue maintained in the microfluidic device following exposure to different perfusion flow rates. Clearly defined blue nuclei were evident in the rat liver sections from the tissue maintained at flow rates up to and including 12µl/minute. However, at 15µl/minute the nuclei were no longer clearly defined and only a small impression of a nucleus is evident with the vast majority of the section being eosin stained only (n=2).

Comparing the BrdU stained slides, BrdU incorporation was noted at flow rates of 2µl, 5µl, 7µl, 10µl and 12µl/minute. With the flow rate of 5µl/minute, BrdU incorporation was seen however the nuclei were few in number. No BrdU incorporation was seen with 15µl/minute.

A

B

C

D

E

F

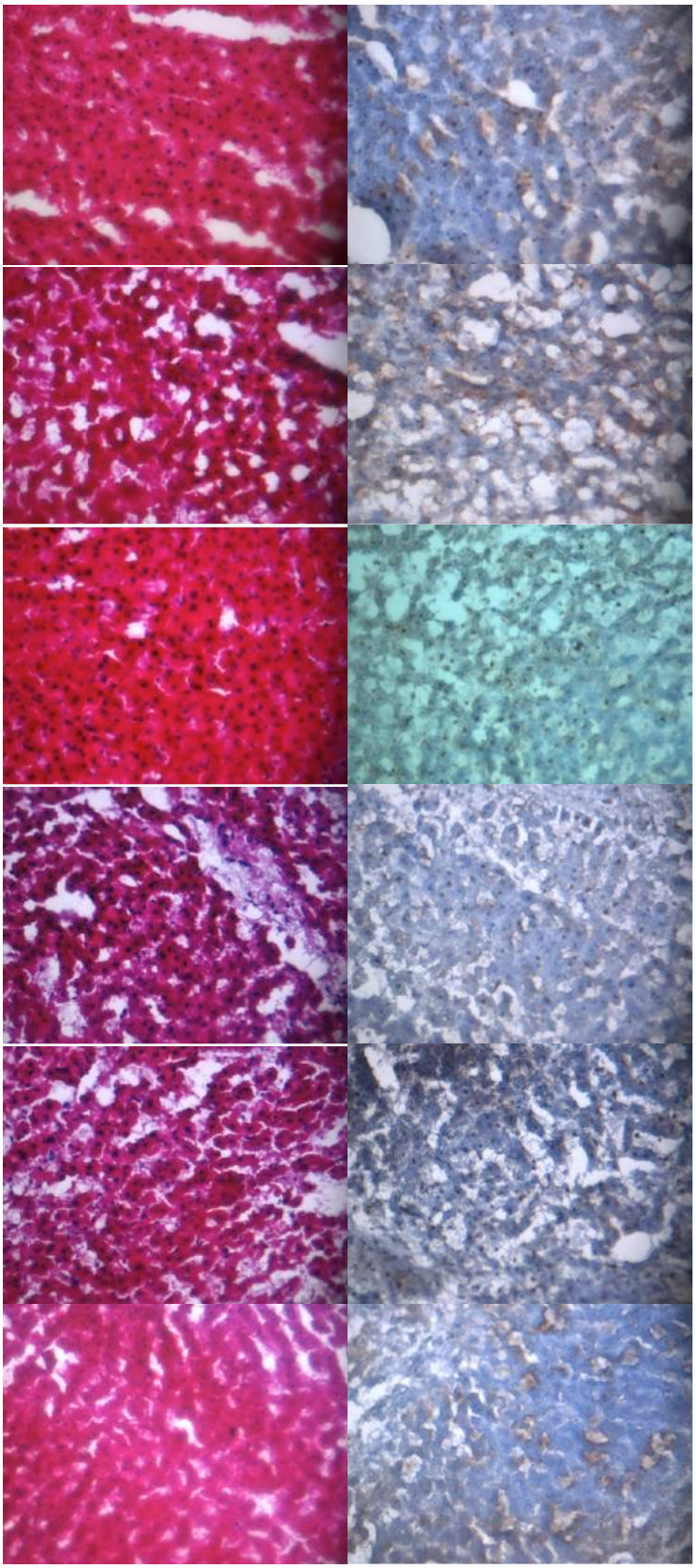

Figure 3.8 Images of rat liver maintained for 4 days in a microfluidic device and subjected to various flow rates following both H&E staining and BrdU immunohistochemistry. A) 2ul/min, B) 5ul/min, C) 7ul/min, D) 10ul/min, E) 12ul/min, F) 15ul/min. Magnification x400.

3.3.5 HEPES buffer

Following H&E staining the nuclei in the tissue section were clearly evident surrounded by pink cytoplasm following days 4 and 5 of incubation with William's E Medium and HEPES, but this was not the case for day 6 (figure 3.9). BrdU incorporation is also seen following 4 and 5 days of incubation but not after day 6. At day 6 all that can be seen is background staining and cytoplasm, there is no evidence of nuclei being present (figure 3.9) (n=2).

A

B

C

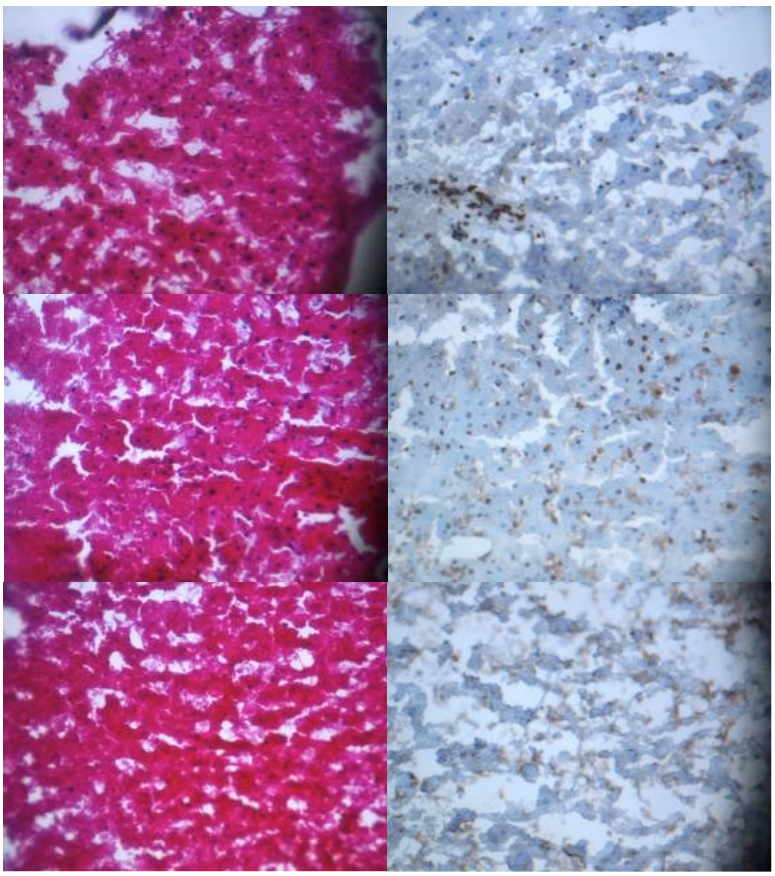

Figure 3.9 Images of sections of rat liver having been perfused with William's E Medium containing HEPES, for A) 4 days, B) 5 days and C) 6 days in a microfluidic device. They were exposed to H&E staining (left) and BrdU IHC (right). Magnification x400.

3.3.6 The oxygen tension in the medium

Following 4, 5 and 6 days of incubation, the architecture of the rat liver tissue demonstrated loss of nuclei; and all that was present was the eosin stained cytoplasm (Figure 3.10). There was lack of cellular cohesion seen and in addition no convincing evidence of BrdU incorporation was observed following any of the incubation times (Figure 3.10) (n=2).

A

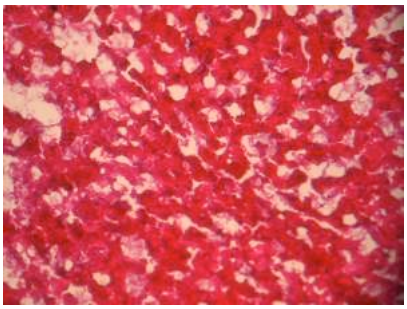

B

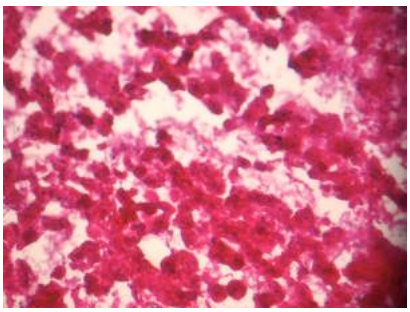

C

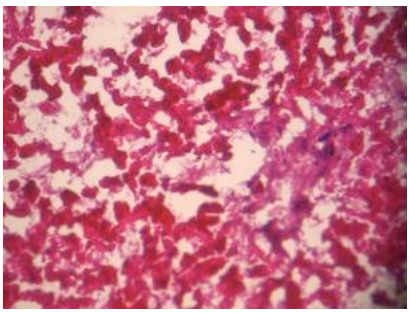

Figure 3.10 Images of sections of rat liver having been perfused with oxygenated William's E Medium containing HEPES, for A) 4 days, B) 5 days and C) 6 days in a microfluidic device. They were exposed to H&E staining. BrdU sections not displayed as no incorporation seen. Magnification x400.

3.4 Discussion

3.4.1 Evaluation of the duration of maintenance of rat liver tissue

The high levels of LDH observed within the first 24 hours were not unexpected and were attributed to the thawing and manipulation of the rat liver tissue during set up of the microfluidic experiment. Between 20 – 30 hours however, the LDH levels generally decreased when the tissue had overcome the initial trauma and became adapted to the culture conditions.

In the majority of the experiments the levels of LDH remained relatively low throughout the remainder of the experiment, however spikes of LDH release were observed during some

experiments. In some experiments the LDH rose as a result of various experimental situations (e.g. leakage of medium at the inlet, blockage of channels due to air bubbles or tissue debris), which ultimately resulted in the tissue not being perfused with the medium or there being a build up of effluent due to a distal blockage. These events explained the graph pattern obtained for tissue maintained for 5 and 6 days. However, for tissue maintained for 4, 7, 8 and 9 days, LDH spikes were seen towards the latter stages of the incubation period and no obvious problems with the device setup were recorded at the time of the experiments. It is therefore assumed that a part of the tissue in the chamber had undergone cell death and hence led to a rise in LDH release. For days 2 and 3, towards the latter part of the experiments, the LDH release decreased.

Even though the LDH graph patterns for days 7, 8 and 9 suggest that the tissue is being maintained; the H&E staining suggests that the rat liver is not in its maximum viable state as compared to the 4 – 6 day period. To ensure the rat liver tissue was viable, lysis buffer addition was performed (figure 3.4) and showed LDH release.

An undergraduate colleague repeated this experiment (n=3) and the results showed the LDH release to be high initially but then gradually decreased (figure 3.3).

These findings were in agreement with Hattersley et al. *(2008 and 2011)* who demonstrated that LDH release initially was high due to tissue handling and preparation for the microfluidic device, when using HNSCC and rat liver. Thereafter, LDH release was low indicating viable tissue. Carr et al. *(2013)* found in their study that rat liver tissue could be maintained for upto 15 days; and as in this study, the LDH cytotoxicity assay had been utilised for assessment of the tissue. The difference of 6 days between the studies could be operator dependent as the method of rat liver tissue preparation was identical. They did not however assess the morphology and proliferation following maintenance of the tissue in the microfluidic device; therefore the results in this study cannot be compared.

Based on the results of this section, in particular the H&E staining, it was felt that the rat liver tissue could be maintained up to a maximum of 6 days for the subsequent optimisation experiments.

3.4.2 Assessment of the optimal time for the BrdU assay

From the results, even though BrdU incorporation was noted at 1, 6 and 24 hours, it was most prominent at 6 hours (figure 3.6). To the author's knowledge, to date there have been no studies that have used the BrdU assay in microfluidic devices per se in assessing rat liver tissue or HNSCC. It has been used in vitro and in vivo as shown in table 3.3. From these studies, it was shown the BrdU incubation period ranged from 0.5 hours to 7 days. It has been reported that cytocidal or teratogenic effects have occurred as a result of prolonged administration of high doses of BrdU and that it may modulate DNA in an unexpected way, it has been recommended that BrdU administration be minimized to avoid unnecessary exposure *(Hoshino et al., 1985).*

For the purposes of the optimisation, it was therefore decided to utilize the BrdU infusion for a 6 hour period.

3.4.3 Serum concentration in the medium

Foetal bovine serum is a popular and good cell growth supplement and is considered as a standard supplement referred over other types of cell culture sera. As well as having a low level of antibodies, it has optimal growth factors and high nutrient levels making it an effective cell growth promoter. Serum-free formulations are ideal for short-term cultures (upto 10 days) while serum-containing medium formulations were developed for long-term cultures (several weeks) *(Shulman and Nahmias, 2013).*

BrdU incorporation was seen with all the media used in this phase of the experiment; however given that 10% FBS is considered the standard in cell culture, it was used as part of the medium for further experiments.

3.4.4 Flow rates supplying the microfluidic system

Following incubation of the rat liver tissue in the microfluidic device at all flow rate except (except 15µl/minute), BrdU incorporation was observed. On visual assessment, there was no clear difference in incorporation between the flow rates. However, at 15*µ*l/min the nuclei

were no longer evident and so incorporation of BrdU could not be observed. It is possible that with higher flow rates, the flow may have been turbulent and hence the rat liver tissue was not in a satisfactory environment in the MF system. This could be a reason for the sparse architecture observed with the H&E slides.

Schumacher et al. *(2007)* compared conventional culture methods with perfusion culture of liver tissue slices. Their study showed key protein marker expressions were more clearly detectable than in culture methods; but stated that perfusion culture system will in general be associated with shear stress that can affect the hepatocyte function. Van Midwoud et al. *(2010)* used a microfluidic-based biochip to assess drug metabolic activity using precision cut liver slices. In their study they used a flow rate of 10µl/minute. The same group *(2010b)* stated the flow rate could be varied between 4 and 50µl/minute while maintaining a high metabolic activity during the first 3 hours. Domansky et al. *(2010)* developed a bioreactor that allowed maintenance of 3D liver tissue cultures under constant perfusion and integrated multiple bioreactors into an array in a multiwall plate format. Based on previously calculated shear stress calculations, they stated a flow rate of 0.3µl/minute/channel should not exceed a shear stress of 30mPa.

From the results of this section, it was decided that the standard flow rate of 2µl/minute would continue to be utilised as no benefit was gained with the higher flow rates.

3.4.5 HEPES buffer

HEPES is a zwitterionic organic chemical buffering agent and is one of the twenty Good's buffers. It has been widely used in cell culture, as it is better at maintaining physiological pH (range 7.2 – 7.6) despite changes in carbon dioxide concentration (which is produced by cellular respiration) when compared to bicarbonate buffers (another widely used buffer in cell culture). Unlike the bicarbonate buffering system, which requires the use of a CO_2 (carbon dioxide) incubator, an advantage of using the HEPES buffering system is that it can be used with or without a CO_2 atmosphere.

Following days 4 and 5 of incubation with the medium and HEPES buffer, the nuclei are evident and architecture maintained on H&E staining and BrdU incorporation noted. HEPES buffer has been used by previous groups whom have used an identical

microfluidic device for their studies *(Hattersley et al. 2011; Hattersley et al. 2012; Carr et al. 2013)* involving rat liver and HNSCC. There is very little in the literature regarding the effectiveness of HEPES buffer in the microfluidic devices. However Elaut et al. *(2005)* performed a study to critically evaluate the influence of incubation medium on the viability and functioning of rat hepatocytes in suspension for 3 hours at 37 ^{o} C under continuous movement. They found that hepatocytes suspended in HEPES buffer and William's E Medium have a lower basal level of spontaneous cell death; and are therefore more suitable for studying apoptotic effects of xenobiotics. In addition, the relative high pH of the HEPES buffer has been found optimal for hepatic respiration, glycolysis and protein synthesis.

Considering the results obtained in this part of the optimisation process along with the above reasons, the HEPES buffer was used in the William's E medium for further experiments.

3.4.6 Oxygen tension in the medium

Oxygen is a requirement by cells for respiration *in vivo*; however, cultured cells (for example) mainly rely on glycolysis (the majority of which will be anaerobic) for their supply. The purpose of this part of the study was to see if oxygenated medium would improve the viability of rat liver tissue incubated in the microfluidic system. As can be seen from the results, the nuclei were not evident on the H&E stained sections even after only 4 days of incubation and there was also no BrdU incorporation seen in the sections that underwent the immunohistochemistry protocol. The reason for this could be the oxygen levels and oxygen tension were toxic to the tissues and hence the conditions were not viable for the tissue in the microfluidic system.

Yamada et al. *(2012)* examined the effect of the oxygen tension on the viability and function of hepatocytes in micro-organoids, on the basis that oxygen plays a vital role in hepatocyte culture. They showed that under high oxygen tension, hepatocyte viability was better than hepatocytes under lower oxygen tension. Our results are not comparable with this study.

Funamoto et al. *(2012)* introduced the use of a microfluidic device that allowed for control of the oxygen tension for the study of different 3D cell cultures. They studied the migration characteristics of human breast cancer cells (MDA-MB-231) under normoxia and hypoxia. They found the invasive behaviour of these cancer cells under hypoxia increased. This was confirmed by immunostaining against hypoxia inducible factor 1-alpha and found an increase in its expression in cancer cells compared to normoxia. These findings were echoed by Yang et al. *(2015)*.

Conclusion

At the end of the optimisation process and analysis of results, it was decided that the maximum period the tissues were to be kept in the microfluidic system was 4 days. The flow rate used was 2µl/minute, with the medium containing 10% FBS and HEPES and no additional oxygen. The time decided for BrdU perfusion prior to termination of the microfluidic experiment was 6 hours. These parameters were applied for use of head and neck squamous cell carcinoma tissue biopsies in the microfluidic system.

Chapter 4

Radiation response of HNSCC using early markers of apoptosis and proliferation, utilising a microfluidic approach

4.1 Introduction

Radiotherapy is one of the modalities used in the treatment of HNSCC. Its role depends on the site and stage of the SCC; and can be used with curative intent or as a palliative measure. There are situations where there is a lack of tumour response or only a partial response to radiotherapy; and these cases are termed radioresistant, which strongly affects the clinical outcome of HNSCC patients *(Ganci et al., 2015)*. It is a major problem as the quality of life of the patient is greatly affected and potentially subjects them to invasive surgical treatment *(Perri et al., 2015)*.

Dinshaw et al. (*2006*) demonstrated patients receiving higher doses of radiotherapy compared to those who had lower doses, had a significantly better outcome. The purpose of this section of the study was to assess the effects of differing doses of radiation on HNSCC tissue biopsies from various head and neck subsites. These consisted of the oral cavity, oropharynx, larynx, maxillary sinus and the metastatic cervical lymph node. The aim is to develop a microfluidics system that can predict a patient's tumour response prior to initiating treatment, potentially avoiding the morbidity associated with surgery.

There were 5 methods used to analyse the effects of radiation on the HNSCC tissue. LDH was measured in the effluent to assess radiation induced cell death. Haematoxylin and eosin staining was used to assess the architecture of HNSCC tissue taken straight from the patient; tissue incubated in the microfluidic device that had not been irradiated and tissue maintained in the device and had been irradiated. The BrdU assay was used to indicate if cells were replicating their DNA and therefore undergoing proliferation in the HNSCC tissue. Immunohistochemistry was performed using cytokeratins and an anti-cytokeratin monoclonal antibody.

Cytokeratins (CK) are the largest subgroup of the intermediate filament proteins and are a major component in the cytoskeleton of mammalian epithelial cells. CK can be divided into type II (basic to neutral, molecular weight 52-68kDa; CK no's 1-8) and type I (acidic,

molecular weight 40-64 kDa; CK no's 9-20) *(van der Velden et al., 1993)*. The cytokeratin antibody was used to identify the carcinomatous components in the HNSCC tissue. This was HNSCC tissue taken straight from the patient, HNSCC tissue incubated in the microfluidic device that had not been irradiated and HNSCC tissue maintained in the device and had been irradiated.

The M30 CytoDEATH™ antibody detects apoptosis in epithelially derived cells, by identifying cytokeratin 18 that has been cleaved by caspases *(Caulin et al., 1997; Leers et al., 1999)*. It was used to identify apoptosis in HNSCC tissue taken straight from the patient, HNSCC tissue incubated in the microfluidic device that had not been irradiated and HNSCC tissue maintained in the device and had been irradiated.

4.2 Materials and methods

4.2.1 Head and neck tissue sample collection

Patients were identified and HNSCC biopsies were collected as described in section 2.1. They were obtained from 4 primary sites and 1 metastatic site. The primary sites were the tonsil, supraglottis, floor of mouth and the maxillary sinus; and the metastatic site was a lymph node. Patients were excluded from the study if they met the criteria described in section 2.2.

4.2.2 The microfluidics system and irradiation administration

The microfluidic device was setup and maintained with the HNSCC tissue as described in sections 2.3 and 2.4. It was transported to the radiotherapy suite and irradiated using the Varian Medical Linear Accelerator as described in section 2.5. In each experiment, 4 samples from each site were irradiated with single doses of 5 Gy, 10 Gy, 15 Gy and 20 Gy. A control sample that was maintained in the microfluidic device was not irradiated. The experiment was repeated 3 times for each site and they were completed as described in section 2.4.

4.2.3 Tissue cryostat sectioning, LDH assay and Haematoxylin and Eosin staining

The tissue specimens and subsequent sections were prepared as described in section 2.6. The sections underwent haematoxylin and eosin staining as described in section 2.7. The LDH assays were performed on all effluent samples, collected from irradiated and non-irradiated tissues maintained in the microfluidic devices.

4.2.4 Immunohistochemistry and analyses

The HNSCC frozen tissue sections underwent pancytokeratin and M30 CytoDEATH™ immunohistochemistry as described in section 2.8. The pancytokeratin immunohistochemistry was performed using a mouse monocloncal anti-human antibody (1.16 mg/ml; clone MNF116, Dako, Cambridgeshire, UK) and the matched isotype control antibody was mouse IgG1 (AbD Serotec, UK); both diluted in a ratio of 1:100. The M30 CytoDEATH™ immunohistochemistry was performed using a mouse monoclonal antibody (0.05 mg/ml; clone M30; IgG2b; Peviva, UK) and the matched isotype control antibody was mouse IgG2b (AbD Serotec, UK); both diluted in a ratio of 1:100.

This was performed on HNSCC tissue not incubated in the microfluidic device, tissue incubated in the device but not irradiated and tissue incubated and irradiated. The apoptotic labelling indices were calculated as described in section 2.9. HNSCC tissues that were incubated in the microfluidic device whether irradiated or not, underwent BrdU immunohistochemistry as described in section 2.8. The analysis was different here as the BrdU incorporation was not to the level achieved with the rat liver. Therefore 5 areas at x400 magnification were chosen to represent the areas of incorporation

4.3 Results

4.3.1 Maintenance of HNSCC tissue in the microfluidics system by measuring LDH release

Figure 4.1 shows the LDH release pattern from HNSCC tissue maintained in the microfluidic device (n=15). Typically the levels of LDH released would rise initially; however at 18 – 20 hours they would decrease but remain at minimal yet detectable levels throughout the incubation period. The results are similar to LDH release patterns found in the rat liver maintained in the microfluidic device. The LDH is detected due to cell death and the graph shows the HNSCC tissue is maintained.

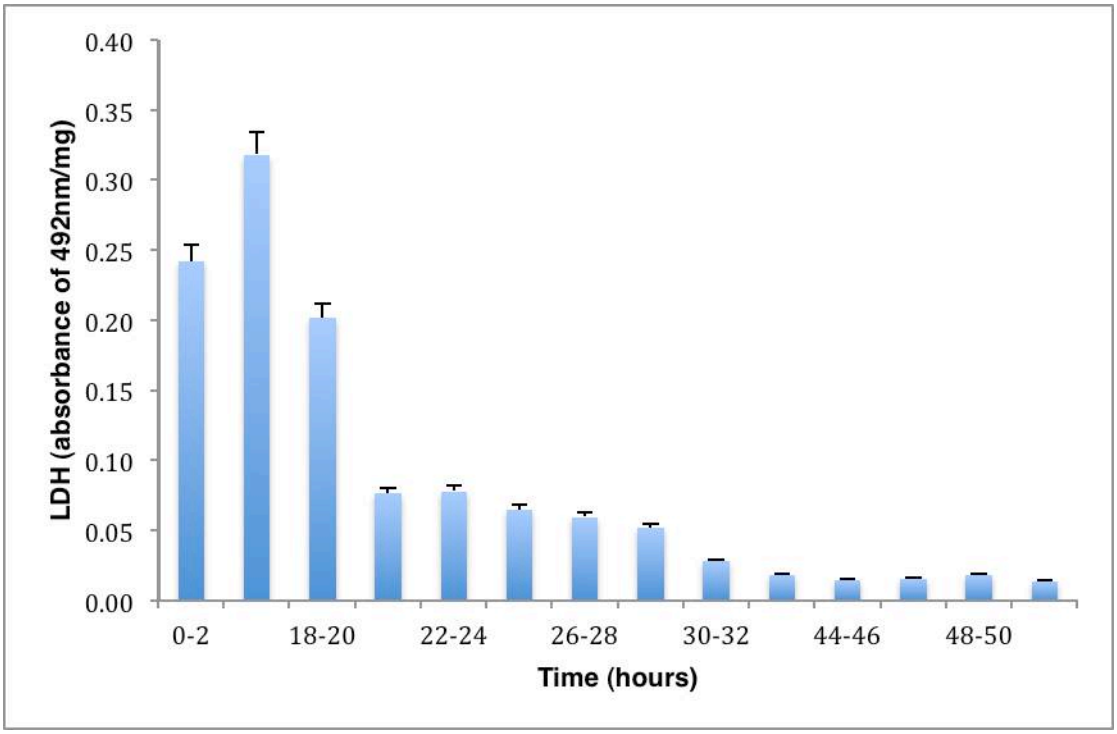

Figure 4.1 A graph showing the LDH assays performed on effluent from non-irradiated HNSCC tissue maintained in the microfluidic device (n=15).

Figure 4.2 shows the LDH release pattern from HNSCC tissue maintained in the microfluidic device (n=5), with the lysis reagent added 6 hours prior to termination of incubation. In a similar fashion to the rat liver tissue, the graph shows the LDH levels rise post lysis addition, however this was not statistically significant (p=0.123) (paired T-test).

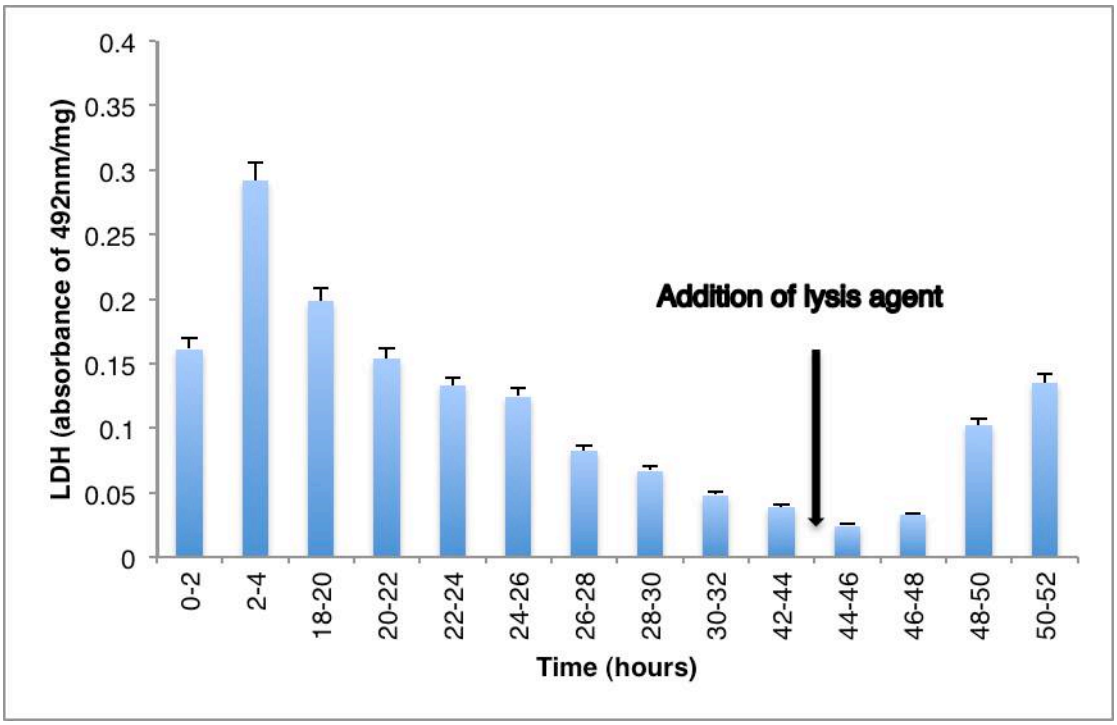

Figure 4.2 A graph showing the LDH assays performed on effluent from non-irradiated HNSCC tissue maintained in the microfluidic device (n=5) and the lysis agent added 6 hours prior to termination of the experiment.

4.3.2 Irradiation of HNSCC tissue in the microfluidics system and measuring LDH release to analyse cell death

HNSCC tissues from five subsites (oral cavity, oropharynx, larynx, maxillary sinus and the metastatic cervical lymph node) were each irradiated with single doses of 5Gy, 10Gy, 15Gy and 20Gy. This was performed three times for each subsite. For the larynx HNSCC tissue, this was performed three times at 10Gy but twice at 5Gy, 15Gy and 20Gy. This was due to a lack of available tissue.

Figures 4.3 and 4.4 show the LDH release patterns from all HNSCC subsites exposed to the increasing doses of irradiation. The graphs demonstrate an initial rise then fall in LDH in the first 24 hours of incubation, similar to the rat liver and non-irradiated HNSCC tissue in the microfluidic device. Post irradiation, there is an initial increase in LDH seen in HNSCC tissue that received 5Gy (p=0.089) and 10Gy (p=0.292) but not with 15Gy

(p=0.701) and 20Gy (p=0.601). There was no overall statistical significance (p=0.275) in LDH levels pre and post irradiation.

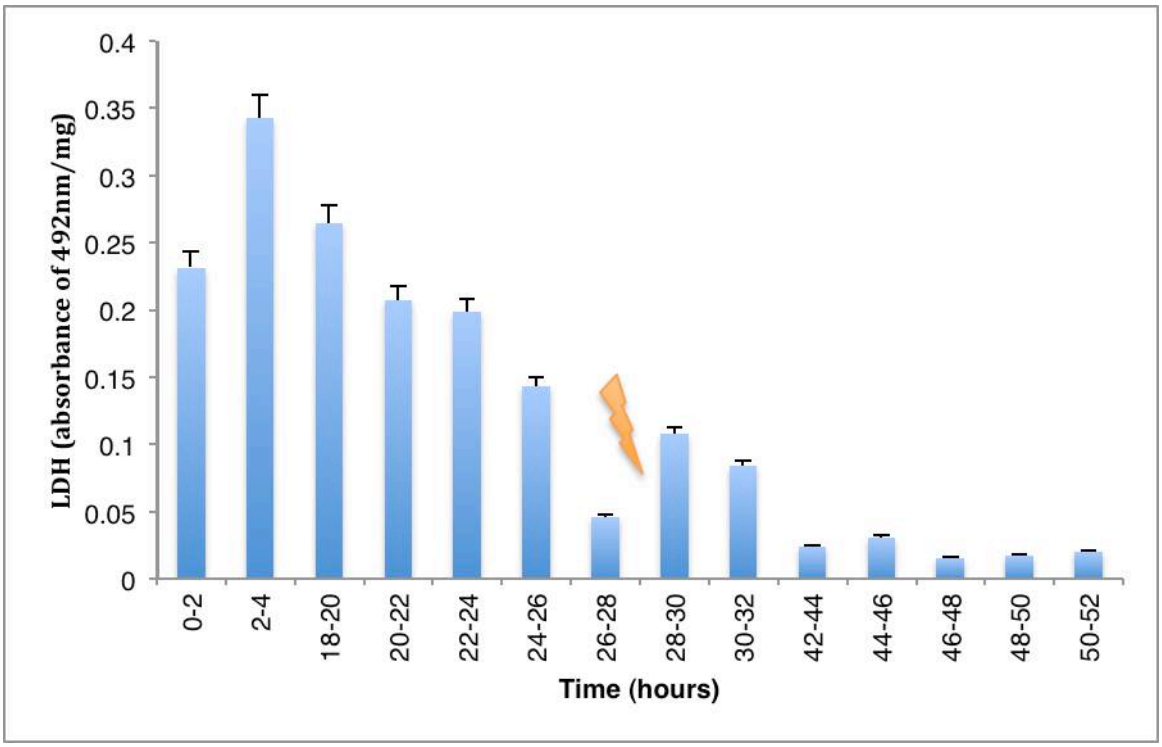

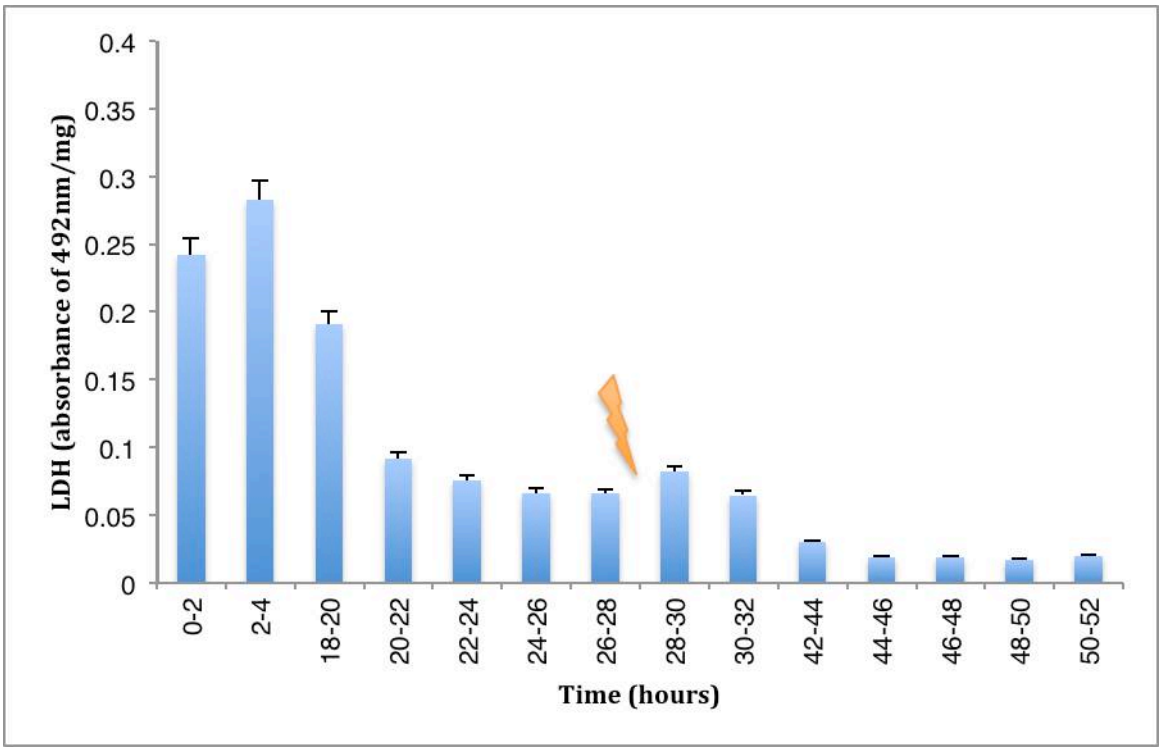

Figure 4.3 Graphs showing LDH assays performed on effluent obtained from HNSCC tissue. The top graph shows HNSCC tissue irradiated with 5Gy (n=14) and the bottom graph shows HNSCC tissue irradiated with 10Gy (n=15).

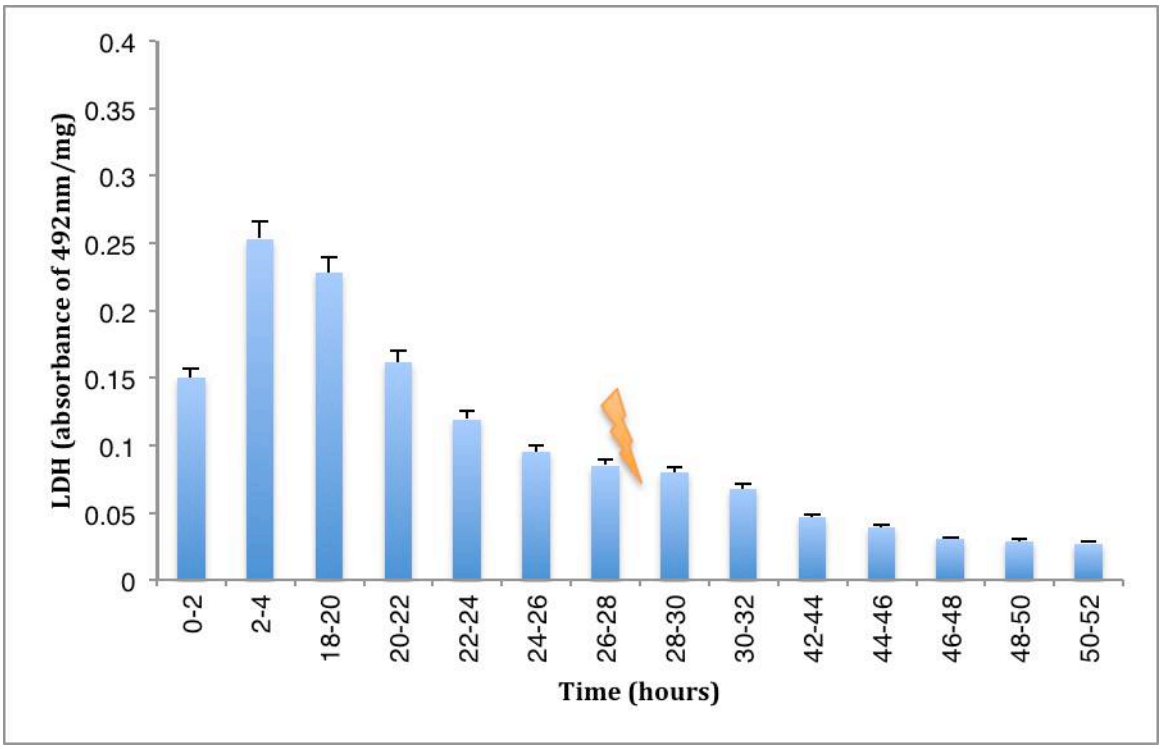

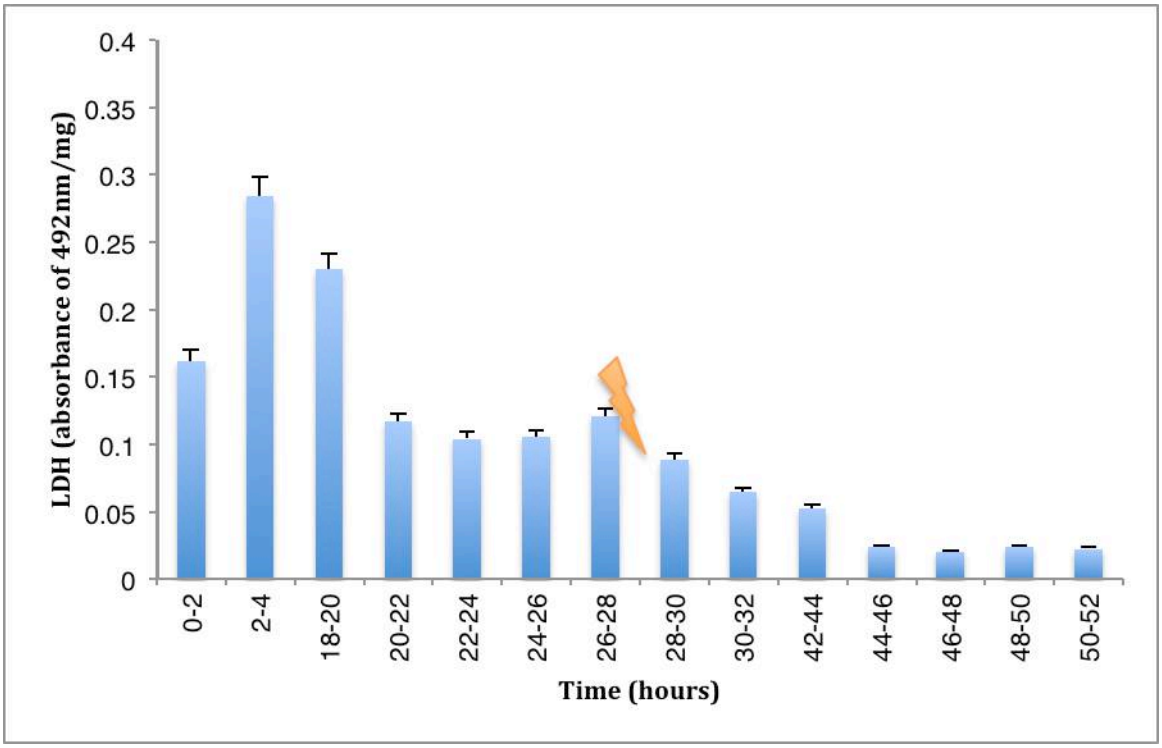

Figure 4.4 Graphs showing LDH assays performed on effluent obtained from HNSCC tissue. The top graph shows HNSCC tissue irradiated with 15Gy (n=14) and the bottom graph shows HNSCC tissue irradiated with 20Gy (n=14).

4.3.3 The effects of irradiation on the morphology of HNSCC tissue in the microfluidic device

All pre-microfluidic and control HNSCC tissue specimens maintained their architecture and morphology. The maxillary sinus, oral cavity and metastatic lymph node at 5Gy and 10Gy exposure showed no obvious changes; however after exposure to 15Gy and 20Gy, some loss of intercellular cohesion could be seen. The oropharynx and laryngeal HNSCC tissues showed more obvious when exposed to all doses of irradiation. There is loss of cohesion in the tissues but also change in the number of the nuclei. Figure 4.5 shows an example of the metastatic lymph node compared with the oropharyngeal tissue.

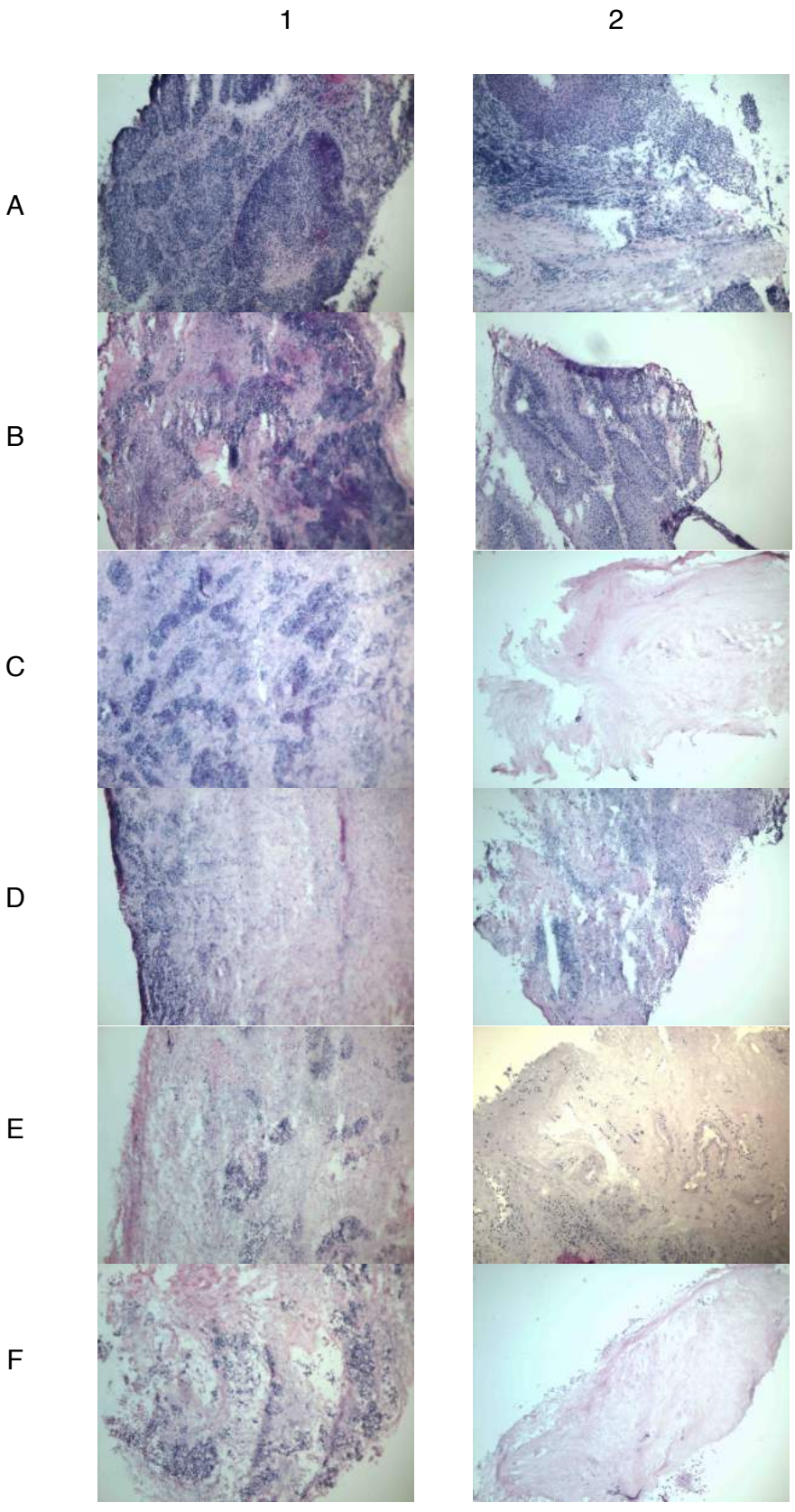

Figure 4.5 Column 1 represents the metastatic lymph node and column 2 the oropharyngeal tissue. A) pre MF B) control C) 5Gy D) 10Gy E) 15Gy F) 20Gy. This shows how the oropharyngeal tissue has reacted to the irradiation compared with the cervical lymph node.

4.3.4 Detection of 5-bromo-2-deoxyuridine (BrdU) as a marker of proliferation

Increased BrdU incorporation with the oropharyngeal and laryngeal tissues observed and calculated compared with the metastatic lymph node. Statistically there was a difference between BrdU incorporation in the metastatic lymph node and the oropharynx *(p=0.012)* and the larynx and oropharynx *(p=0.047).* Statistically there was no significant difference between the metastatic lymph node and the larynx *(p=0.165)*. These results however are based on a small number experiments where BrdU incorporation was noted (n=2 metastatic lymph node, n=1 oropharynx, n=1 larynx) (figure 4.6 and figure 4.7)

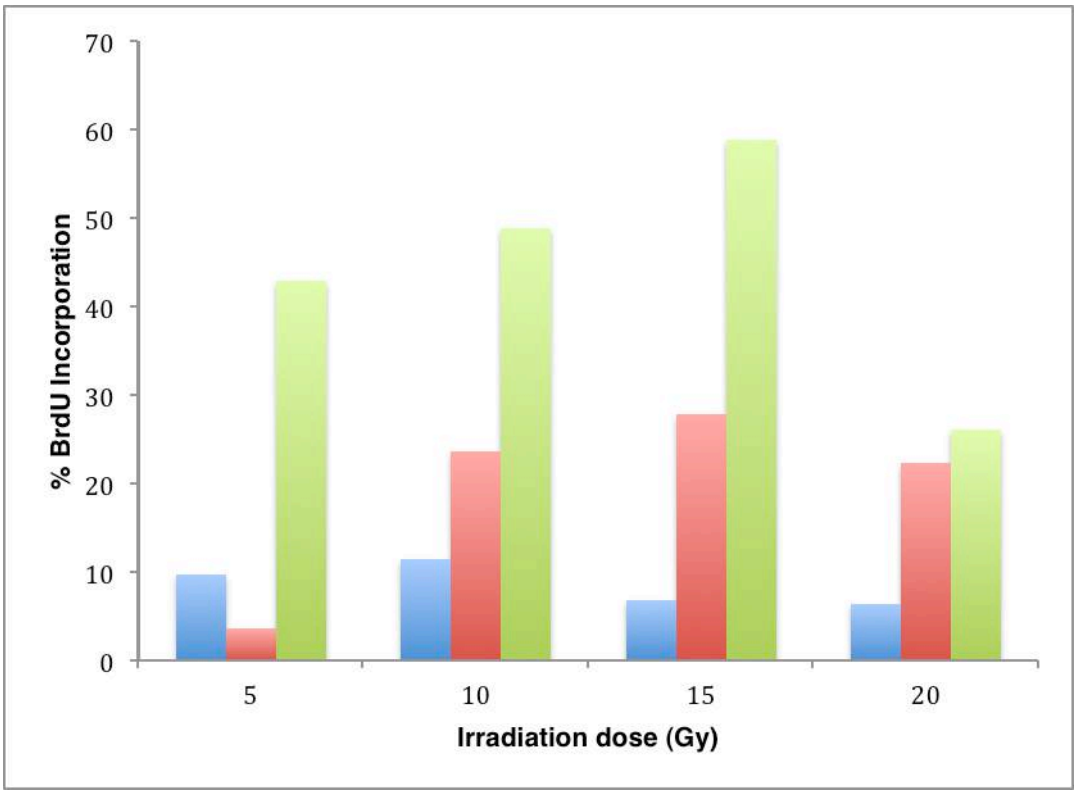

Figure 4.6 A graph representing the percentage of BrdU incorporation. Blue - metastatic lymph node, red – oropharynx, green – larynx.

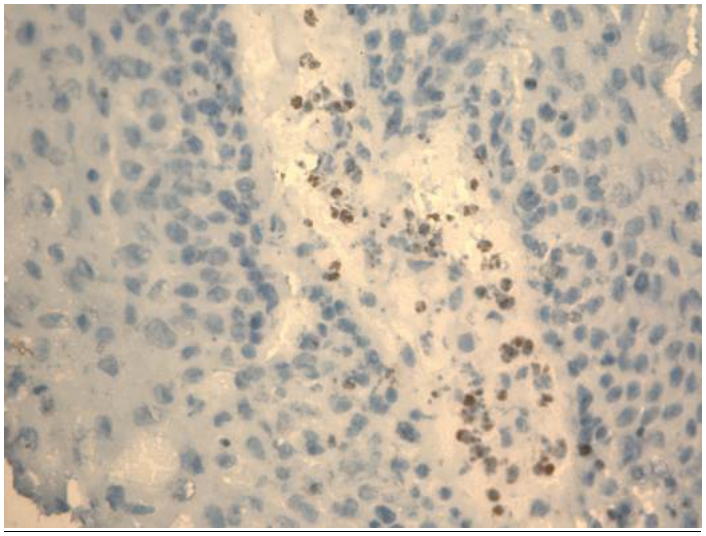

Figure 4.7 An example of BrdU incorporation in the oropharyngeal tissue showing the nuclei as a brown colour.

4.3.5 Detection of pancytokeratin and the M30 antibody as a marker of apoptosis

From figure 4.8, it can be seen the apoptotic indices (AI's) are generally low for the pre-microfluidic samples. The highest was 21.52% for the maxillary sinus sample on the third set of experiments. It is assumed the part of the tissue has undergone apoptosis while undergoing the thawing and freezing process prior to cryostat sectioning. The AI's for the maxillary sinus and oropharynx control samples are low. The highest AI's in the controls obtained were for the larynx control specimens (56.78%). Apoptosis could explain these results however this did not correlate with the LDH values and H&E staining.

From the results it could be seen there was not a dose dependent relationship and that apoptotic indices would vary for the same subsite from the same patient. The largest difference noted was for the larynx. The lowest value was 15.13% and the highest 59.12% after irradiation with 10Gy. Even though these differences were observed, statistically there was no significant difference between the apoptotic indices obtained for the 5Gy, 10Gy, 15Gy or 20Gy. Of significance was the difference between the pre microfluidic samples and 10Gy ($p=0.038$) and between the pre-microfluidic samples and 15Gy ($p=0.039$).

A

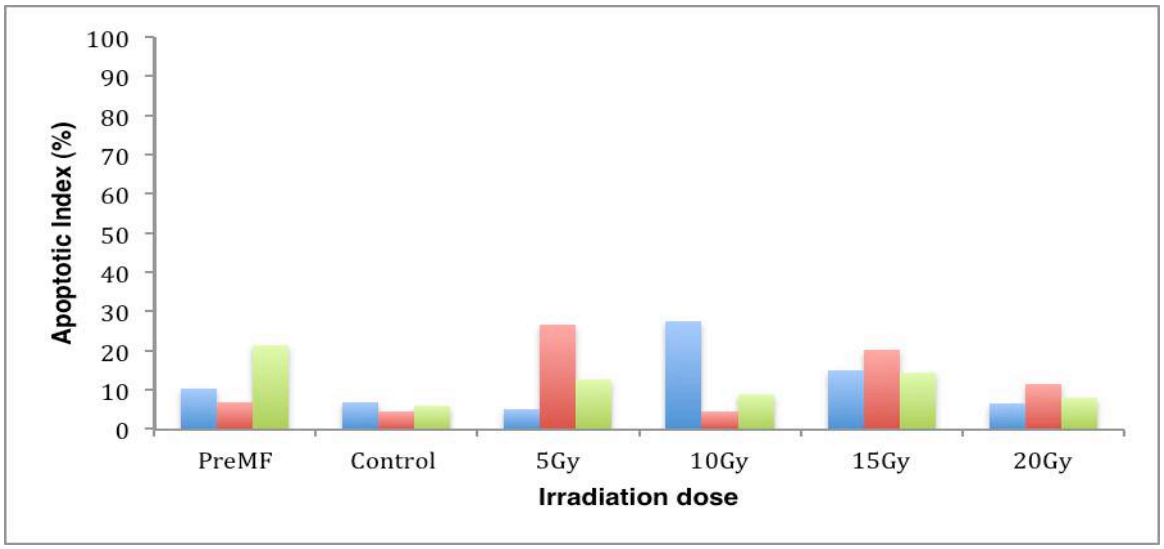
Apoptotic Index (%)
100
90
80
70
60
50
40
30
20
10
0
PreMF
Control
5Gy
10Gy
15Gy
20Gy
Irradiation dose

B

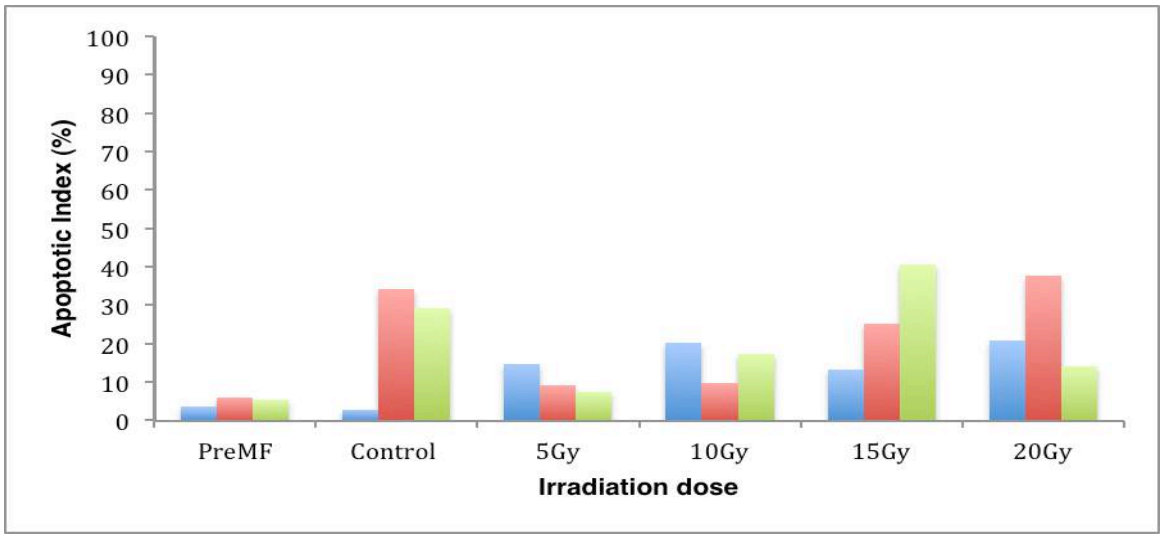
Apoptotic Index (%)
100
90
80
70
60
50
40
30
20
10
0
PreMF
Control
5Gy
10Gy
15Gy
20Gy
Irradiation dose

C

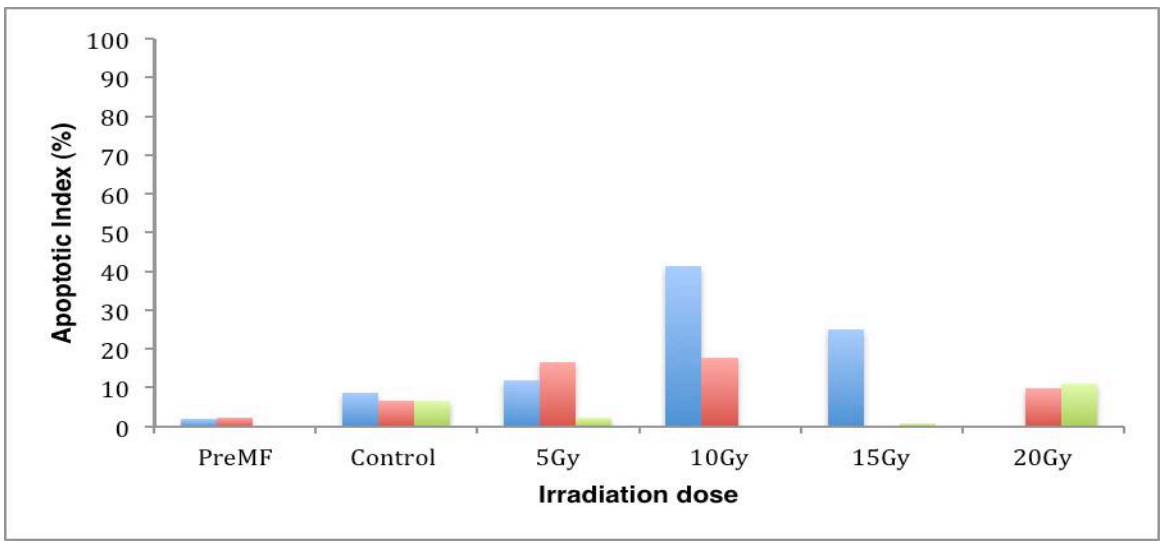
Apoptotic Index (%)
100
90
80
70
60
50
40
30
20
10
0
PreMF
Control
5Gy
10Gy
15Gy
20Gy
Irradiation dose

D

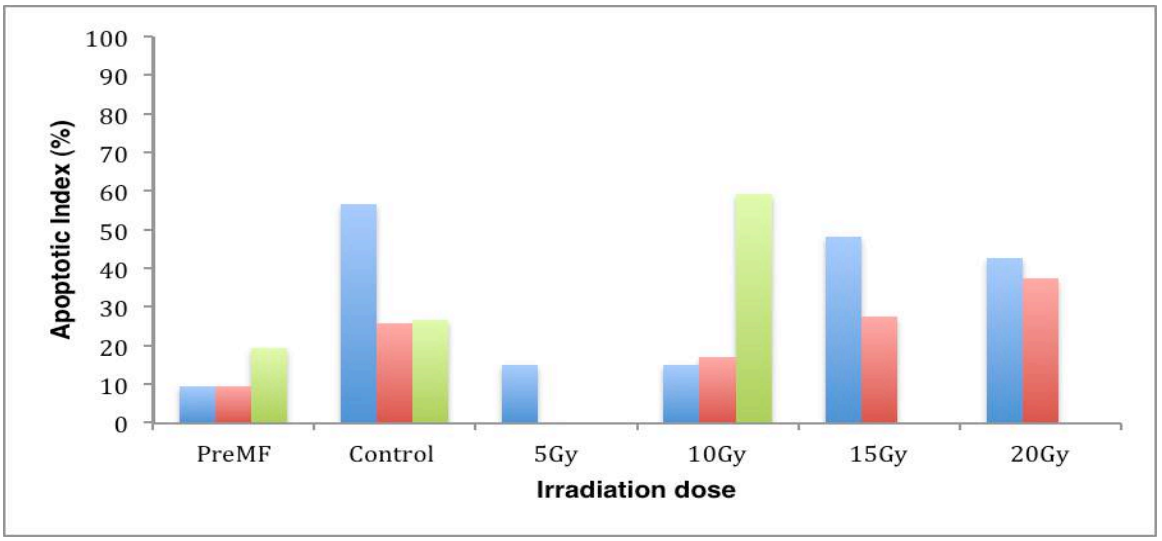

E

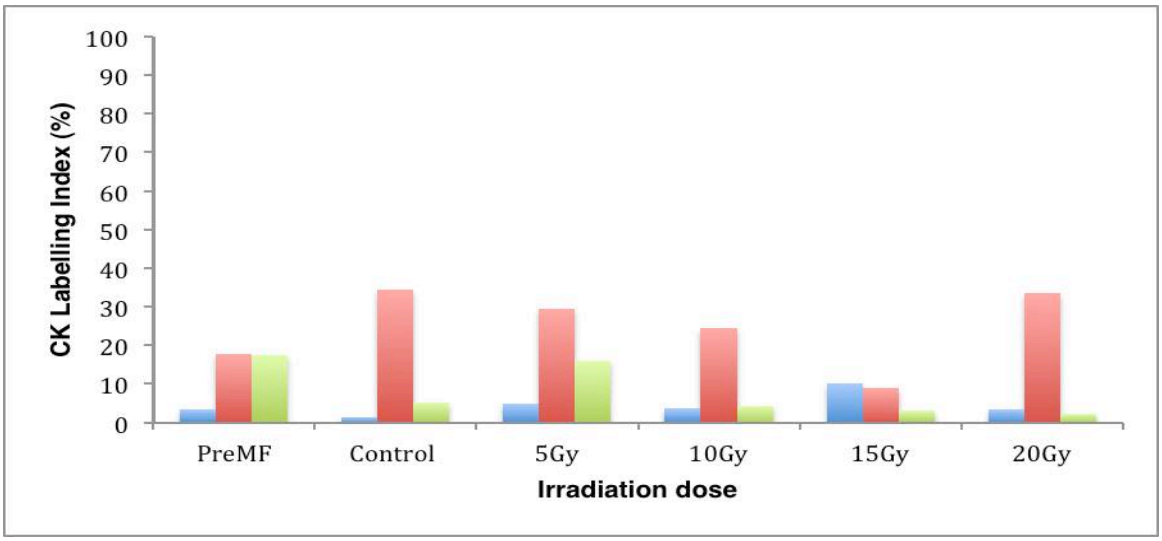

Figure 4.8 Five graphs representing the apoptotic labeling indices for the 5 head and neck subsites tested in this study. A) maxillary sinus B) metastatic lymph node C) oropharynx D) larynx and E) oral cavity. Blue – first experiment, red – second experiment, green – third experiment.

Figure 4.9 demonstrates what the tiled photomicrographs look like and how they stain with the pancytokeratin and the M30 antibody.

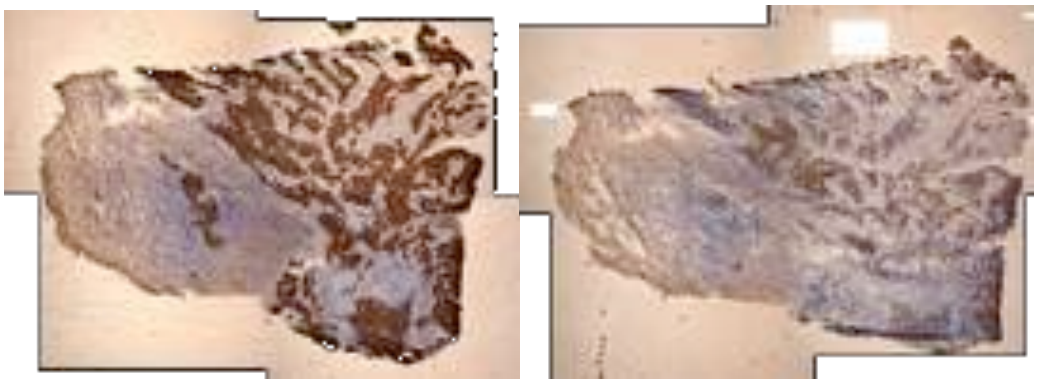

Figure 4.9 The left photomicrograph represents the metastatic lymph node having been irradiated with 20Gy and stained with cytokeratin. The right photomicrograph shows the staining with the M30 antibody. Both areas stain brown however as described in section 2.10, these areas can calculated and the apoptotic index obtained.

4.3.6 Summary of results

	Pre microfluidic	Control	Control + Lysis agent	5Gy	10Gy	15Gy	20Gy
LDH	NP	15	5	14	15	14	14
H&E	14	15	NP	14	15	13	14
CK & M30 staining	14	15	NP	13	14	12	13
BrdU incorporation	NP	15	NP	4	4	4	4

Table 4.1 A table summarising the numbers of measurements obtained. HNSCC tissue specimens from one subsite would not undergo the microfluidic process (pre-microfluidic), would be maintained in the microfluidic device and not irradiated (control;) and they would be exposed to 4 escalating doses of irradiation. This was performed 3 times for each subsite. LDH assays with addition of the lysis agent prior to termination of the experiment (non-irradiated samples) were performed 5 times. LDH and BrdU incorporation assays were not performed on pre-microfluidic samples. Haematoxylin and eosin, cytokeratin and M30 IHC staining and BrdU incorporation assay were not performed on non-irradiated samples exposed to the lysis agent. (NP – not performed).

4.4 Discussion

LDH measurement to analyse radiation induced cell death

LDH is a marker of both apoptotic and necrotic cell death *(Ka-Ming Chan et al., 2013)* and was utilised in this study as a marker of cell death post irradiation of HNSCC tissue. High LDH levels were observed in the first 24 hours when HNSCC was maintained in the microfluidic device. This is due to the tissue dissection and preparation when establishing the experiments and is in keeping with similar findings in previous studies. Hattersley et al. *(2012)* studied the effects of chemotherapeutic agents to HNSCC and metastatic lymph node samples in the microfluidic device identical to the system utilised in this study. Their study showed an initial peak in LDH release followed by low levels for the next 48 hours. Carr et al. *(2013) also* demonstrated similar findings with HNSCC tissue maintained in the microfluidic device.

In this study, after addition of the lysis agent, an immediate rise was not seen in the first measurement of LDH levels but was more an exponential rise. The results are not in keeping with Carr et al. *(2013)* who noted an immediate rise in the first LDH levels post lysis addition (n=9). Their addition took place approximately 6 days post commencement of the experiment, whereas in this study the addition of the lysis agent was 44 hours after the start of the experiment. An explanation for the difference in results is in this study, the tissue was in a more viable state and the tissue took more time to react to the addition of the lysis agent. Whereas in the study by Carr et al. *(2013)*, the tissue was in the microfluidic environment for a longer period and perhaps was in a far less viable state reacted more rapidly to the addition of the lysis agent.

Statistically, there was no overall significance in the LDH release levels post irradiation at 5Gy, 10Gy, 15Gy and 20Gy. These findings are in agreement with Carr et al. *(2013)* who found that LDH release was only statistically significant post irradiation at 40Gy; and this difference is thought to be due to the intrinsic radiosensitivity of HNSCC. These results are supported by a study from Cai et al., *(2000)* who looked at the role of metallothionen in the brain by exposing human central nervous system cultures to 30Gy and 60Gy irradiation. It showed cells exposed to 30Gy or less exhibited some apoptotic cell death; whereas exposure to 60Gy caused a marked increase in LDH release.

The effects of irradiation on the morphology of HNSCC tissue in the microfluidic device

There was no apparent difference between the histological appearance of the pre-microfluidic HNSCC tissue samples and the non-irradiated HNSCC tissue incubated in the microfluidic device. This was in keeping with the results by Hattersley et al. *(2012)* and Carr et al. *(2013).* The architecture was maintained; the nuclei had retained their shape and there was no obvious loss of intercellular cohesion. Irradiated HNSCC tissue from the maxillary sinus, oral cavity and metastatic lymph node had shown some loss of intercellular cohesion and change in nuclei after exposure to 15Gy and 20Gy. HNSCC from the oropharynx and larynx showed these changes at 5Gy, 10Gy, 15Gy and 20Gy. Carr et al. (*2013)* showed an architectural change in the tissue following 5 fractions of 2Gy and 7 days of incubation in the microfluidic device.

Shinomiya *(2001)* characterised the hallmarks of radiation-induced apoptosis, which consisted of pyknosis, cell condensation and internucleosomal breakage of chromatin. The results of this study are supported by the findings of Kellolumpu-Lehtinen et al. *(1990).* Their group had analysed HNSCC tissue samples from patients before and during irradiation treatment. Histologically there were several cellular changes, the most prominent of which was nuclear atypia considered to be due to cell death. The tumour invasion pattern remained unchanged but the numbers of desmosomes associated with intercellular junctions to allow for cellular adhesion were reduced in epithelial tumours.

Beyzadeoglu *(2010)* stated the most radiosensitive stages during the cell cycle are the early G_2 and M stages and radioresistance is high in the S, late G_1 and G_0 phases. Nordman et al. *(1989)* indicated radio-responsiveness was not a consistent characteristic of tumours with a high percentage of S-phase cells. This as well as tumour heterogeneity *(Mantyla et al., 1979, Kellokumou-Lehtinen et al., 1990)* can account for the architectural observations with HNSCC from the oropharynx and larynx exposed to different doses of irradiation; compared with the findings with the HNSCC from remaining subsites exposed to the higher doses of 15Gy and 20Gy.

Detection of 5-bromo-2-deoxyuridine (BrdU) as a marker of proliferation

BrdU is a thymidine analogue that incorporates DNA of dividing cells during the S-phase of the cell cycle. It is used not only for monitoring cell proliferation, it is a marker of DNA synthesis and can label cells undergoing DNA repair as a prelude to apoptosis *(Taupin, 2007)*.

Overall, there was not a dose dependent relationship observed with the metastatic lymph node, oropharynx and laryngeal subsites. Although there was increased BrdU incorporation with the oropharyngeal and laryngeal tissues, there was no statistically significant difference between the subsites where BrdU incorporation was seen.

Earlier studies have utilised BrdU *in vivo* to evaluate cell kinetics in HNSCC *(Cooke et al., 1994, Wilson et al., 1995, Corvo et al., 1996, Corvo et al., 2000)*. Cooke et al. *(1994)* revealed no difference in survival between patients who had high and low values for the labeling indices, the duration of the S phase and potential doubling time for tumours. Wilson et al. *(1995)* assessed cell kinetics to predict which patients would benefit from accelerated radiotherapy, so the overall duration of treatment could be reduced and the time minimised for cellular repopulation. They showed it did not predict success or failure in these patients. Corvo et al. *(1996)* observed a strong correlation between the tumour potential doubling time below 5 days and a major tumour response at 40Gy; whereas the same group *(2000)* suggested that pretreatment cell kinetics offered only a weak prognostic role in the outcome of HNSCC.

Taupin *(2007)* commented that BrdU is potentially a toxic and mutagenic substance that can induce many side effects. Table 3.3 provides a summary of the use of BrdU in HNSCC studies and it is noticeable that more recent reports are the results of *in vitro* studies. Bertrand et al. *(2014)* investigated the resistance of cancer stem-like cells (CSC's) in radioresistant HNSCC cell lines (SQ20B). BrdU proliferation studies were performed here and it showed 24 hours to 120 hours post photon or carbon ion exposure, the proliferation of this subpopulation of SQ20B was greatly reduced. Their explanation for this finding is that CSC's are capable of prolonged G2/M phase arrest in response to carbon or photon irradiation.

Our study shows the BrdU incorporation was greater in the oropharynx and laryngeal tissue compared with the metastatic lymph node. This suggests the cells are undergoing increased apoptosis compared with the metastatic lymph node post irradiation. However the BrdU incorporation was more prominent with the rat liver as part of the optimisation process. The methodology had been addressed to ensure a thorough process had been exercised. This included using fresh solutions every 3 experiments, reducing the time the slides spent in 2M HCl to allow the DNA to be denatured and histone proteins removed, thorough deep cleaning of the equipment between experiments and ensuring all materials were in date. The variation in consistency with the results could be explained by the heterogeneity in HNSCC compared with the homogeneity of rat liver tissue.

To the author's knowledge, this is the first study utilising BrdU as a marker of proliferation in HNSCC in a microfluidic setting.

Detection of pancytokeratin and the M30 antibody as a marker of apoptosis

Statistically, there was no significant difference in the apoptotic indices between the pre-microfluidic HNSCC tissues and the non-irradiated HNSCC tissues maintained in the microfluidic device. This would suggest the HNSCC tissues were kept in a viable state and had minimal loss of function. These results are in agreement with Carr et al. *(2013)*. Their study also demonstrated a significant increase in apoptosis following irradiation of HNSCC tissue for both a single dose of 2Gy and five fractions of 2GY compared with non-irradiated HNSCC tissue. A dose dependent relationship was established; so the higher the dose of irradiation administered, the higher the apoptotic index was observed.

In our study a dose dependent relationship was not observed. Statistically, there was no significant difference between the doses of irradiation administered and the apoptotic indices obtained for the various HNSCC tissues from the 5 subsites.

In this study, there is a clearer association between dose dependent irradiated tissues as manifested morphologically with H&E staining compared with the LDH levels and the values obtained for the apoptotic indices. It would be expected that with a higher dose of irradiation, there would be higher LDH levels and apoptotic indices obtained. Given the

lack of this, it is suspected that the discrepancies are due to the fact that the method used in this study is not repeatable and hence the variability in the results obtained.

Brieger et al. *(2011)* performed an *in vitro* study to evaluate pharmacological genome demethylation for the increase of irradiation treatment effectiveness in HNSCC. HNSCC cells were cultured with 2 different concentrations of 5-azacytidine for 72 hours, followed by a single fraction of 4Gy or 50Gy. They found apoptosis was strongly increased after a combined 4Gy/5-azacytidine treatment; however irradiation treatment of 50Gy resulted in no further increased levels of apoptosis, remaining comparable to the combined 4Gy/5-azacytidine treatment. Wozny et al. *(2016)* studied the effect of a dose rate variation during high or low linear energy transfer irradiations in terms of cell survival and DNA double strand breaks repair. They used two HNSCC cell lines, one radioresistant and the other radiosensitive; and they were irradiated with 0.5, 2 or 10Gy per minute. They found that the higher the dose the lower the relative biological effectiveness; and in contrast to photon irradiation, a carbon ion dose rate variation did not significantly affect cell survival regardless of the HNSCC cell line used. Their hypothesis was that damage spreads more over a time at a low dose rate and can allow cells to have more time to detect DNA damages and activate their repair systems *(Nunez et al., 1996)*.

Intratumour heterogeneity can also provide an explanation for the findings of a non-dose dependent relationship *(Mroz et al., 2013, Zhang et al., 2013, Ledgerwood et al., 2016)*.

Ledgerwood et al. *(2016)* characterised the degree of intratumour mutational heterogeneity in HNSCC. Their study employed mutli-region sequencing of primary and metastatic DNA of 24 distinct samples from 7 patients with HNSCC of the larynx, floor of mouth and oral tongue. In depth sequencing of 202 genes was performed and they observed the larynx and floor of mouth tumours had more than 69% unique single nucleotide variants compared with 33.3% in the oral tongue HNSCC's. There were also fewer mutations in the oral tongue. Their data was consistent with data from the Cancer Genome Atlas and they concluded the findings are relevant to clinicians developing personalised cancer treatments based on the mutations in tumour biopsies.

Zhang et al. *(2013)* performed whole-genome sequencing on three separate regions of HPV positive oropharygneal SCC and two separate regions from one corresponding

cervical lymph node metastasis. Their approach covered under 98% of the genome across all samples. All of their tumour samples shared 41% of single point mutations, 57% of the 1805 genes with single point mutations and 34 out of 55 cancer genes. Not only were they able to show the metastatic samples arose as a late event, their approach suggested a single biopsy may not represent the entire mutational map of HNSCC tumours.

In a study by Mroz et al. *(2013)*, they examined the association between mutant allele tumour heterogeneity and a HNSCC data set utilising next generation sequencing as a quantitative measure of intratumour genetic heterogeneity. They found the higher the heterogeneity, the worse the clinical outcome in patients with HNSCC.

Conclusion

This study has shown that HNSCC tissue specimens can be maintained in a microfluidic device, in a pseudo *in vivo* environment. Use of the pancytokeratin and M30 antibody has revealed that repeated irradiation of HNSCC tissue from the same patient has shown the variability in apoptotic indices obtained. Even though intratumour heterogeneity is a valid explanation, it is felt that discrepancies in the results shown could be explained by the fact the method isn't particularly repeatable and gives rise to variable results. The microfluidic device is useful to assess a patient's personalised response to radiotherapy; however from this study, it can be seen this method would need to be reevaluated to assess the response to irradiation. In the clinical setting, patients who have not responded to radiotherapy or chemoradiotherapy would require salvage surgery with the intention to cure if deemed possible. Both methods of treatment are associated with morbidity and mortality; and the microfluidic device provides the opportunity to assess a patient's response to radiotherapy and potentially decide which mode of treatment a patient would benefit from the most. Given the current financial climate in the NHS, it also provides a hypothetical benefit in cost reduction.

During this study, frozen HNSCC specimens were consistently used to facilitate efficient utilisation of multiple microfluidic devices. Future work should consider usage of freshly obtained tumour tissue; as this potentially reduces any cell death that will occur with the freezing and thawing process, allowing an *in vivo* environment to be simulated more closely. Even though previous studies have used urea, albumin and LDH release as

markers of rat liver tissue viability in the microfluidic device (*Hattersley et al., 2008; Hattersley et al., 2011; Carr et al., 2013)*, unfortunately there is no universal constant secretable measureable marker of HNSCC that can be tested to ensure adequate function.

In this study, even though certain problems with the device were identified and managed during the optimisation phase, a new design would need to be considered that could prevent them from occurring with future studies. These include leakage of effluent from the well of the device, as well as the output channels becoming blocked with parts of the HNSCC tissue. If the device was modified taking these factors into account, the fallibilities could be kept to a minimum and could allow a more precise assessment of HNSCC tissue.

There has been an increased perception in the molecular mechanisms involved in HNSCC. Being able to identify markers of radioresistance of HNSCC tissue could not only be cost effective, it could possibly prevent unnecessary morbidity with non-surgical treatment and allow patient centred treatment success. As mentioned above, Silva et al. *(2007)* described certain genes that can act as potential markers of radiation-induced DNA damage response and hence determine a tumour's intrinsic radiosensitivity. In clinical practice, there are certain biomarkers that are tested e.g. EGFR which is associated with a poorer outcome and HPV positivity (especially in the oropharynx) which is known to have a favourable prognosis. Other biomarkers maybe utilised in the early diagnosis and intervention of patients with HNSCC and include the following: chemokine receptors 2, 4 and 7; microsatellite instability, methylation, metalloproteinases 1, 3, 8, 9 and 10; interleukins 6 and 8; micro RNA, melanoma associated gene, centrosome abnormalities, actin and myosin, cytokeratins, p53, eukaryotic translation factor 4E and loss of function of DNA repair genes *(Dahiya and Dhankhar, 2016)*.

It is possible the application of different therapeutic modalities for detection of the above biomarkers in conjunction with a modified microfluidic system, would allow a more specific approach in the treatment of patients with HNSCC. This could provide great potential to contribute to the concept of personalised medicine.

References

Abbe, R. (1915). Cancer of the Mouth. *The Laryngoscope*, 25(8), p.559.

Abend, M. (2003). Reasons to reconsider the significance of apoptosis for cancer therapy. *International Journal of Radiation Biology*, 79(12), pp.927-941.

Alberts, B. (2002). *Molecular biology of the cell*. New York: Garland Science.

Alos, L., Moyano, S., Nadal, A., Alobid, I., Blanch, J., Ayala, E., Lloveras, B., Quint, W., Cardesa, A. and Ordi, J. (2009). Human papillomaviruses are identified in a subgroup of sinonasal squamous cell carcinomas with favorable outcome. *Cancer*, 115(12), pp.2701-2709.

Alvarez, S., Drané, P., Meiller, A., Bras, M., Deguin-Chambon, V., Bouvard, V. and May, E. (2006). A comprehensive study of p53 transcriptional activity in thymus and spleen of γ irradiated mouse: High sensitivity of genes involved in the two main apoptotic pathways. *International Journal of Radiation Biology*, 82(11), pp.761-770.

Ang, K., Berkey, B. and Tu, X. (2002). Impact of epidermal growth factor receptor expression on survival and pattern of relapse in patients with advanced head and neck carcinoma. *Cancer Res*, 62, pp.7350-7356.

Ang, K., Harris, J., Wheeler, R., Weber, R., Rosenthal, D., Nguyen-Tân, P., Westra, W., Chung, C., Jordan, R., Lu, C., Kim, H., Axelrod, R., Silverman, C., Redmond, K. and Gillison, M. (2010). Human Papillomavirus and Survival of Patients with Oropharyngeal Cancer. *New England Journal of Medicine*, 363(1), pp.24-35.

Ansa, B., Goodman, M., Ward, K., Kono, S., Owonikoko, T., Higgins, K., Beitler, J., Grist, W., Wadsworth, T., El-Deiry, M., Chen, A., Khuri, F., Shin, D. and Saba, N. (2013). Paranasal sinus squamous cell carcinoma incidence and survival based on Surveillance, Epidemiology, and End Results data, 1973 to 2009. *Cancer*, 119(14), pp.2602-2610.

Areca nut and betel-quid chewing bibliography. (2002). *Addiction Biology*, 7(1), pp.155-168.

Argiris, A., Karamouzis, M., Raben, D. and Ferris, R. (2008). Head and neck cancer. *The Lancet*, 371(9625), pp.1695-1709.

Ariyoshi, Y., Shimahara, M. and Tanigawa, N. (2003). Study on chemosensitivity of oral squamous cell carcinomas by histoculture drug response assay. *Oral Oncology*, 39(7), pp.701-707.

Axelsson, L., Nyman, J., Haugen-Cange, H., Bove, M., Johansson, L., De Lara, S., Kovács, A. and Hammerlid, E. (2017). Prognostic factors for head and neck cancer of unknown primary including the impact of human papilloma virus infection. *Journal of Otolaryngology - Head & Neck Surgery*, 46(1).

Baicu, S. and Taylor, M. (2002). Acid–base buffering in organ preservation solutions as a function of temperature: new parameters for comparing buffer capacity and efficiency. *Cryobiology*, 45(1), pp.33-48.

Baker, F., Spitzer, G., Ajani, J., Brock, W., Lukeman, J., Pathak, S., Tomasovic, B., Thielvoldt, D., Williams, M. and Vines, C. (1986). Drug and radiation sensitivity measurements of successful primary monolayer culturing of human tumor cells using cell-adhesive matrix and supplemented medium. *Cancer Res*, 46, pp.1263-1274.

Balis, F. (2002). Evolution of Anticancer Drug Discovery and the Role of Cell-Based Screening. *JNCI Journal of the National Cancer Institute*, 94(2), pp.78-79.

Barker, H., Paget, J., Khan, A. and Harrington, K. (2015). The tumour microenvironment after radiotherapy: mechanisms of resistance and recurrence. *Nature Reviews Cancer*, 15(7), pp.409-425.

Begg, A. (2012). Predicting Recurrence After Radiotherapy in Head and Neck Cancer. *Seminars in Radiation Oncology*, 22(2), pp.108-118.

Begg, A., Stewart, F. and Vens, C. (2011). Strategies to improve radiotherapy with targeted drugs. *Nature Reviews Cancer*, 11(4), pp.239-253.

Bentzen, S., Atasoy, B., Daley, F., Dische, S., Richman, P., Saunders, M., Trott, K. and Wilson, G. (2005). Epidermal Growth Factor Receptor Expression in Pretreatment

Biopsies From Head and Neck Squamous Cell Carcinoma As a Predictive Factor for a Benefit From Accelerated Radiation Therapy in a Randomized Controlled Trial. *Journal of Clinical Oncology*, 23(24), pp.5560-5567.

Bertrand, G., Maalouf, M., Boivin, A., Battiston-Montagne, P., Beuve, M., Levy, A., Jalade, P., Fournier, C., Ardail, D., Magné, N., Alphonse, G. and Rodriguez-Lafrasse, C. (2013). Targeting Head and Neck Cancer Stem Cells to Overcome Resistance to Photon and Carbon Ion Radiation. *Stem Cell Rev and Rep*, 10(1), pp.114-126.

Besic Gyenge, E., Forny, P., Lüscher, D., Laass, A., Walt, H. and Maake, C. (2012). Effects of hypericin and a chlorin based photosensitizer alone or in combination in squamous cell carcinoma cells in the dark. *Photodiagnosis and Photodynamic Therapy*, 9(4), pp.321-331.

Beyzadeoglu, M., Ozyigit, G. and Ebruli, C. (2010). *Basic radiation oncology*. Berlin: Springer.

Bignold, L. (2006). *Cancer*. Basel: Birhäuser.

Bishop, J., Guo, T., Smith, D., Wang, H., Ogawa, T., Pai, S. and Westra, W. (2013). Human Papillomavirus-related Carcinomas of the Sinonasal Tract. *The American Journal of Surgical Pathology*, 37(2), pp.185-192.

Björk-Eriksson, T., West, C., Karlsson, E. and Mercke, C. (2000). Tumor radiosensitivity (SF2) is a prognostic factor for local control in head and neck cancers. *International Journal of Radiation Oncology*Biology*Physics*, 46(1), pp.13-19.

Bonner, J., Harari, P., Giralt, J., Azarnia, N., Shin, D., Cohen, R., Jones, C., Sur, R., Raben, D., Jassem, J., Ove, R., Kies, M., Baselga, J., Youssoufian, H., Amellal, N., Rowinsky, E. and Ang, K. (2006). Radiotherapy plus Cetuximab for Squamous-Cell Carcinoma of the Head and Neck. *New England Journal of Medicine*, 354(6), pp.567-578.

Boscolo-Rizzo, P., Schroeder, L., Romeo, S. and Pawlita, M. (2015). The prevalence of human papillomavirus in squamous cell carcinoma of unknown primary site metastatic

to neck lymph nodes: a systematic review. *Clinical & Experimental Metastasis*, 32(8), pp.835-845.

Bourke, E., Dodson, H., Merdes, A., Cuffe, L., Zachos, G., Walker, M., Gillespie, D. and Morrison, C. (2007). DNA damage induces Chk1-dependent centrosome amplification. *EMBO Rep*, 8(6), pp.603-609.

Braakhuis, B., Tabor, M., Leemans, R., Kummer, A. and Brakenhoff, R. (2013). A genetic explanation of Slaughter's concept of field cancerization. *Cancer Research*, 15(8), pp.1727-1730.

Brennan, M., Rexius-Hall, M., Elgass, L. and Eddington, D. (2014). Oxygen control with microfluidics. *Lab Chip*, 14(22), pp.4305-4318.

Brieger, J. (2011). Pharmacological genome demethylation increases radiosensitivity of head and neck squamous carcinoma cells. *International Journal of Molecular Medicine*.

Brizel, D., Sibley, G., Prosnitz, L., Scher, R. and Dewhirst, M. (1997). Tumor hypoxia adversely affects the prognosis of carcinoma of the head and neck. *International Journal of Radiation Oncology*Biology*Physics*, 38(2), pp.285-289.

Broadwell, I., Fletcher, P., Haswell, S., McCreedy, T. and Zhang, X. (2001). Quantitative 3-dimensional profiling of channel networks within transparent ‘lab-on-a-chip’ microreactors using a digital imaging method. *Lab Chip*, 1(1), pp.66-71.

Brock, W., Baker, F., Wike, J., Sivon, S. and Peters, L. (1990). Cellular radiosensitivity of primary head and neck squamous cell carcinomas and local tumor control. *International Journal of Radiation Oncology*Biology*Physics*, 18(6), pp.1283-1286.

Brockton, N., Dort, J., Lau, H., Hao, D., Brar, S., Klimowicz, A., Petrillo, S., Diaz, R., Doll, C. and Magliocco, A. (2011). High Stromal Carbonic Anhydrase IX Expression Is Associated With Decreased Survival in p16-Negative Head-and-Neck Tumors. *International Journal of Radiation Oncology*Biology*Physics*, 80(1), pp.249-257.

Burns, T., Bernhard, E. and El-Deiry, W. (2001). Tissue specific expression of p53 target genes suggests a key role for KILLER/DR5 in p53-dependent apoptosis in vivo. *Oncogene*, 20(34), pp.4601-4612.

Cai, M. G. Cherian, S. Iskander, M., L. (2000). Metallothionein induction in human CNS in vitro : neuroprotection from ionizing radiation. *International Journal of Radiation Biology*, 76(7), pp.1009-1017.

Califano III, J., Clayman, G., Sidransky, D., Koch, W., Piantadosi, S., Vander Riet, P., Nawroz, H., Westra, W. and Corio, R. (1996). A genetic progression model for head and neck cancer: Implications for field cancerization. *Otolaryngology - Head and Neck Surgery*, 115(2), pp.P79-P79.

Cancer Research UK. (2016). *Cancer Research UK*. [online] Available at: http://www.cancerresearch.org.uk [Accessed 17 Aug. 2016].

Carey, T., Hay, R., Park, J. and Gazdar, A. (1994). *Head and NEck Tumour Cell Lines. In atlas of hum tumour cell lines*. San Diego: Academic Press Inc, pp.79-120.

Carr, S., Green, V., Stafford, N. and Greenman, J. (2013). Analysis of Radiation-Induced Cell Death in Head and Neck Squamous Cell Carcinoma and Rat Liver Maintained in Microfluidic Devices. *Otolaryngology -- Head and Neck Surgery*, 150(1), pp.73-80.

Castedo, M., Perfettini, J., Roumier, T., Valent, A., Raslova, H., Yakushijin, K., Horne, D., Feunteun, J., Lenoir, G., Medema, R., Vainchenker, W. and Kroemer, G. (2004). Mitotic catastrophe constitutes a special case of apoptosis whose suppression entails aneuploidy. *Oncogene*, 23(25), pp.4362-4370.

Cattani, P., Hohaus, S. and Bellacosa, A. (2016). Association between cyclin D1 (CCND1) gene amplification and human papillomavirus infection in human laryngeal squmous cell carcinoma. *Clin Cancer Res*, (4), p.2585.

Caulín, C., Salvesen, G. and Oshima, R. (1997). Caspase Cleavage of Keratin 18 and Reorganization of Intermediate Filaments during Epithelial Cell Apoptosis. *J Cell Biol*, 138(6), pp.1379-1394.

Champion, A., Hanson, J., Venables, S., McGregor, A. and Gaffney, C. (1997). Determination of radiosensitivity in established and primary squamous cell carcinoma cultures using the micronucleus assay. *European Journal of Cancer*, 33(3), pp.453-462.

Chan, F., Moriwaki, K. and De Rosa, M. (2013). Detection of Necrosis by Release of Lactate Dehydrogenase Activity. *Methods in Molecular Biology*, pp.65-70.

Chaturvedi, A., Engels, E., Pfeiffer, R., Hernandez, B., Xiao, W., Kim, E., Jiang, B., Goodman, M., Sibug-Saber, M., Cozen, W., Liu, L., Lynch, C., Wentzensen, N., Jordan, R., Altekruse, S., Anderson, W., Rosenberg, P. and Gillison, M. (2011). Human Papillomavirus and Rising Oropharyngeal Cancer Incidence in the United States. *Journal of Clinical Oncology*, 29(32), pp.4294-4301.

Chaudhuri, P., Ebrahimi Warkiani, M., Jing, T., Kenry, K. and Lim, C. (2016). Microfluidics for research and applications in oncology. *The Analyst*, 141(2), pp.504-524.

Chen, A., Felix, C., Wang, P., Hsu, S., Basehart, V., Garst, J., Beron, P., Wong, D., Rosove, M., Rao, S., Melanson, H., Kim, E., Palmer, D., Qi, L., Kelly, K., Steinberg, M., Kupelian, P. and Daly, M. (2017). Reduced-dose radiotherapy for human papillomavirus-associated squamous-cell carcinoma of the oropharynx: a single-arm, phase 2 study. *The Lancet Oncology*, 18(6), pp.803-811.

Chen, P., Kuo, C., Pan, C. and Chou, M. (2002). Risk of oral cancer associated with human papillomavirus infection, betel quid chewing, and cigarette smoking in Taiwan - an integrated molecular and epidemiological study of 58 cases. *J Oral Pathol Med*, 31(6), pp.317-322.

Chen, Y., Cheng, Y., Kim, H., Ingram, P., Nor, J. and Yoon, E. (2014). Paired single cell co-culture microenvironments isolated by two-phase flow with continuous nutrient renewal. *Lab on a Chip*, 14(16), p.2941.

Chung, C., Ely, K., McGavran, L., Varella-Garcia, M., Parker, J., Parker, N., Jarrett, C., Carter, J., Murphy, B., Netterville, J., Burkey, B., Sinard, R., Cmelak, A., Levy, S., Yarbrough, W., Slebos, R. and Hirsch, F. (2006). Increased Epidermal Growth Factor

Receptor Gene Copy Number Is Associated With Poor Prognosis in Head and Neck Squamous Cell Carcinomas. *Journal of Clinical Oncology*, 24(25), pp.4170-4176.

Chung, C., Levy, S., Chaurand, P. and Carbone, D. (2007). Genomics and proteomics: Emerging technologies in clinical cancer research. *Critical Reviews in Oncology/Hematology*, 61(1), pp.1-25.

Ciriello, G., Miller, M., Aksoy, B., Senbabaoglu, Y., Schultz, N. and Sander, C. (2013). Emerging landscape of oncogenic signatures across human cancers. *Nature Genetics*, 45(10), pp.1127-1133.

Clarke, P. (1990). Developmental cell death: morphological diversity and multiple mechanisms. *Anat Embryol*, 181(3).

Cleary, C., Leeman, J., Higginson, D., Katabi, N., Sherman, E., Morris, L., McBride, S., Lee, N. and Riaz, N. (2016). Biological Features of Human Papillomavirus-related Head and Neck Cancers Contributing to Improved Response. *Clinical Oncology*, 28(7), pp.467-474.

Contemporary Issues in Head and Neck Cancer Management. (2015). InTech.

Cooke, L., Cooke, T., Forster, G., Jones, A. and Stell, P. (1994). Prospective evaluation of cell kinetics in head and neck squamous carcinoma: the relationship to tumour factors and survival. *Br J Cancer*, 69(4), pp.717-720.

Coppé, J., Desprez, P., Krtolica, A. and Campisi, J. (2010). The Senescence-Associated Secretory Phenotype: The Dark Side of Tumor Suppression. *Annu. Rev. Pathol. Mech. Dis.*, 5(1), pp.99-118.

Corvo, R., Giaretti, W., Geido, E., Sanguineti, G., Orecchia, R., Scala, M., Garaventa, G., Mora, E. and Vitale, V. (1996). Cell kinetics and tumor regression during radiotherapy in head and neck squamous-cell carcinomas. *International Journal of Cancer*, 68(2), pp.151-155.

Corvò, R., Paoli, G., Giaretti, W., Sanguineti, G., Geido, E., Benasso, M., Margarino, G. and Vitale, V. (2000). Evidence of cell kinetics as predictive factor of response to

radiotherapy alone or chemoradiotherapy in patients with advanced head and neck cancer. *International Journal of Radiation Oncology*Biology*Physics*, 47(1), pp.57-63.

Coutard, H. (1934). Principles of x ray therapy of malignant diseases. *The Lancet*, 224(5784), pp.1-8.

Coutard, H. (1937). The results and methods of treatment of cancer by radiation. *Annals of Surgery*, 106(4), pp.584-598.

Couture, C., Raybaud-Diogène, H., Têtu, B., Bairati, I., Murry, D., Allard, J. and Fortin, A. (2002). p53 and Ki-67 as markers of radioresistance in head and neck carcinoma. *Cancer*, 94(3), pp.713-722.

Critchley, J. (2003). Health effects associated with smokeless tobacco: a systematic review. *Thorax*, 58(5), pp.435-443.

Dahiya, K. and Dhankhar, R. (2016). Updated overview of current biomarkers in head and neck carcinoma. *World Journal of Methodology*, 6(1), p.77.

Dai, C. and Enders, G. (2000). p16INK4a can initiate an autonomous senescence program. *Oncogene*, 19(13), pp.1613-1622.

Das, S., Raj, L., Zhao, B., Kimura, Y., Bernstein, A., Aaronson, S. and Lee, S. (2007). Hzf Determines Cell Survival upon Genotoxic Stress by Modulating p53 Transactivation. *Cell*, 130(4), pp.624-637.

de Jong, M., Pramana, J., Knegjens, J., Balm, A., van den Brekel, M., Hauptmann, M., Begg, A. and Rasch, C. (2010). HPV and high-risk gene expression profiles predict response to chemoradiotherapy in head and neck cancer, independent of clinical factors. *Radiotherapy and Oncology*, 95(3), pp.365-370.

De Stefani, E., Oreggia, F., Boffetta, P., Deneo-Pellegrini, H., Ronco, A. and Mendilaharsu, M. (2000). Tomatoes, tomato-rich foods, lycopene and cancer of the upper aerodigestive tract: a case-control in Uruguay. *Oral Oncology*, 36(1), pp.47-53.

Deng, Y., Chan, S. and Chang, S. (2008). Telomere dysfunction and tumour suppression: the senescence connection. *Nature Reviews Cancer*, 8(6), pp.450-458.

Desouky, O., Ding, N. and Zhou, G. (2015). Targeted and non-targeted effects of ionizing radiation. *Journal of Radiation Research and Applied Sciences*, 8(2), pp.247-254.

Dinshaw, K., Agarwal, J., Ghosh-Laskar, S., Gupta, T. and Shrivastava, S. (2006). Radical Radiotherapy in Head and Neck Squamous Cell Carcinoma: An Analysis of Prognostic and Therapeutic Factors. *Clinical Oncology*, 18(5), pp.383-389.

Dodson, H., Wheatley, S. and Morrison, C. (2007). Involvement of Centrosome Amplification in Radiation-Induced Mitotic Catastrophe. *Cell Cycle*, 6(3), pp.364-370.

Dohmen, A., Swartz, J., Van Den Brekel, M., Willems, S., Spijker, R., Neefjes, J. and Zuur, C. (2015). Feasibility of Primary Tumor Culture Models and Preclinical Prediction Assays for Head and Neck Cancer: A Narrative Review. *Cancers*, 7(3), pp.1716-1742.

Dok, R., Kalev, P., Van Limbergen, E., Asbagh, L., Vázquez, I., Hauben, E., Sablina, A. and Nuyts, S. (2014). p16INK4a Impairs Homologous Recombination–Mediated DNA Repair in Human Papillomavirus–Positive Head and Neck Tumors. *Cancer Research*, 74(6), pp.1739-1751.

Domansky, K., Inman, W., Serdy, J., Dash, A., Lim, M. and Griffith, L. (2010). Perfused multiwell plate for 3D liver tissue engineering. *Lab Chip*, 10(1), pp.51-58.

El-Ali, J., Sorger, P. and Jensen, K. (2006). Cells on chips. *Nature*, 442(7101), pp.403-411.

Elaut, G., Vanhaecke, T., Heyden, Y. and Rogiers, V. (2005). Spontaneous apoptosis, necrosis, energy status, glutathione levels and biotransformation capacities of isolated rat hepatocytes in suspension: Effect of the incubation medium. *Biochemical Pharmacology*, 69(12), pp.1829-1838.

Elprana, D., Schwachofer, J., Kuiipers, W., van den Broek, P. and Wagener, D. (1989). Cytotoxic drug sensitivity of squamous cell carcinoma as predicted by an in vitro testing model. *Anticancer Res*, 9, pp.1089-1094.

El-Serag, H., Hepworth, E., Lee, P. and Sonnenberg, A. (2001). Gastroesophageal reflux disease is a risk factor for laryngeal and pharyngeal cancer. *The American Journal of Gastroenterology*, 96(7), pp.2013-2018.

Embree-Ku, M. (2002). Fas Is Involved in the p53-Dependent Apoptotic Response to Ionizing Radiation in Mouse Testis. *Biology of Reproduction*, 66(5), pp.1456-1461.

Emedicine.com. (2016). *Diseases & Conditions - Medscape Reference*. [online] Available at: http://emedicine.com [Accessed 17 Aug. 2016].

Erenpreisa, J. And Cragg, M. (2007). Cancer: A matter of life cycle?. *Cell Biology International*, 31(12), pp.1507-1510.

Erenpreisa, J., Kalejs, M., Ianzini, F., Kosmacek, E., Mackey, M., Emzinsh, D., Cragg, M., Ivanov, A. And Illidge, T. (2005). Segregation of genomes in polyploid tumour cells following mitotic catastrophe. *Cell Biology International*, 29(12), pp.1005-1011.

Eriksen, J., Steiniche, T. and Overgaard, J. (2005). The role of epidermal growth factor receptor and E-cadherin for the outcome of reduction in the overall treatment time of radiotherapy of supraglottic larynx squamous cell carcinoma. *Acta Oncologica*, 44(1), pp.50-58.

Eriksson, D. and Stigbrand, T. (2010). Radiation-induced cell death mechanisms. *Tumor Biol.*, 31(4), pp.363-372.

Eriksson, D., Blomberg, J., Lindgren, T., Löfroth, P., Johansson, L., Riklund, K. and Stigbrand, T. (2008). Iodine-131 induces Mitotic Catastrophes and Activates Apoptotic Pathways in HeLa Hep2 Cells. *Cancer Biotherapy & Radiopharmaceuticals*, pp.1-10.

Eriksson, D., Joniani, H., Sheikholvaezin, A., Löfroth, P., Johansson, L., Riklund Åhlström, K. and Stigbrand, T. (2003). Combined low dose radio- and radioimmunotherapy of experimental HeLa Hep 2 tumours. *European Journal of Nuclear Medicine and Molecular Imaging*, 30(6), pp.895-906.

Eriksson, D., Lofroth, P., Johansson, L., Riklund, K. and Stigbrand, T. (2007). Cell Cycle Disturbances and Mitotic Catastrophes in HeLa Hep2 Cells following 2.5 to 10 Gy of Ionizing Radiation. *Clinical Cancer Research*, 13(18), pp.5501s-5508s.

Erlich, R., Rickwood, D., Coman, W., Saunders, N. and Guminski, A. (2008). Valproic acid as a therapeutic agent for head and neck squamous cell carcinomas. *Cancer Chemotherapy and Pharmacology*, 63(3), pp.381-389.

Eschwege, F., Bourhis, J., Girinski, T., Lartigau, E., Guichard, M., Deblé, D., Kepta, L., Wilson, G. and Luboinski, B. (1997). Predictive assays of radiation response in patients with head and neck squamous cell carcinoma: A review of the institute gustave roussy experience. *International Journal of Radiation Oncology*Biology*Physics*, 39(4), pp.849-853.

Fearon, E. and Vogelstein, B. (1990). A genetic model for colorectal tumorigenesis. *Cell*, 61(5), pp.759-767.

Ferlay, J., Soerjomataram, I., Dikshit, R., Eser, S., Mathers, C., Rebelo, M., Parkin, D., Forman, D. and Bray, F. (2014). Cancer incidence and mortality worldwide: Sources, methods and major patterns in GLOBOCAN 2012. *International Journal of Cancer*, 136(5), pp.E359-E386.

Findley, H., Gu, L., Yeager, A. and Zhou, M. (1997). Expression and regulation of bcl-2, bcl-xl, and bax correlate with p53 status and sensitivity to apoptosis in childhood acute lymphoblastic leukemia. *Blood*, 89, pp.2986-93.

Flaitz, C. and Hicks, M. (1998). Molecular piracy: the viral link to carcinogenesis. *Oral Oncology*, 34(6), pp.448-453.

Freshney, R. (2010). *Culture of animal cells*. Hoboken, NJ: Wiley-Blackwell.

Freudlsperger, C., Horn, D., Weißfuß, S., Weichert, W., Weber, K., Saure, D., Sharma, S., Dyckhoff, G., Grabe, N., Plinkert, P., Hoffmann, J., Freier, K. and Hess, J. (2014). Phosphorylation of AKT(Ser473) serves as an independent prognostic marker for

radiosensitivity in advanced head and neck squamous cell carcinoma. *International Journal of Cancer*, 136(12), pp.2775-2785.

Fumic-Dunkic, L., Katic, V., Janjanin, S., Klapan, I., Simuncic, A. and Vcev, A. (2003). Retrospective analysis of Ki-67 antigen expression in paraffin tissue blocks of laryngeal squamous cell carcinoma. *American Journal of Otolaryngology*, 24(2), pp.106-110.

Funamoto, K., Zervantonakis, I., Liu, Y., Ochs, C., Kim, C. and Kamm, R. (2012). A novel microfluidic platform for high-resolution imaging of a three-dimensional cell culture under a controlled hypoxic environment. *Lab on a Chip*, 12(22), p.4855.

Galluzzi, L., Maiuri, M., Vitale, I., Zischka, H., Castedo, M., Zitvogel, L. and Kroemer, G. (2007). Cell death modalities: classification and pathophysiological implications. *Cell Death Differ*, 14(7), pp.1237-1243.

Galluzzi, L., Vitale, I., Abrams, J., Alnemri, E., Baehrecke, E., Blagosklonny, M., Dawson, T., Dawson, V., El-Deiry, W., Fulda, S., Gottlieb, E., Green, D., Hengartner, M., Kepp, O., Knight, R., Kumar, S., Lipton, S., Lu, X., Madeo, F., Malorni, W., Mehlen, P., Nuñez, G., Peter, M., Piacentini, M., Rubinsztein, D., Shi, Y., Simon, H., Vandenabeele, P., White, E., Yuan, J., Zhivotovsky, B., Melino, G. and Kroemer, G. (2011). Molecular definitions of cell death subroutines: recommendations of the Nomenclature Committee on Cell Death 2012. *Cell Death Differ*, 19(1), pp.107-120.

Ganci, F., Sacconi, A., Manciocco, V., Spriano, G., Fontemaggi, G., Carlini, P. and Blandino, G. (2015). Radioresistance in Head and Neck Squamous Cell Carcinoma — Possible Molecular Markers for Local Recurrence and New Putative Therapeutic Strategies. *Contemporary Issues in Head and Neck Cancer Management*.

Ganem, N. and Pellman, D. (2007). Limiting the Proliferation of Polyploid Cells. *Cell*, 131(3), pp.437-440.

Ganem, N., Storchova, Z. and Pellman, D. (2007). Tetraploidy, aneuploidy and cancer. *Current Opinion in Genetics & Development*, 17(2), pp.157-162.

Garozzo, A., Rossi, M., Denaro, A., Allegra, E., Santangelo, G., Amato, M. and Tomasello, C. (1989). In VitroShort-Term Chemosensitivity Test in Head and Neck Tumors. *Journal of Chemotherapy*, 1(1), pp.59-63.

Gewirtz, D., Holt, S. and Elmore, L. (2008). Accelerated senescence: An emerging role in tumor cell response to chemotherapy and radiation. *Biochemical Pharmacology*, 76(8), pp.947-957.

Girinsky, T., Bernheim, A., Lubin, R., Tavakoli-Razavi, T., Baker, F., Janot, F., Wibault, P., Cosset, J., Duvillard, P., Duverger, A. and Fertil, B. (1994). In vitro parameters and treatment outcome in head and neck cancers treated with surgery and/or radiation: Cell characterization and correlations with local control and overall survival. *International Journal of Radiation Oncology*Biology*Physics*, 30(4), pp.789-794.

Gleeson, M. and Scott-Brown, W. (2008). *Scott-Brown's otorhinolaryngology*. London: Hodder Arnold.

Gregoire, V., Lefebvre, J., Licitra, L. and Felip, E. (2010). Squamous cell carcinoma of the head and neck: EHNS-ESMO-ESTRO Clinical Practice Guidelines for diagnosis, treatment and follow-up. *Annals of Oncology*, 21(Supplement 5), pp.v184-v186.

Gronbak, M., Becker, U., Johansen, D., Tonnesen, H., Jensen, G. and Sorensen, T. (1998). Population based cohort study of the association between alcohol intake and cancer of the upper digestive tract. *BMJ*, 317(7162), pp.844-848.

Gstraunthaler, G. (2003). Alternatives to the use of fetal bovine serum: serum-free cell culture. *Altex*, 20(4), pp.275-81.

Gupta, A., McKenna, W. and Weber, C. (2002). Local recurrence in head and neck cancer: Relationship to radiation resistance and signal transduction. *Clin Cancer Res*, 8, pp.885-892.

Ha, P. and Califano, J. (2003). The Molecular Biology of Mucosal Field Cancerization of the Head and Neck. *Critical Reviews in Oral Biology & Medicine*, 14(5), pp.363-369.

Haddad, R. and Shin, D. (2008). Recent Advances in Head and Neck Cancer. *New England Journal of Medicine*, 359(11), pp.1143-1154.

Haldar, S., Negrini, M., Monne, M., Sabbioni, S. and Croce, C. (1994). Downregulation of bcl-2 by p53 in breast cancer cells. 54, pp.2095-7.

Hall, E. and Giaccia, A. (2012). *Radiobiology for the radiologist*. Philadelphia: Wolters Kluwer Health/Lippincott Williams & Wilkins.

Harris, B., Barberis, A., West, C. and Buffa, F. (2015). Gene Expression Signatures as Biomarkers of Tumour Hypoxia. *Clinical Oncology*, 27(10), pp.547-560.

Hasegawa, Y., Goto, M., Hanai, N., Ijichi, K., Adachi, M., Terada, A., Hyodo, I., Ogawa, T. and Furukawa, T. (2007). Evaluation of optimal drug concentration in histoculture drug response assay in association with clinical efficacy for head and neck cancer. *Oral Oncology*, 43(8), pp.749-756.

Hashibe, M., Brennan, P., Benhamou, S., Castellsague, X., Chen, C., Curado, M., Maso, L., Daudt, A., Fabianova, E., Wunsch-Filho, V., Franceschi, S., Hayes, R., Herrero, R., Koifman, S., La Vecchia, C., Lazarus, P., Levi, F., Mates, D., Matos, E., Menezes, A., Muscat, J., Eluf-Neto, J., Olshan, A., Rudnai, P., Schwartz, S., Smith, E., Sturgis, E., Szeszenia-Dabrowska, N., Talamini, R., Wei, Q., Winn, D., Zaridze, D., Zatonski, W., Zhang, Z., Berthiller, J. and Boffetta, P. (2007). Alcohol Drinking in Never Users of Tobacco, Cigarette Smoking in Never Drinkers, and the Risk of Head and Neck Cancer: Pooled Analysis in the International Head and Neck Cancer Epidemiology Consortium. *JNCI Journal of the National Cancer Institute*, 99(10), pp.777-789.

Hattersley, S., Dyer, C., Greenman, J. and Haswell, S. (2008). Development of a microfluidic device for the maintenance and interrogation of viable tissue biopsies. *Lab on a Chip*, 8(11), p.1842.

Hattersley, S., Greenman, J. and Haswell, S. (2011). Study if ethanol induced toxicity in liver explants using microfluidic devices. *Biomedical Microdevices*, 13(6), pp.1005-1014.

Hattersley, S., Sylvester, D., Dyer, C., Stafford, N., Haswell, S. and Greenman, J. (2011). A Microfluidic System for Testing the Responses of Head and Neck Squamous Cell Carcinoma Tissue Biopsies to Treatment with Chemotherapy Drugs. *Annals of Biomedical Engineering*, 40(6), pp.1277-1288.

Heck, J., Berthiller, J., Vaccarella, S., Winn, D., Smith, E., Shan'gina, O., Schwartz, S., Purdue, M., Pilarska, A., Eluf-Neto, J., Menezes, A., McClean, M., Matos, E., Koifman, S., Kelsey, K., Herrero, R., Hayes, R., Franceschi, S., Wünsch-Filho, V., Fernández, L., Daudt, A., Curado, M., Chen, C., Castellsagué, X., Ferro, G., Brennan, P., Boffetta, P. and Hashibe, M. (2009). Sexual behaviours and the risk of head and neck cancers: a pooled analysis in the International Head and Neck Cancer Epidemiology (INHANCE) consortium. *International Journal of Epidemiology*, 39(1), pp.166-181.

Helton, E. and Chen, X. (2007). p53 modulation of the DNA damage response. *Journal of Cellular Biochemistry*, 100(4), pp.883-896.

Herrero, R. (2003). Human Papillomavirus and Oral Cancer: The International Agency for Research on Cancer Multicenter Study. *CancerSpectrum Knowledge Environment*, 95(23), pp.1772-1783.

Hill, R. (2006). Identifying Cancer Stem Cells in Solid Tumors: Case Not Proven. *Cancer Research*, 66(4), pp.1891-1896.

Höckel, M., Knoop, C., Schlenger, K., Vorndran, B., Baußnann, E., Mitze, M., Knapstein, P. and Vaupel, P. (1993). Intratumoral pO2 predicts survival in advanced cancer of the uterine cervix. *Radiotherapy and Oncology*, 26(1), pp.45-50.

Hoffman, W., Biade, S., Zilfou, J., Chen, J. and Murphy, M. (2001). Transcriptional Repression of the Anti-apoptoticsurvivin Gene by Wild Type p53. *Journal of Biological Chemistry*, 277(5), pp.3247-3257.

Hoffmann, D., Brunnemann, K., Prokopczyk, B. and Djordjevic, M. (1994). Tobacco-specific N -nitrosamines and ARECA- derived N -nitrosamines: Chemistry, biochemistry, carcinogenicity, and relevance to humans. *Journal of Toxicology and Environmental Health*, 41(1), pp.1-52.

Hoshino, T., Nagashima, T., Murovic, J., Levin, E., Levin, V. and Rupp, S. (1985). Cell kinetic studies of in situ human brain tumors with bromodeoxyuridine. *Cytometry*, 6(6), pp.627-632.

Hu, Z., Müller, S., Qian, G., Xu, J., Kim, S., Chen, Z., Jiang, N., Wang, D., Zhang, H., Saba, N., Shin, D. and Chen, Z. (2014). Human papillomavirus 16 oncoprotein regulates the translocation of β-catenin via the activation of epidermal growth factor receptor. *Cancer*, 121(2), pp.214-225.

Huang, S., Waldron, J., Milosevic, M., Shen, X., Ringash, J., Su, J., Tong, L., Perez-Ordonez, B., Weinreb, I., Bayley, A., Kim, J., Hope, A., Cho, B., Giuliani, M., Razak, A., Goldstein, D., Shi, W., Liu, F., Xu, W. and O'Sullivan, B. (2014). Prognostic value of pretreatment circulating neutrophils, monocytes, and lymphocytes in oropharyngeal cancer stratified by human papillomavirus status. *Cancer*, 121(4), pp.545-555.

Huebner, A., Srisa-Art, M., Holt, D., Abell, C., Hollfelder, F., deMello, A. and Edel, J. (2007). Quantitative detection of protein expression in single cells using droplet microfluidics. *Chemical Communications*, (12), p.1218.

Hung, S., Ho, J., Shih, Y., Lo, T. and Lee, O. (2011). Hypoxia promotes proliferation and osteogenic differentiation potentials of human mesenchymal stem cells. *Journal of Orthopaedic Research*, 30(2), pp.260-266.

Ianzini, F., Bertoldo, A., Kosmacek, E., Phillips, S. and Mackey, M. (2006). Lack of p53 function promotes radiation-induced mitotic catastrophe in mouse embryonic fibroblast cells. *Cancer Cell Int*, 26(6), p.11.

IARC monographs on the evaluation of the carcinogenic risk of chemicals to humans. Vol. 37. Tobacco habits other than smoking; Betel-quid and Areca-nut chewing; and some related nitrosamines. (1986). *Food and Chemical Toxicology*, 24(8), pp.885-886.

Igney, F. and Krammer, P. (2002). Death and anti-death: tumour resistance to apoptosis. *Nature Reviews Cancer*, 2(4), pp.277-288.

Ijichi, K., Adachi, M., Hasegawa, Y., Ogawa, T., Nakamura, H., Kudoh, A., Yasui, Y., Murakami, S. and Ishizaki, K. (2007). Pretreatment with 5-FU enhances cisplatin cytotoxicity in head and neck squamous cell carcinoma cells. *Cancer Chemotherapy and Pharmacology*, 62(5), pp.745-752.

Jensen, D., Hedback, N., Specht, L., Høgdall, E., Andersen, E., Therkildsen, M., Friis-Hansen, L., Norrild, B. and von Buchwald, C. (2014). Human Papillomavirus in Head and Neck Squamous Cell Carcinoma of Unknown Primary Is a Common Event and a Strong Predictor of Survival. *PLoS ONE*, 9(11), p.e110456.

Jiang, X. and Wang, X. (2000). Cytochrome c Promotes Caspase-9 Activation by Inducing Nucleotide Binding to Apaf-1. *Journal of Biological Chemistry*, 275(40), pp.31199-31203.

Jones, K., Elmore, L., Jackson-Cook, C., Demasters, G., Povirk, L., Holt, S. and Gewirtz, D. (2005). p53-Dependent accelerated senescence induced by ionizing radiation in breast tumour cells. *International Journal of Radiation Biology*, 81(6), pp.445-458.

Junqueira, L. and Carneiro, J. (2005). *Basic histology*. New York: McGraw-Hill, Medical Pub. Division.

Kastan, M. (1997). On the TRAIL from p53 to apoptosis?. *Nature Genetics*, 17(2), pp.130-131.

Kawamura, K., Fujikawa-Yamamoto, K., Ozaki, M., Iwabuchi, K., Nakashima, H., Domiki, C., Morita, N., Inoue, M., Tokunaga, K., Shiba, N., Ikeda, R. and Suzuki, K. (2005). Centrosome Hyperamplification and Chromosomal Damage after Exposure to Radiation. *Oncology*, 67(5-6), pp.460-470.

Kawamura, K., Morita, N., Domiki, C., Fujikawa-Yamamoto, K., Hashimoto, M., Iwabuchi, K. and Suzuki, K. (2006). Induction of centrosome amplification in p53 siRNA-treated human fibroblast cells by radiation exposure. *Cancer Science*, 97(4), pp.252-258.

Kellokumpu-Lehtinen, P., Söderström, K., Kortekangas, A. and Nordman, E. (1990). Radiation-Induced Morphological Changes and Radiocurability in Squamous Cell

Carcinoma of the Head and Neck Region: A preliminary report. *Acta Oncologica*, 29(4), pp.517-520.

Kerr, J., Wyllie, A. and Currie, A. (1972). Apoptosis: A Basic Biological Phenomenon with Wideranging Implications in Tissue Kinetics. *Br J Cancer*, 26(4), pp.239-257.

Kim, I., Bae, S. and Fernandes, A. (2005). Selective inhibition of Ras, phosphoinositide 3 kinase, and Akt isoforms increases the radiosensitivity of human carcinoma cell lines. *Cancer Res*, 65, pp.7902-7910.

Kim, L., Toh, Y., Voldman, J. and Yu, H. (2007). A practical guide to microfluidic perfusion culture of adherent mammalian cells. *Lab on a Chip*, 7(6), p.681.

Kim, L., Vahey, M., Lee, H. and Voldman, J. (2006). Microfluidic arrays for logarithmically perfused embryonic stem cell culture. *Lab on a Chip*, 6(3), p.394.

Kimple, R., Smith, M., Blitzer, G., Torres, A., Martin, J., Yang, R., Peet, C., Lorenz, L., Nickel, K., Klingelhutz, A., Lambert, P. and Harari, P. (2013). Enhanced Radiation Sensitivity in HPV-Positive Head and Neck Cancer. *Cancer Research*, 73(15), pp.4791-4800.

Knekt,, P., Järvinen, R., Dich, J. and Hakulinen, T. (1999). Risk of colorectal and other gastro-intestinal cancers after exposure to nitrate, nitrite and N-nitroso compounds: a follow-up study. *International Journal of Cancer*, 80(6), pp.852-856.

Kobayashi, H., Man, S., Graham, C., Kapitain, S., Teicher, B. and Kerbel, R. (1993). Acquired multicellular-mediated resistance to alkylating agents in cancer. *Proceedings of the National Academy of Sciences*, 90(8), pp.3294-3298.

Kobayashi, T., Ruan, S., Jabbur, J., Consoli, U., Clodi, K., Shiku, H., Owen-Schaub, L., Andreeff, M., Reed, J. and Zhang, W. (1998). Differential p53 phosphorylation and activation of apoptosis-promoting genes Bax and Fas/APO-1 by irradiation and ara-C treatment. *Cell Death Differ*, 5(7), pp.584-591.

Kofler, B., Laban, S., Busch, C., Lörincz, B. and Knecht, R. (2013). New treatment strategies for HPV-positive head and neck cancer. *Eur Arch Otorhinolaryngol*, 271(7), pp.1861-1867.

Koniggreger, D., Riechelmann, H., Wittich, U. and Gronau, S. (2004). Genotype and phenotype of glutathione-s-transferase in patients with head and neck carcinoma1. *Otolaryngology - Head and Neck Surgery*, 130(6), pp.718-725.

Konry, T., Dominguez-Villar, M., Baecher-Allan, C., Hafler, D. and Yarmush, M. (2011). Droplet-based microfluidic platforms for single T cell secretion analysis of IL-10 cytokine. *Biosensors and Bioelectronics*, 26(5), pp.2707-2710.

Köpf-Maier, P. and Kolon, B. (1992). An organoid culture assay (OCA) for determining the drug sensitivity of human tumors. *International Journal of Cancer*, 51(1), pp.99-107.

Krause, C., Otieno, B., Bishop, G., Phadke, G., Choquette, L., Lalla, R., Peterson, D. and Rusling, J. (2015). Ultrasensitive microfluidic array for serum pro-inflammatory cytokines and C-reactive protein to assess oral mucositis risk in cancer patients. *Anal Bioanal Chem*, 407(23), pp.7239-7243.

Kreimer, A., Clifford, G., Snijders, P., Castellsagué, X., Meijer, C., Pawlita, M., Viscidi, R., Herrero, R. and Franceschi, S. (2005). HPV16 semiquantitative viral load and serologic biomarkers in oral and oropharyngeal squamous cell carcinomas. *International Journal of Cancer*, 115(2), pp.329-332.

Kropveld, A., Slootweg, P., Blankenstein, M., Terhaard, C. and Hordijk, G. (1998). Ki-67 and p53 in T2 laryngeal cancer. *Laryngoscope*, 108(10), pp.1548-1552.

Kross, K., Heimdal, J., Olsnes, C., Olofsson, J. and Aarstad, H. (2005). Head and neck squamous cell carcinoma spheroid- and monocyte spheroid-stimulated IL-6 and monocyte chemotactic protein-1 secretion are related to TNM stage, inflammatory state and tumor macrophage density. *Acta Oto-Laryngologica*, 125(10), pp.1097-1104.

Kufe, D., Pollock, R., Weichselbaum, R., Bast, R., Gansler, T., Holland, J. and Frei, E. (2003). *Holland-Frei Cancer medicine*. Hamilton, Ont.: B C Decker.

Lambrecht, M., Dirix, P., Van den Bogaert, W. and Nuyts, S. (2009). Incidence of isolated regional recurrence after definitive (chemo-) radiotherapy for head and neck squamous cell carcinoma. *Radiotherapy and Oncology*, 93(3), pp.498-502.

Larque, A., Hakim, S., Ordi, J., Nadal, A., Diaz, A., Pino, M., Marimon, L., Alobid, I., Cardesa, A. and Alos, L. (2013). High-risk human papillomavirus is transcriptionally active in a subset of sinonasal squamous cell carcinomas. *Modern Pathology*.

Lassen, P., Eriksen, J., Hamilton-Dutoit, S., Tramm, T., Alsner, J. and Overgaard, J. (2009). Effect of HPV-Associated p16INK4A Expression on Response to Radiotherapy and Survival in Squamous Cell Carcinoma of the Head and Neck. *Journal of Clinical Oncology*, 27(12), pp.1992-1998.

Lassen, P., Eriksen, J., Hamilton-Dutoit, S., Tramm, T., Alsner, J. and Overgaard, J. (2010). HPV-associated p16-expression and response to hypoxic modification of radiotherapy in head and neck cancer. *Radiotherapy and Oncology*, 94(1), pp.30-35.

Ledgerwood, L., Kumar, D., Eterovic, A., Wick, J., Chen, K., Zhao, H., Tazi, L., Manna, P., Kerley, S., Joshi, R., Wang, L., Chiosea, S., Garnett, J., Tsue, T., Chien, J., Mills, G., Grandis, J. and Thomas, S. (2016). The degree of intratumor mutational heterogeneity varies by primary tumor sub-site. *Oncotarget*.

Lee, S., Lee, T., Park, J., Cho, E. and Chung, C. (1989). In vitro immunohistochemical localization of S-phase cells by a monoclonal antibody to bromodeoxyuridine. *Journal of Korean Medical Science*, 4(4), p.193.

Leemans, C., Braakhuis, B. and Brakenhoff, R. (2010). The molecular biology of head and neck cancer. *Nature Reviews Cancer*, 11(1), pp.9-22.

Leers, M., Kolgen, W., Bjorklund, V., Bergman, T., Tribbick, G., Persson, B., Bjorklund, P., Ramaekers, F., Bjorklund, B., Nap, M., Jornvall, H. and Schutte, B. (1999). Immunocytochemical detection and mapping of a cytokeratin 18 neo-epitope exposed during early apoptosis. *J. Pathol.* 187(5), pp.567-572.

Lehmann, B., McCubrey, J., Jefferson, H., Paine, M., Chappell, W. and Terrian, D. (2007). A Dominant Role for p53-Dependent Cellular Senescence in Radiosensitization of Human Prostate Cancer Cells. *Cell Cycle*, 6(5), pp.595-605.

Lei, K., Wu, M., Hsu, C. and Chen, Y. (2014). Real-time and non-invasive impedimetric monitoring of cell proliferation and chemosensitivity in a perfusion 3D cell culture microfluidic chip. *Biosensors and Bioelectronics*, 51, pp.16-21.

Lenarduzzi, M., Hui, A., Yue, S., Ito, E., Shi, W., Williams, J., Bruce, J., Sakemura-Nakatsugawa, N., Xu, W., Schimmer, A. and Liu, F. (2013). Hemochromatosis Enhances Tumor Progression via Upregulation of Intracellular Iron in Head and Neck Cancer. *PLoS ONE*, 8(8), p.e74075.

Leong, H., Chong, F., Sew, P., Lau, D., Wong, B., Teh, B., Tan, D. and Iyer, N. (2014). Targeting Cancer Stem Cell Plasticity Through Modulation of Epidermal Growth Factor and Insulin-Like Growth Factor Receptor Signaling in Head and Neck Squamous Cell Cancer. *Stem Cells Translational Medicine*, 3(9), pp.1055-1065.

Lewis, J. (2016). Sinonasal Squamous Cell Carcinoma: A Review with Emphasis on Emerging Histologic Subtypes and the Role of Human Papillomavirus. *Head and Neck Pathology*, 10(1), pp.60-67.

Liang, C., McClean, M., Marsit, C., Christensen, B., Peters, E., Nelson, H. and Kelsey, K. (2009). A Population-Based Case-Control Study of Marijuana Use and Head and Neck Squamous Cell Carcinoma. *Cancer Prevention Research*, 2(8), pp.759-768.

Lim, Y., Oh, S., Cha, Y., Kim, S., Jin, X. and Kim, H. (2011). Cancer stem cell traits in squamospheres derived from primary head and neck squamous cell carcinomas. *Oral Oncology*, 47(2), pp.83-91.

Lin, C., Grandis, J., Carey, T., Gollin, S., Whiteside, T., Koch, W., Ferris, R. and Lai, S. (2007). Head and neck squamous cell carcinoma cell lines: Established models and rationale for selection. *Head Neck*, 29(2), pp.163-188.

Ling, Y., Rubin, J., Deng, Y., Huang, C., Demirci, U., Karp, J. and Khademhosseini, A. (2007). A cell-laden microfluidic hydrogel. *Lab on a Chip*, 7(6), p.756.

Linz, U. (2012). *Ion beam therapy*. Berlin: Springer.

Lohavanichbutr, P., Houck, J., Fan, W., Yueh, B., Mendez, E., Futran, N., Doody, D., Upton, M., Farwell, D., Schwartz, S., Zhao, L. and Chen, C. (2009). Genomewide Gene Expression Profiles of HPV-Positive and HPV-Negative Oropharyngeal Cancer. *Arch Otolaryngol Head Neck Surg*, 135(2), p.180.

Lothaire, P., de Azambuja, E., Dequanter, D., Lalami, Y., Sotiriou, C., Andry, G., Castro, G. and Awada, A. (2006). Molecular markers of head and neck squamous cell carcinoma: Promising signs in need of prospective evaluation. *Head Neck*, 28(3), pp.256-269.

Luo, X., Budihardjo, I., Zou, H., Slaughter, C. and Wang, X. (1998). Bid, a Bcl2 Interacting Protein, Mediates Cytochrome c Release from Mitochondria in Response to Activation of Cell Surface Death Receptors. *Cell*, 94(4), pp.481-490.

Ma, H., Zhang, M. and Qin, J. (2012). Probing the role of mesenchymal stem cells in salivary gland cancer on biomimetic microdevices. *Integr. Biol.*, 4(5), p.522.

Maalouf, M., Alphonse, G., Colliaux, A., Beuve, M., Trajkovic-Bodennec, S., Battiston-Montagne, P., Testard, I., Chapet, O., Bajard, M., Taucher-Scholz, G., Fournier, C. and Rodriguez-Lafrasse, C. (2009). Different Mechanisms of Cell Death in Radiosensitive and Radioresistant P53 Mutated Head and Neck Squamous Cell Carcinoma Cell Lines Exposed to Carbon Ions and X-Rays. *International Journal of Radiation Oncology*Biology*Physics*, 74(1), pp.200-209.

Maier, H. and Tisch, M. (2001). Occupations and social habits and head and neck cancer. *Current Opinion in Otolaryngology & Head and Neck Surgery*, 9(2), pp.71-73.

Majchrzak, E., Szybiak, B., Wegner, A., Pienkowski, P., Pazdrowski, J., Luczewski, L., Sowka, M., Golusinski, P., Malicki, J. and Golusinski, W. (2014). Oral cavity and oropharyngeal squamous cell carcinoma in young adults: a review of the literature. *Radiology and Oncology*, 48(1), pp.1-10.

Malhotra, R., Patel, V., Chikkaveeraiah, B., Munge, B., Cheong, S., Zain, R., Abraham, M., Dey, D., Gutkind, J. and Rusling, J. (2012). Ultrasensitive Detection of Cancer Biomarkers in the Clinic by Use of a Nanostructured Microfluidic Array. *Analytical Chemistry*, 84(14), pp.6249-6255.

Mamouni, J. and Yang, L. (2011). Interdigitated microelectrode-based microchip for electrical impedance spectroscopic study of oral cancer cells. *Biomedical Microdevices*, 13(6), pp.1075-1088.

Mantel, F., Frey, B., Haslinger, S., Schildkopf, P., Sieber, R., Ott, O., Lödermann, B., Rödel, F., Sauer, R., Fietkau, R. and Gaipl, U. (2010). Combination of Ionising Irradiation and Hyperthermia Activates Programmed Apoptotic and Necrotic Cell Death Pathways in Human Colorectal Carcinoma Cells. *Strahlenther Onkol*, 186(11), pp.587-599.

Mäntylä, M., Kortekangas, A., Valavaara, R. and Nordman, E. (1979). Tumour regression during radiation treatment as a guide to prognosis. *The British Journal of Radiology*, 52(624), pp.972-977.

Marusyk, A. and Polyak, K. (2010). Tumor heterogeneity: Causes and consequences. *Biochimica et Biophysica Acta (BBA) - Reviews on Cancer*, 1805(1), pp.105-117.

Masunaga, S., Uto, Y., Nagasawa, H., Hori, H., Nagata, K., Suzuki, M., Kinashi, Y. and Ono, K. (2006). Evaluation of hypoxic cell radio-sensitizers in terms of radio-sensitizing and repair-inhibiting potential. Dependency on p53 status of tumor cells and the effects on intratumor quiescent cells. *Anticancer Res*, 26(2A), pp.1261-70.

Mazutis, L., Araghi, A., Miller, O., Baret, J., Frenz, L., Janoshazi, A., Taly, V., Miller, B., Hutchison, J., Link, D., Griffiths, A. and Ryckelynck, M. (2009). Droplet-Based Microfluidic Systems for High-Throughput Single DNA Molecule Isothermal Amplification and Analysis. *Analytical Chemistry*, 81(12), pp.4813-4821.

Mehanna, H., Jones, T., Gregoire, V. and Ang, K. (2010). Oropharyngeal carcinoma related to human papillomavirus. *BMJ*, 340(mar25 1), pp.c1439-c1439.

Mehanna, H., Paleri, V., West, C. and Nutting, C. (2010). Head and neck cancer--Part 1: Epidemiology, presentation, and prevention. *BMJ*, 341(sep20 1), pp.c4684-c4684.

Merchant, A., Husain, S., Hosain, M., Fikree, F., Pitiphat, W., Siddiqui, A., Hayder, S., Haider, S., Ikram, M., Chuang, S. and Saeed, S. (2000). Paan without tobacco: An independent risk factor for oral cancer. *International Journal of Cancer*, 86(1), pp.128-131.

Merletti, F., Boffetta, P., Ciccone, G., Mashberg, A. and Terracini, B. (1989). Role of tobacco and alcoholic beverages in the etiology of cancer of the oral cavity/oropharynx in Torino, Italy. *Cancer Res*, 1(49), pp.4919-24.

Meyvantsson, I. and Beebe, D. (2008). Cell Culture Models in Microfluidic Systems. *Annual Review of Analytical Chemistry*, 1(1), pp.423-449.

Miller, A. (1987). IARC monographs on the evaluation of the carcinogenic risk of chemicals to humans. Vol. 38. Tobacco smoking. *Food and Chemical Toxicology*, 25(8), pp.627-628.

Miller, B., Miller, F. and Heppner, G. (1984). Assessing tumor drug sensitivity by a new in vitro assay which preserves tumor heterogeneity and subpopulation interactions. *J. Cell. Physiol.*, 121(S3), pp.105-116.

Mirghani, H., Amen, F., Moreau, F., Guigay, J., Hartl, D. and Lacau St. Guily, J. (2014). Oropharyngeal cancers: Relationship between epidermal growth factor receptor alterations and human papillomavirus status. *European Journal of Cancer*, 50(6), pp.1100-1111.

Mirghani, H., Amen, F., Tao, Y., Deutsch, E. and Levy, A. (2015). Increased radiosensitivity of HPV-positive head and neck cancers: Molecular basis and therapeutic perspectives. *Cancer Treatment Reviews*, 41(10), pp.844-852.

Mirzayans, R., Scott, A., Cameron, M. and Murray, D. (2005). Induction of Accelerated Senescence by γ Radiation in Human Solid Tumor-Derived Cell Lines Expressing Wild-Type TP53. *Radiation Research*, 163(1), pp.53-62.

Miyashita, T., Harigai, M., Hanada, M. and reed, J. (1994). Identification of a p53-dependent negative response element in the bcl-2 gene. *Cancer Res*, 54, pp.3131-5.

Mroz, E. and Rocco, J. (2013). MATH, a novel measure of intratumor genetic heterogeneity, is high in poor-outcome classes of head and neck squamous cell carcinoma. *Oral Oncology*, 49(3), pp.211-215.

Mroz, E., Tward, A., Pickering, C., Myers, J., Ferris, R. and Rocco, J. (2013). High intratumor genetic heterogeneity is related to worse outcome in patients with head and neck squamous cell carcinoma. *Cancer*, 119(16), pp.3034-3042.

Muhanna, N., Mepham, A., Mohamadi, R., Chan, H., Khan, T., Akens, M., Besant, J., Irish, J. and Kelley, S. (2015). Nanoparticle-based sorting of circulating tumor cells by epithelial antigen expression during disease progression in an animal model. *Nanomedicine: Nanotechnology, Biology and Medicine*, 11(7), pp.1613-1620.

Nakanishi, J., Takarada, T., Yamaguchi, K. And Maeda, M. (2008). Recent Advances in Cell Micropatterning Techniques for Bioanalytical and Biomedical Sciences. *Analytical Sciences*, 24(1), pp.67-72.

Näsman, A., Attner, P., Hammarstedt, L., Du, J., Eriksson, M., Giraud, G., Ährlund-Richter, S., Marklund, L., Romanitan, M., Lindquist, D., Ramqvist, T., Lindholm, J., Sparén, P., Ye, W., Dahlstrand, H., Munck-Wikland, E. and Dalianis, T. (2009). Incidence of human papillomavirus (HPV) positive tonsillar carcinoma in Stockholm, Sweden: An epidemic of viral-induced carcinoma?. *International Journal of Cancer*, 125(2), pp.362-366.

Nevill, J., Cooper, R., Dueck, M., Breslauer, D. and Lee, L. (2007). Integrated microfluidic cell culture and lysis on a chip. *Lab on a Chip*, 7(12), p.1689.

Nomiya, T. (2013). Discussions on target theory: past and present. *Journal of Radiation Research*, 54(6), pp.1161-1163.

Nordman, E., Joensuu, H., Kellokumpu-Lehtinen, P., Minn, H. and Mäntylä, M. (1990). Is It Possible to Predict the Outcome of Radiation Therapy of Head and Neck Cancer?. *Acta Oncologica*, 29(4), pp.521-524.

Nordsmark, M., Bentzen, S., Rudat, V., Brizel, D., Lartigau, E., Stadler, P., Becker, A., Adam, M., Molls, M., Dunst, J., Terris, D. and Overgaard, J. (2005). Prognostic value of tumor oxygenation in 397 head and neck tumors after primary radiation therapy. An international multi-center study. *Radiotherapy and Oncology*, 77(1), pp.18-24.

Novakova, Z., Hubackova, S., Kosar, M., Janderova-Rossmeislova, L., Dobrovolna, J., Vasicova, P., Vancurova, M., Horejsi, Z., Hozak, P., Bartek, J. and Hodny, Z. (2009). Cytokine expression and signaling in drug-induced cellular senescence. *Oncogene*, 29(2), pp.273-284.

Nowell, P. (1976). The clonal evolution of tumor cell populations. *Science*, 194(4260), pp.23-28.

Núñez, M., McMillan, T., Valenzuela, M., de Almodóvar, J. and Pedraza, V. (1996). Relationship between DNA damage, rejoining and cell killing by radiation in mammalian cells. *Radiotherapy and Oncology*, 39(2), pp.155-165.

Nutting, C. (2016). Radiotherapy in head and neck cancer management: United Kingdom National Multidisciplinary Guidelines. *The Journal of Laryngology & Otology*, 130(S2), pp.S66-S67.

O'Rourke, S., McAneney, H. and Hillen, T. (2008). Linear quadratic and tumour control probability modelling in external beam radiotherapy. *J. Math. Biol.*, 58(4-5), pp.799-817.

Olsen, J., Sabroe, S. and Ipsen, J. (1985). Effect of combined alcohol and tobacco exposure on risk of cancer of the hypopharynx. *Journal of Epidemiology & Community Health*, 39(4), pp.304-307.

Olshan, A., Weissler, M., Pei, H. and Conway, K. (1997). p53 mutations in head and neck cancer: new data and evaluation of mutational spectra. *Cancer Epidemiol Biomarkers Prev*, 6, pp.499-504.

Oreggia, F., De Stefani, E., Boffetta, P., Brennan, P., Deneo-Pellegrini, H. and Ronco, A. (2001). Meat, fat and risk of laryngeal cancer: a case-control study in Uruguay. *Oral Oncology*, 37(2), pp.141-145.

Orth, M., Lauber, K., Niyazi, M., Friedl, A., Li, M., Maihöfer, C., Schüttrumpf, L., Ernst, A., Niemöller, O. and Belka, C. (2013). Current concepts in clinical radiation oncology. *Radiat Environ Biophys*, 53(1), pp.1-29.

Otieno, B., Krause, C., Latus, A., Chikkaveeraiah, B., Faria, R. and Rusling, J. (2014). On-line protein capture on magnetic beads for ultrasensitive microfluidic immunoassays of cancer biomarkers. *Biosensors and Bioelectronics*, 53, pp.268-274.

Overgaard, J. (2011). Hypoxic modification of radiotherapy in squamous cell carcinoma of the head and neck – A systematic review and meta-analysis. *Radiotherapy and Oncology*, 100(1), pp.22-32.

Pai, S. and Westra, W. (2009). Molecular Pathology of Head and Neck Cancer: Implications for Diagnosis, Prognosis, and Treatment. *Annu. Rev. Pathol. Mech. Dis.*, 4(1), pp.49-70.

Pajares, B., Trigo, J., Toledo, M., Álvarez, M., González-Hermoso, C., Rueda, A., Medina, J., Luque, V., Jerez, J. and Alba, E. (2013). Differential outcome of concurrent radiotherapy plus epidermal growth factor receptor inhibitors versus radiotherapy plus cisplatin in patients with human papillomavirus-related head and neck cancer. *BMC Cancer*, 13(1).

Paleri, V. and Roland, N. (2016). Introduction to the United Kingdom National Multidisciplinary Guidelines for Head and Neck Cancer. *The Journal of Laryngology & Otology*, 130(S2), pp.S3-S4.

Park, C., Bissell, M. and Barcellos-Hoff, M. (2000). The influence of the microenvironment on the malignant phenotype. *Molecular Medicine Today*, 6(8), pp.324-329.

Patel, V., Martin, D., Malhotra, R., Marsh, C., Doçi, C., Veenstra, T., Nathan, C., Sinha, U., Singh, B., Molinolo, A., Rusling, J. and Gutkind, J. (2013). DSG3 as a biomarker for the ultrasensitive detection of occult lymph node metastasis in oral cancer using nanostructured immunoarrays. *Oral Oncology*, 49(2), pp.93-101.

Pathak, K., Juvekar, A., Radhakrishnan, D., Deshpande, M., Pai, V., Chaturvedi, P., Pai, P., Chaukar, D., D'Cruz, A. and Parikh, P. (2007). In vitro chemosensitivity profile of oral squamous cell cancer and its correlation with clinical response to chemotherapy. *Indian Journal of Cancer*, 44(4), p.142.

Pathologyoutlines.com. (2016). *Pathology Outlines*. [online] Available at: http://www.pathologyoutlines.com [Accessed 17 Aug. 2016].

Paydarfar, J. and Birkmeyer, N. (2006). Complications in Head and Neck Surgery. *Archives of Otolaryngology–Head & Neck Surgery*, 132(1), p.67.

Perri, F., Pacelli, R., Della Vittoria Scarpati, G., Cella, L., Giuliano, M., Caponigro, F. and Pepe, S. (2015). Radioresistance in head and neck squamous cell carcinoma: Biological bases and therapeutic implications. *Head Neck*, 37(5), pp.763-770.

Philip, B., Ito, K., Moreno-Sanchez, R. and Ralph, S. (2013). HIF expression and the role of hypoxic microenvironments within primary tumours as protective sites driving cancer stem cell renewal and metastatic progression. *Carcinogenesis*, 34(8), pp.1699-1707.

Pignon, J., Sylvester, R. and Bourhis, J. (2000). Hyperfractionated and/or accelerated radiotherapy versus conventional radiotherapy for head and neck cancer. *Cochrane Database of Systematic Reviews*.

Podgorsak, E. (2005). *Radiation oncology physics*. Vienna: International Atomic Energy Agency.

Podgoršak, E. (2006). *Radiation Physics for Medical Physicists*. Berlin, Heidelberg: Springer-Verlag Berlin Heidelberg.

Poeta, M., Manola, J., Goldwasser, M., Forastiere, A., Benoit, N., Califano, J., Ridge, J., Goodwin, J., Kenady, D., Saunders, J., Westra, W., Sidransky, D. and Koch, W. (2007). TP53 Mutations and Survival in Squamous-Cell Carcinoma of the Head and Neck. *New England Journal of Medicine*, 357(25), pp.2552-2561.

Price, P., Sikora, K. and Illidge, T. (2008). *Treatment of cancer*. London: Hodder Arnold.

Puleo, C., Yeh, H. and Wang, T. (2007). Applications of MEMS Technologies in Tissue Engineering. *Tissue Engineering*, 13(12), pp.2839-2854.

Quick, Q. and Gewirtz, D. (2006). An accelerated senescence response to radiation in wild-type p53 glioblastoma multiforme cells. *Journal of Neurosurgery*, 105(1), pp.111-118.

Raybaud, H., Fortin, A., Bairati, I., Morency, R., Monteil, R. and Tetu, B. (2000). Nuclear DNA content, an adjunct to p53 and Ki-67 as a marker of resistance to radiation therapy in oral cavity and pharyngeal squamous cell carcinoma. *International Journal of Oral and Maxillofacial Surgery*, 29(1), pp.36-41.

Remmerbach, T., Wottawah, F., Dietrich, J., Lincoln, B., Wittekind, C. and Guck, J. (2009). Oral Cancer Diagnosis by Mechanical Phenotyping. *Cancer Research*, 69(5), pp.1728-1732.

Rexius-Hall, M., Mauleon, G., Malik, A., Rehman, J. and Eddington, D. (2014). Microfluidic platform generates oxygen landscapes for localized hypoxic activation. *Lab Chip*, 14(24), pp.4688-4695.

Rheinwald, J. and Beckett, M. (1981). Tumorigenic keratinocyte lines requiring anchorage and fibroblast support cultured from human squamous cell carcinomas. *Cancer Res*, 41, pp.1657-1663.

Rieckmann, T., Tribius, S., Grob, T., Meyer, F., Busch, C., Petersen, C., Dikomey, E. and Kriegs, M. (2013). HNSCC cell lines positive for HPV and p16 possess higher cellular

radiosensitivity due to an impaired DSB repair capacity. *Radiotherapy and Oncology*, 107(2), pp.242-246.

Riedel, F., Gotte, K., Bergler, W., Rojas, W. and Hormann, K. (2000). Expression of basic fibroblast growth factor protein and its down-regulation by interferons in head and neck cancer. *Head Neck*, 22(2), pp.183-189.

Rieder, C. and Maiato, H. (2004). Stuck in Division or Passing through. *Developmental Cell*, 7(5), pp.637-651.

Riesz, P. (1995). The life of Wilhelm Conrad Roentgen. *American Journal of Roentgenology*, 165(6), pp.1533-1537.

Robbins, K., Connors, K., Storniolo, A., Hanchett, C. and Hoffman, R. (1994). Sponge-Gel-Supported Histoculture Drug-Response Assay for Head and Neck Cancer: Correlations With Clinical Response to Cisplatin. *Archives of Otolaryngology - Head and Neck Surgery*, 120(3), pp.288-292.

Robin, P., Powell, D. And Stansbie, J. (1979). Carcinoma of the nasal cavity and paranasal sinuses: incidence and presentation of different histological types. *Clinical Otolaryngology*, 4(6), pp.431-456.

Rodier, F., Coppé, J., Patil, C., Hoeijmakers, W., Muñoz, D., Raza, S., Freund, A., Campeau, E., Davalos, A. and Campisi, J. (2009). Persistent DNA damage signalling triggers senescence-associated inflammatory cytokine secretion. *Nature Cell Biology*, 11(8), pp.973-979.

Rodriguez, J. and Lazebnik, Y. (1999). Caspase-9 and APAF-1 form an active holoenzyme. *Genes & Development*, 13(24), pp.3179-3184.

Rofstad, E., Wahl, A. and Brustad, T. (1987). Radiation sensitivity in vitro of cells isolated from human tumor surgical specimens. *Cancer Res*, 47, pp.106-110.

Roninson, I., Broude, E. and Chang, B. (2001). If not apoptosis, then what? Treatment-induced senescence and mitotic catastrophe in tumor cells. *Drug Resistance Updates*, 4(5), pp.303-313.

Rosenblatt, K. (2004). Marijuana Use and Risk of Oral Squamous Cell Carcinoma. *Cancer Research*, 64(11), pp.4049-4054.

Ruth, A. and Roninson, I. (2000). Effects of the multidrug transporter pglycoprotein on cellular responses to ionizing radiation. *Cancer Res*, 60, pp.2576-8.

Sacks, P. (1996). Cell, tissue and organ culture as in vitro models to study the biology of squamous cell carcinomas of the head and neck. *Cancer and Metastasis Review*, 15(1), pp.27-51.

Sasco, A., Secretan, M. and Straif, K. (2004). Tobacco smoking and cancer: a brief review of recent epidemiological evidence. *Lung Cancer*, 45, pp.S3-S9.

Scaffidi, C., Srinivasan, A., Friesen, C., Li, F. and Tomaselli, K. (1998). Two cd95 (apo-1/fas) signaling pathways. 17, pp.1675-87.

Schaerli, Y. and Hollfelder, F. (2009). The potential of microfluidic water-in-oil droplets in experimental biology. *Mol. BioSyst.*, 5(12), p.1392.

Scheffner, M., Werness, B., Huibregtse, J., Levine, A. and Howley, P. (1990). The E6 oncoprotein encoded by human papillomavirus types 16 and 18 promotes the degradation of p53. *Cell*, 63(6), pp.1129-1136.

Schildkopf, P., Frey, B., Mantel, F., Ott, O., Weiss, E., Sieber, R., Janko, C., Sauer, R., Fietkau, R. and Gaipl, U. (2010). Application of hyperthermia in addition to ionizing irradiation fosters necrotic cell death and HMGB1 release of colorectal tumor cells. *Biochemical and Biophysical Research Communications*, 391(1), pp.1014-1020.

Schumacher, K., Khong, Y., Chang, S., Ni, J., Sun, W. and Yu, H. (2007). Perfusion Culture Improves the Maintenance of Cultured Liver Tissue Slices. *Tissue Engineering*, 13(1), pp.197-205.

Schweichel, J. and Merker, H. (1973). The morphology of various types of cell death in prenatal tissues. *Teratology*, 7(3), pp.253-266.

Seethala, R. (2009). Current State of Neck Dissection in the United States. *Head and Neck Pathol*, 3(3), pp.238-245.

Semenza, G. (2003). Targeting HIF-1 for cancer therapy. *Nature Reviews Cancer*, 3(10), pp.721-732.

Semenza, G. (2004). Intratumoral hypoxia, radiation resistance, and HIF-1. *Cancer Cell*, 5(5), pp.405-406.

Shapira, A., Wagner, J., Wollner, I., Maybaum, J., Stetson, P., Ensminger, W. and Carey, T. (1988). Dynamics of bromodeoxyuridine incorporation into DNA of squamous carcinoma cells during mid and late logarithmic growth. *Pharm Res*, 5(8), pp.518-22.

Shay, J. and Roninson, I. (2004). Hallmarks of senescence in carcinogenesis and cancer therapy. *Oncogene*, 23(16), pp.2919-2933.

Sheard, M., Uldrijan, S. and Vojtesek, B. (2003). Role of p53 in regulating constitutive and x-radiation-inducible cd95 expression and function in carcinoma cells. *Cancer Res*, 63, pp.7176-84.

Sheard, M., Vojtesek, B., Janakova, L., Kovarik, J. and Zaloudik, J. (1997). Up-regulation of Fas (CD95) in human p53wild-type cancer cells treated with ionizing radiation. *International Journal of Cancer*, 73(5), pp.757-762.

Sheikh, M., Burns, T., Huang, Y., Wu, G., Amundson, S. and Brooks, K. (1998). P53-dependent and -independent regulation of the death receptor killer/dr5 gene expression in response to genotoxic stress and tumor necrosis factor alpha. *Cancer Res*, 58, pp.1593-8.

Sherwin, R., Richters, A., Yellin, A. and Donovan, A. (1980). Histoculture of human breast cancers. *Journal of Surgical Oncology*, 13(1), pp.9-20.

Shinomiya, N. (2001). New concepts in radiation-induced apoptosis: premitotic apoptosis and postmitotic apoptosis. *Journal of Cellular and Molecular Medicine*, 5(3), pp.240-253.

Shulman, M. and Nahmias, Y. (2012). Long-Term Culture and Coculture of Primary Rat and Human Hepatocytes. *Methods in Molecular Biology*, pp.287-302.

Silva, P., Homer, J., Slevin, N., Musgrove, B., Sloan, P., Price, P. and West, C. (2007). Clinical and biological factors affecting response to radiotherapy in patients with head and neck cancer: a review. *Clinical Otolaryngology*, 32(5), pp.337-345.

Singh, B., Li, R., Xu, L., Poluri, A., Patel, S., Shaha, A., Pfister, D., Sherman, E., Goberdhan, A., Hoffman, R. and Shah, J. (2002). Prediction of survival in patients with head and neck cancer using the histoculture drug response assay. *Head Neck*, 24(5), pp.437-442.

Skinner, H., Sandulache, V., Ow, T., Meyn, R., Yordy, J., Beadle, B., Fitzgerald, A., Giri, U., Ang, K. and Myers, J. (2011). TP53 Disruptive Mutations Lead to Head and Neck Cancer Treatment Failure through Inhibition of Radiation-Induced Senescence. *Clinical Cancer Research*, 18(1), pp.290-300.

Skinner, H., Sandulache, V., Ow, T., Meyn, R., Yordy, J., Beadle, B., Fitzgerald, A., Giri, U., Ang, K. and Myers, J. (2011). TP53 Disruptive Mutations Lead to Head and Neck Cancer Treatment Failure through Inhibition of Radiation-Induced Senescence. *Clinical Cancer Research*, 18(1), pp.290-300.

Slebos, R. (2006). Gene Expression Differences Associated with Human Papillomavirus Status in Head and Neck Squamous Cell Carcinoma. *Clinical Cancer Research*, 12(3), pp.701-709.

Smith, E., Pawlita, M., Rubenstein, L., Haugen, T., Hamsikova, E. and Turek, L. (2009). Risk factors and survival by HPV-16 E6 and E7 antibody status in human papillomavirus positive head and neck cancer. *International Journal of Cancer*, 127(1), pp.111-117.

Soussi, T. and Béroud, C. (2001). Assessing TP53 status in human tumours to evaluate clinical outcome. *Nature Reviews Cancer*, 1(3), pp.233-239.

Soussi, T. and Lozano, G. (2005). p53 mutation heterogeneity in cancer. *Biochemical and Biophysical Research Communications*, 331(3), pp.834-842.

Stausbøl-Grøn, B., Bundgaard, T. and Overgaard, J. (1999). In vitro radiosensitivity of tumour cells and fibroblasts derived from head and neck carcinomas: mutual relationship and correlation with clinical data. *Br J Cancer*, 79(7/8), pp.1074-1084.

Steiner, M., Wang, Y., Zhang, Y., Zhang, X. and Lu, Y. (2000). p16/MTS1/INK4A suppresses prostate cancer by both pRb dependent and independent pathways. *Oncogene*, 19(10), pp.1297-1306.

Storchova, Z. and Pellman, D. (2004). From polyploidy to aneuploidy, genome instability and cancer. *Nature Reviews Molecular Cell Biology*, 5(1), pp.45-54.

Stryker, J. (2007). Why Is the Liver a Radiosensitive Organ?. *Radiology*, 242(1), pp.1-2.

Sugrue, M., Shin, D., Lee, S. and Aaronson, S. (1997). Wild-type p53 triggers a rapid senescence program in human tumor cells lacking functional p53. *Proceedings of the National Academy of Sciences*, 94(18), pp.9648-9653.

Swanton, C. (2012). Intratumor Heterogeneity: Evolution through Space and Time. *Cancer Research*, 72(19), pp.4875-4882.

Syrjänen, K., Syrjänen, S. and Pyrhönen, S. (1982). Human Papilloma Virus (HPV) Antigens in Lesions of Laryngeal Squamous Cell Carcinomas. *ORL*, 44(6), pp.323-334.

Takayama, S., Ostuni, E., LeDuc, P., Naruse, K., Ingber, D. and Whitesides, G. (2003). Selective Chemical Treatment of Cellular Microdomains Using Multiple Laminar Streams. *Chemistry & Biology*, 10(2), pp.123-130.

Talamini, R., Bosetti, C., La Vecchia, C., Dal Maso, L., Levi, F., Bidoli, E., Negri, E., Pasche, C., Vaccarella, S., Barzan, L. and Franceschi, S. (2002). Journal search results - Cite This For Me. *Cancer Causes and Control*, 13(10), pp.957-964.

Tanaka, T., Ohkubo, S., Tatsuno, I. and Prives, C. (2007). hCAS/CSE1L Associates with Chromatin and Regulates Expression of Select p53 Target Genes. *Cell*, 130(4), pp.638-650.

Tanweer, F., Louise Green, V., David Stafford, N. and Greenman, J. (2012). Application of microfluidic systems in management of head and neck squamous cell carcinoma. *Head Neck*, 35(5), pp.756-763.

Taupin, P. (2007). BrdU immunohistochemistry for studying adult neurogenesis: Paradigms, pitfalls, limitations, and validation. *Brain Research Reviews*, 53(1), pp.198-214.

Temam, S., Kawaguchi, H., El-Naggar, A., Jelinek, J., Tang, H., Liu, D., Lang, W., Issa, J., Lee, J. and Mao, L. (2007). Epidermal Growth Factor Receptor Copy Number Alterations Correlate With Poor Clinical Outcome in Patients With Head and Neck Squamous Cancer. *Journal of Clinical Oncology*, 25(16), pp.2164-2170.

Teresewinslow.com. (2016). [online] Available at: http://teresewinslow.com [Accessed 17 Aug. 2016].

Toustrup, K., Sorensen, B., Nordsmark, M., Busk, M., Wiuf, C., Alsner, J. and Overgaard, J. (2011). Development of a Hypoxia Gene Expression Classifier with Predictive Impact for Hypoxic Modification of Radiotherapy in Head and Neck Cancer. *Cancer Research*, 71(17), pp.5923-5931.

Vakifahmetoglu, H., Olsson, M. and Zhivotovsky, B. (2008). Death through a tragedy: mitotic catastrophe. *Cell Death Differ*, 15(7), pp.1153-1162.

Van Der Velden, L., Schaafsma, H., Manni, J., Ramaekers, F. and Kuijpers, W. (1993). Cytokeratin expression in normal and (pre)malignant head and neck epithelia: An overview. *Head Neck*, 15(2), pp.133-146.

van Midwoud, P., Groothuis, G., Merema, M. and Verpoorte, E. (2010). Microfluidic biochip for the perifusion of precision-cut rat liver slices for metabolism and toxicology studies. *Biotechnol. Bioeng.*, 105(1), pp.184-194.

van Midwoud, P., Merema, M., Verweij, N., Groothuis, G. and Verpoorte, E. (2011). Hydrogel embedding of precision-cut liver slices in a microfluidic device improves drug metabolic activity. *Biotechnol. Bioeng.*, 108(6), pp.1404-1412.

Vandenabeele, P., Galluzzi, L., Vanden Berghe, T. and Kroemer, G. (2010). Molecular mechanisms of necroptosis: an ordered cellular explosion. *Nature Reviews Molecular Cell Biology*, 11(10), pp.700-714.

Vaupel, P., Kelleher, D. and Hockel, M. (2001). Oxygenation status of malignant tumors: Pathogenesis of hypoxia and significance for tumor therapy. *Seminars in Oncology*, 28(2F), pp.29-35.

Vent, J., Haidle, B., Wedemeyer, I., Huebbers, C., Siefer, O., Semrau, R., Preuss, S. and Klussmann, J. (2013). p16 Expression in carcinoma of unknown primary: Diagnostic indicator and prognostic marker. *Head & Neck*, 35(11), pp.1521-1526.

Vermeer, D., Spanos, W., Vermeer, P., Bruns, A., Lee, K. and Lee, J. (2013). Radiation-induced loss of cell surface CD47 enhances immune-mediated clearance of human papillomavirus-positive cancer. *International Journal of Cancer*, 133(1), pp.120-129.

Wang, X. (2001). The expanding role of mitochondria in apoptosis. *Genes Dev*, 15, pp.2922-33.

Wang, Y., Ji, P., Liu, J., Broaddus, R., Xue, F. and Zhang, W. (2009). Centrosome-associated regulators of the G2/M checkpoint as targets for cancer therapy. *Molecular Cancer*, 8(1), p.8.

Wang, Z., Fan, Y., Chen, J., Guo, Y., Wu, W., He, Y., Xu, L. and Fu, F. (2013). A microfluidic chip-based fluorescent biosensor for the sensitive and specific detection of label-free single-base mismatch via magnetic beads-based “sandwich” hybridization strategy. *Electrophoresis*, 34(15), pp.2177-2184.

Weaver, B. and Cleveland, D. (2005). Decoding the links between mitosis, cancer, and chemotherapy: The mitotic checkpoint, adaptation, and cell death. *Cancer Cell*, 8(1), pp.7-12.

Webb, S. and Evans, P. (2006). Innovative Techniques in Radiation Therapy: Editorial, Overview, and Crystal Ball Gaze to the Future. *Seminars in Radiation Oncology*, 16(4), pp.193-198.

Weber, R., Berkey, B., Forastiere, A., Cooper, J., Maor, M., Goepfert, H., Morrison, W., Glisson, B., Trotti, A., Ridge, J., Chao, K., Peters, G., Lee, D., Leaf, A. and Ensley, J. (2003). Outcome of Salvage Total Laryngectomy Following Organ Preservation Therapy. *Archives of Otolaryngology–Head & Neck Surgery*, 129(1), p.44.

Weibel, D. And Whitesides, G. (2006). Applications of microfluidics in chemical biology. *Current Opinion in Chemical Biology*, 10(6), pp.584-591.

Weigum, S., Floriano, P., Christodoulides, N. and McDevitt, J. (2007). Cell-based sensor for analysis of EGFR biomarker expression in oral cancer. *Lab on a Chip*, 7(8), p.995.

Williams, M. (2006). Radiotherapy Dose Fractionation. *The Royal College of Radiologists*.

Wilson, G., Dische, S. and Saunders, M. (1995). Studies with bromodeoxyuridine in head and neck cancer and accelerated radiotherapy. *Radiotherapy and Oncology*, 36(3), pp.189-197.

Wilson, J. (2008). Does Pharma Fund the Pipers? – Scottish Intercollegiate Guidelines Network (SIGN) Guidelines 90 — Diagnosis and Management of Head and Neck Cancer, October 2006. *Clinical Oncology*, 20(9), pp.661-663.

Wozny, A., Alphonse, G., Battiston-Montagne, P., Simonet, S., Poncet, D., Testa, E., Guy, J., Rancoule, C., Magné, N., Beuve, M. and Rodriguez-Lafrasse, C. (2016). Influence of Dose Rate on the Cellular Response to Low- and High-LET Radiations. *Front. Oncol.*, 6.

Wu, G., Burns, T., McDonald, E., Jiang, W., Meng, R., Krantz, I., Kao, G., Gan, D., Zhou, J., Muschel, R., Hamilton, S., Spinner, N., Markowitz, S., Wu, G. and El-Deiry, W. (1997). KILLER/DR5 is a DNA damage–inducible p53–regulated death receptor gene. *Nature Genetics*, 17(2), pp.141-143.

www. histology.med.umich.edu/medical. (2016). [online] Available at: http://www. histology.med.umich.edu/medical [Accessed 17 Aug. 2016].

Wynder, E., Bross, I. and Feldman, R. (1957). A study of the etiological factors in cancer of the mouth. *Cancer*, 10(6), pp.1300-1323.

Yamada, H. and Gorbsky, G. (2006). Spindle checkpoint function and cellular sensitivity to antimitotic drugs. *Molecular Cancer Therapeutics*, 5(12), pp.2963-2969.

Yamada, M., Utoh, R., Ohashi, K., Tatsumi, K., Yamato, M., Okano, T. and Seki, M. (2012). Controlled formation of heterotypic hepatic micro-organoids in anisotropic hydrogel microfibers for long-term preservation of liver-specific functions. *Biomaterials*, 33(33), pp.8304-8315.

Yang, C., Brooks, E., Li, Y., Denny, P., Ho, C., Qi, F., Shi, W., Wolinsky, L., Wu, B., Wong, D. and Montemagno, C. (2005). Detection of picomolar levels of interleukin-8 in human saliva by SPR. *Lab on a Chip*, 5(10), p.1017.

Yang, W., Luo, C., Lai, L. and Ouyang, Q. (2015). A novel microfluidic platform for studying mammalian cell chemotaxis in different oxygen environments under zero-flow conditions. *Biomicrofluidics*, 9(4), p.044121.

Yu, H., Alexander, C. and Beebe, D. (2007). Understanding microchannel culture: parameters involved in soluble factor signaling. *Lab on a Chip*, 7(6), p.726.

Zafereo, M., Hanasono, M., Rosenthal, D., Sturgis, E., Lewin, J., Roberts, D. and Weber, R. (2009). The role of salvage surgery in patients with recurrent squamous cell carcinoma of the oropharynx. *Cancer*, 115(24), pp.5723-5733.

Zaravinos, A. (2014). An updated overview of HPV-associated head and neck carcinomas. *Oncotarget*, 5(12), pp.3956-3969.

Zhan, Q., Fan, S., Bae, I., Guillouf, C., Liebermann, D. and O'Connor, P. (1994). Induction of bax by genotoxic stress in human cells correlates with normal p53 status and apoptosis. *Oncogene*, 9, pp.3743-51.

Zhang, H. (2006). Molecular signaling and genetic pathways of senescence: Its role in tumorigenesis and aging. *J. Cell. Physiol.*, 210(3), pp.567-574.

Zhang, X., Xu, C., Mitchell, R., Zhang, B., Zhao, D., Li, Y., Huang, X., Fan, W., Wang, H., Lerma, L., Upton, M., Hay, A., Méndez, E. and Zhao, L. (2013). Tumor Evolution and Intratumor Heterogeneity of an Oropharyngeal Squamous Cell Carcinoma Revealed by Whole-Genome Sequencing. *Neoplasia*, 15(12), pp.1371-IN7.

Zhang, Z., Morgenstern, H., Spitz, M., Tashkin, D. and Yu, G. (1999). Marijuana use and increased risk of squmous cell carcinoma of the head and neck. *Cancer Epidemiol Biomarkers*, 8, pp.1071-1078.

Zheng, C., Cotrim, A., Rowzee, A., Swaim, W., Sowers, A., Mitchell, J. and Baum, B. (2011). Prevention of Radiation-Induced Salivary Hypofunction Following hKGF Gene Delivery to Murine Submandibular Glands. *Clinical Cancer Research*, 17(9), pp.2842-2851.

Zheng, Z., Park, J., Guillemette, C., Schantz, S. and Lazarus, P. (2001). Tobacco Carcinogen-Detoxifying Enzyme UGT1A7 and Its Association With Orolaryngeal Cancer Risk. *JNCI Journal of the National Cancer Institute*, 93(18), pp.1411-1418.

Ziober, A., Patel, K., Alawi, F., Gimotty, P., Weber, R., Feldman, M., Chalian, A., Weinstein, G., Hunt, J. and Ziober, B. (2006). Identification of a Gene Signature for Rapid Screening of Oral Squamous Cell Carcinoma. *Clinical Cancer Research*, 12(20), pp.5960-5971.

Glossary

APAF 1	Apoptotic Protease Activating Factor
ATM	Ataxia telangiectasia mutated
ATR	Ataxia telangiectasia and Rad3-related protein
BAX B	Cell lymphoma associated X-protein
BCL-2	B Cell Lymphoma 2
BRDU	5-bromo-2'-deoxyuridine
CI	Confidence interval
CNA	Copy number aberrations
CNV	Copy nucleotide variants
CT	Computed tomography
DNA	Deoxyribonucleic acid
EGFR	Epidermal growth factor receptor
EMT	Epithelial mesenchymal transition
FGFR	Fibroblast growth factor receptors
GST	Glutathione S-transferase
HEPES	4-(2-hydroxyethyl)-1-piperazineethanesulfonic acid
HNSCC	Head and neck squamous cell carcinoma
HPV	Human papilloma virus
HR	Hazard ratio
LET	Linear energy transfer
LOH	Loss of heterozygosity
MOMP	Mitochondrial Outer Membrane Permeabilisation
MRI	Magnetic resonance imaging
NKB1	Nuclear factors of kappa light polypeptide gene enhancer in B-cells 1
MAPK	Mitogen activated protein kinases
p16	Cyclin-dependent kinase inhibitor 2A
P53	Tumour protein 53
PARP	Poly-ADP-ribose-polymerase
PI3K	Phosphatidylinositol 3-kinases-AKT-mTOR
PTEN	Phosphatase and tensin homolog

Rb	Retinoblastoma
RIP	Receptor interacting protein
RNA	Ribonucleic acid
ROS	Reactive oxygen species
Ser473	Serine 473
SNV	Single nucleotide variants
TGF- ß	Transforming growth factor beta
Thr308	Threonine 308
TNM	Tumour Node Metastasis
TSNA	Tobacco-specific N-nitrosamines
UADT	Upper aerodigestive tract
XRCC5	X-ray repair cross complementing 5 protein

Appendix

Tris buffered saline (TBS)

1L of dH2O containing 121g (1M) of Tris (Trizma T1503; Sigma-Aldrich) and 170g (3M) of NaCl (S3014; Sigma-Aldrich) was prepared. The pH was adjusted to 7.6 by adding about 80mL of concentrated HCl and measured by using pH meter. The stock solution (20x concentrated stock solution) was stored at room temperature and was added into distilled-water in 50 times dilution before use.

Borate buffer

To make 100mL of borate buffer, 55mL of Boric acid (0.2M) and 45mL of sodium tetraborate (0.05M) were mixed and the pH of the buffer was adjusted to 8.4. The buffer was stored at room temperature.